FACTORS AFFECTING ATHABASCA OIL SAND SLUDGE STABILITY

by

Maurenia Mae Lynds

A thesis submitted to the School of Graduate Studies and Research

in partial fulfilment of the requirements for the

degree of

MASTER OF APPLIED SCIENCE

Department of Chemical Engineering

University of Ottawa

Abstract

The two major oil sand extraction plants, Syncrude Canada Ltd. and Suncor Inc., utilize the Clark Hot Water Extraction Process to remove bitumen from surface mineable Athabasca oil sands. This process produces a waste stream containing dispersed clay, sand, silt, and bitumen which is pumped to tailings ponds. The coarse sand and some of the finer particles settle out and are used to construct containment dykes around the ponds. However, much of the clay, silt, and bitumen remain in suspension and are carried out towards the centre of the pond. These solids eventually form a sludge with a gel-like structure, retaining from 85 to 90 percent of the recyclable process water. The ever-increasing, enormous tailings ponds present a serious environmental hazard to the nearby lakes, rivers, land, and wildlife.

It has been proven that ultrafine (10 to 200 nm) clay particles, capable of forming a highly porous, three-dimensional gel network, are the main components responsible for structure formation within Athabasca oil sand sludge. The ultrafine clay particles, mainly kaolinite and mica, are able to form the gel network in a short period of time (1 to 14 days) and the gel has a high water holding capacity.

The oil sand sludge is also composed of coarse solids, poorly-crystalline inorganic components, and strongly-bound organic matter. The deuterium nuclear magnetic resonance technique was used to study the effect of these components, as well as, the effect of the different sizes of ultrafine clay particles on gel formation. It was observed that the gel forming propensity of the sludge was significantly increased with a decrease in particle size of the ultrafine clays. The presence of coarse solids

slowed the rate of gel formation; however, the poorly-crystalline inorganic components were shown to have no effect on the gel forming propensity.

The ultrafine clay particles were further separated into hydrophilic and biwetted solids. The biwetted ultrafine solids were identified as having surfaces that contained a large percentage of strongly-bound organic matter. The presence of these particles significantly accelerated the rate of gel structure formation.

Lastly, water chemistry (chemical composition of dissolved matter) was proven to play a significant role in sludge structure formation. The ultrafine clay particles would only form a gel when the aqueous media contained an appropriate amount of dissolved electrolytes. Gel structure formation was prevented in an aqueous media of distilled water. As well, a significant increase in the electrolyte concentration of the aqueous media induced coagulation, thereby allowing a dense sediment to be formed and a large volume of trapped water to be released.

These results have revealed that the combination of ultrafine clay particles and appropriate water chemistry is essential before structure formation can occur within oil sand sludge.

Acknowledgements

Special gratitude is reserved for Dr. Luba Kotlyar who supervised this thesis with infinite patience and inspiration. I am very thankful for her advice, technical expertise, and kindness in answering my endless questions.

I would also like to thank Dr. Vladimir Hornof, who also supervised this research, for his advice, guidance, and encouragement.

I would like to acknowledge Dr. John Ripmeester for his assistance and advice on the deuterium nuclear magnetic resonance technique and Dr. Yves Deslandes for conducting the transmission electron microscopy and X-ray photoelectron spectroscopy analyses.

This research has been funded by the Sludge Fundamentals Consortium. Their support is gratefully acknowledged.

Finally, I extend much love and appreciation to my husband, Capt Kirk Lynds, for his enduring patience, moral support, and most importantly, his inexhaustible ability to proofread this document.

Nomenclature

A:	Aqueous colloidal suspension layer
A-200:	Fraction of A sedimented at 200 g
A-500:	Fraction of A sedimented at 500 g
A-1500:	Fraction of A sedimented at 1500 g
A-91500:	Fraction of A sedimented at 91500 g
AS:	Hydrophilic (aqueous) colloidal solids
B:	Bitumen
BS:	Bitumen associated hydrophobic solids
CEC:	Cation exchange capacity
CGC:	Critical gel concentration
DLVO:	Derjaguin, Landau, Verwey, and Overbeek theory
D_o:	^2H NMR residual splitting at zero time, (Hz)
D_t:	^2H NMR residual splitting at a certain time, t (Hz)
DW:	Distilled Water
GCOS:	Great Canadian Oil Sands extraction plant
GOC:	Gel onset concentration
IOCC:	Insoluble organic carbon content
NMR:	Nuclear magnetic resonance technique
NRC:	National Research Council of Canada
ORS:	Organic rich coarse solids
PW:	Pond water
RS:	Residual coarse solids

SAS:	Surface active solids
SOM:	Strongly bound organic matter
TEM:	Transmission electron microscopy
V_A:	Van der Waals attractive interparticle force
XPS:	X-ray photoelectron spectroscopy
XRD:	X-ray diffraction spectroscopy

Table of Contents

List of Tables

List of Figures

Chapter 1

Introduction

1.1 General Overview

Fifteen percent of Canada's oil is recovered from the Athabasca Oil Sand Deposit, located in northeastern Alberta. It is the largest of Alberta's oil sand deposits and is one of the world's largest and best known resources of bitumen. The deposit covers approximately 46,800 square kilometres and contains an estimated 151 billion cubic metres (950 billion barrels) of bitumen (AOSTRA, 1990). It has been estimated that 50 billion barrels of bitumen can be recovered economically using the Clark Hot Water Extraction Process, developed by K.A. Clark of the Alberta Research Council (Clark, 1948).

The two major Canadian oil sand extraction plants, Syncrude Canada Ltd. and Suncor Inc., located near Fort McMurray, Alberta, utilize the Hot Water Extraction Process to remove bitumen from surface mineable oil sands (Figure 1.1). During the first step of this process, oil sand is mixed with hot water (80 to 85 °C) and injected with pressurized steam (for temperature control) in huge tumblers to form a pulp of 70 to 85 wt% solids (Camp, 1977). Sodium hydroxide and other reagents are added as required to maintain the pH in the range of 8.0 to 8.5.

Figure 1.1: Primary Extraction Process Flow Sheet

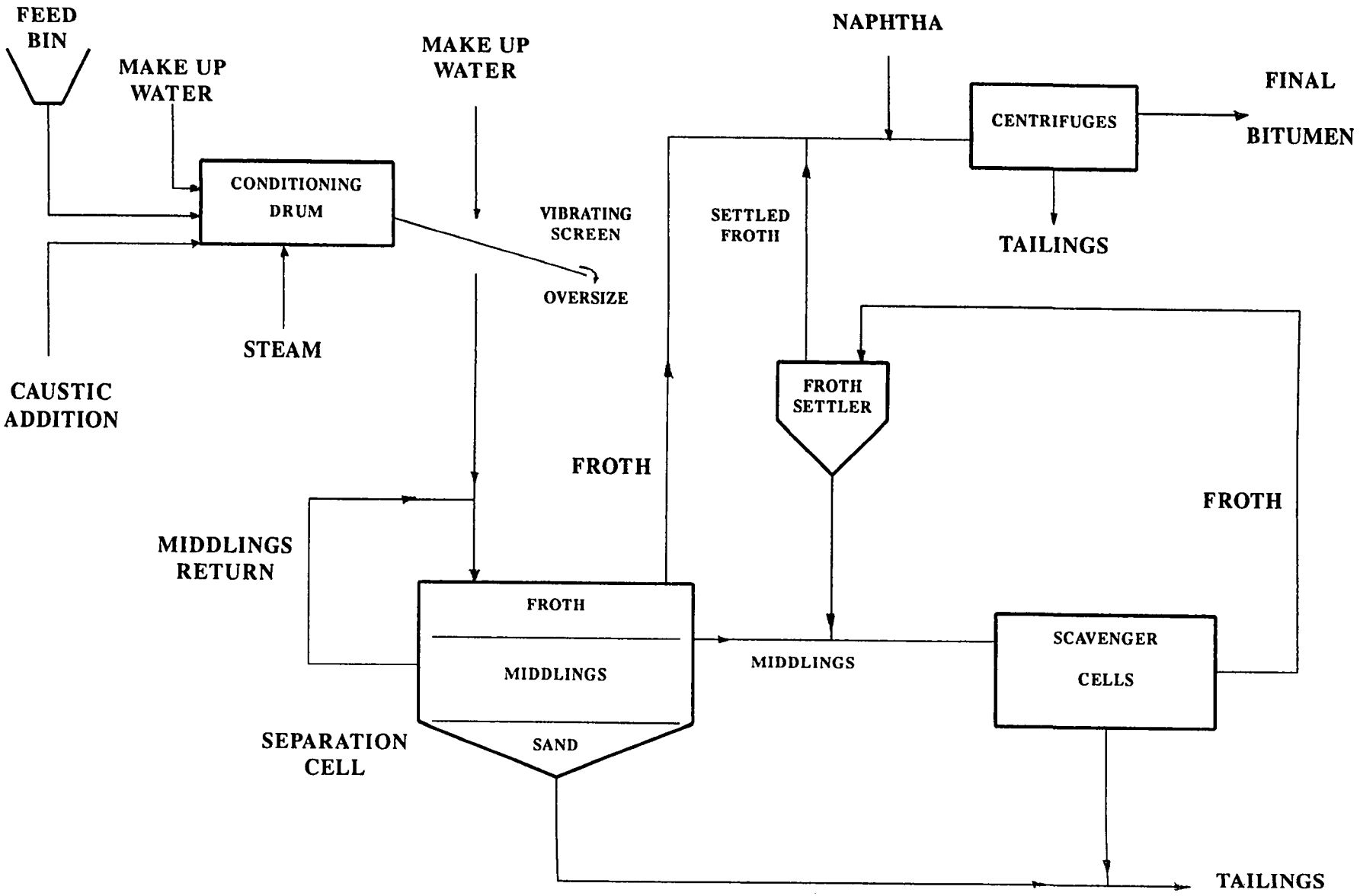

This first conditioning step separates the bitumen from the sand grains, and then mixes the bitumen into the pulp in the form of discrete droplets of a particle size on the same order of magnitude as that of the sand grains. However, the process conditions also cause a large fraction (60-80%) of the clays, occurring naturally in the oil sand feed, to be dispersed throughout the pulp mixture. During dispersion, the naturally occurring aggregates of clay particles are broken down, forming a slurry of individual particles (Camp, 1977). As a result, the conditioning process, which prepares the bitumen for efficient recovery in the following refining steps, also disperses the clays into a form which causes severe problems for the disposal operations.

Following the conditioning process is the separation step. From the tumblers, the pulp mixture is pumped to the primary gravity separation tank where the bitumen floats to the top as a froth. The bituminous froth is then removed for dewatering and upgraded to synthetic crude oil. The middle layer from the primary separation tank undergoes air flotation which results in further bitumen separation from dispersed clay, sand, and silt.

The bottom layer from the primary separation tank, consisting of an aqueous slurry of dispersed clay, sand, silt, and small amounts of bitumen, along with dispersed solids separated from the middle layer, are pumped to tailings or sedimentation ponds. Ideally, the solid particles should settle out thereby releasing process water which could then be recycled back to the extraction process. In reality, the coarse sand and some of the finer particles ($< 40\ \mu m$) do settle out and are used to construct containment dykes around the ponds; however, due to the dispersing action of the conditioning process, about half of the silt and clay and almost all of the unextracted bitumen, remain in suspension and are carried out towards the centre of the pond. These solids eventually form a gel-like structure retaining from 85 to 90 percent of the recyclable process water (Scott and Dusseault, 1982). This has resulted in enormous tailings ponds being generated at a current rate of 55 million cubic

metres (342 million barrels) per year of tailings sludge (AOSTRA, 1990).

The sludge, with its gel-like structure, contains approximately 66 wt% water, 31 wt% solids, and 3 wt% bitumen. It has been estimated that up to 12 percent of the bitumen, originally present in the oil sand, remains with the sludge (Hall and Tollefson, 1980). This means that over 2900 tonnes of bitumen are wasted daily from a plant producing 16,000 cubic metres (100,000 barrels) of synthetic crude oil per day! If the synthetic crude oil is valued at $21 per barrel, approximately $89 million per year worth of bitumen is lost to the tailings ponds.

The residual bitumen, which may be contributing to the stability of the sludge, causes the ponds to be toxic and, therefore, presents a serious environmental hazard (EVS Consultants, 1992). A catastrophic failure of the retaining dyked-wall would cause irreparable damage to the nearby lakes, rivers, land and wildlife.

From the above explanation, it is apparent that there are both environmental and economic incentives to develop an understanding of the factors affecting structure formation in oil sand sludge. This fundamental understanding is necessary to develop a long term economical and environmentally acceptable method to eliminate or minimize the accumulation of oil sand sludge.

1.2 Main Objective of this Research Project

The main objective of this research project is twofold: 1) to gain a thorough understanding of the properties of the different components in oil sand sludge; and 2) to determine the factors and mechanisms affecting structure formation in the sludge.

1.3 Literature Review of the Theories of Structure Formation and Stability Within Oil Sand Sludge

1.3.1 Nature of the Problem

The Great Canadian Oil Sands (GCOS) extraction plant, completed in 1967, was the first large-scale attempt to recover crude oil from the Athabasca oil sand deposit (Fitzgerald, 1978). Using the Clark Hot Water Extraction Process, the GCOS operation produced about 8000 cubic metres (50,000 barrels) of synthetic crude oil daily (Nedapac, 1973). Unfortunately, it also produced about 130,000 cubic metres (34.6 million gallons) of sludge per day! A small fraction of water was released from the sludge and recycled back to the process, but it was not sufficient to replace the fresh water intake that was also necessary. This imbalance caused continuous stockpiling of the sludge and by 1973, the GCOS tailings pond, which was enclosed by a dyke having a height of 91 metres, was approaching full capacity.

As with any new large-scale operation, a pilot plant study was implemented before the full-scale GCOS plant was constructed. None of the studies conducted on the pilot plant revealed this serious sludge accumulation problem. It was anticipated that the bitumen, water, chemicals, clay, and sand would rapidly separate into four distinct layers. Had the bitumen floated to the top, as shown by the pilot plant study, it would have been skimmed off, and the chemicals would have dissipated naturally by the air and wave action. The water could then be recycled back to the process and the clay and sand could be used to fill in the land depressions created by the strip-mining, thereby restoring the whole area to its former growing state (Fitzgerald, 1978). As this problem was not foreseen, GCOS was not prepared to deal with the ever-increasing size of the tailings pond.

GCOS's first step towards coping with the problem was to construct technologically-improved impermeable dykes (Camp, 1977). While this was a

satisfactory short-term fix, GCOS realized that it was not going to solve the problem; therefore, progress was started towards developing an economically and environmentally-acceptable solution.

GCOS immediately initiated a research and development program whose main objectives were to quantify and minimize sludge accumulation. This program endeavoured to develop three strategies: 1) to reduce sludge accumulation; 2) to treat sludge after it was formed; and 3) to permanently impound the sludge (Camp, 1977).

The first strategy, sludge accumulation reduction, would have required process modifications. As this would have been very difficult and expensive to test, minimal time was spent investigating this strategy.

The strategy of sludge treatment after it was formed received the bulk of GCOS's development effort. GCOS tried flocculation/settling, filtration, ultrafiltration, centrifugation, freeze/thaw, evaporation/distillation, electrophoresis, flotation, bioprocessing, and solidification (Camp, 1977). Each of these approaches was ultimately rejected because of either technical or economical limitations.

The last strategy of permanently impounding the sludge was environmentally very sensitive. Impoundment tests, as well as, many surveys of the local topography were conducted. However, a technically, economically, and environmentally-acceptable action plan was never developed.

1.3.2 Theories of Structure Formation and Stability Within Oil Sand Sludge

Following the GCOS program, researchers began to realize that before a solution to the sludge stability and accumulation problem could be devised, the actual interactions between the various solid constituents within the sludge must first be understood. In 1978, Yong and Sethi were contracted by GCOS to investigate these interactions.

Yong and Sethi (1978) examined the stability phenomenon by studying the fundamental interactions between the mineral components in the sludge. They stated that the minerals of importance were montmorillonite, illite, kaolinite and iron oxide. The presence of amorphous matter, which was thought to contribute significantly to the status of the sludge suspension, was also detected. It was found that the fines fraction (solids <40 μm) contained an average of approximately 4% amorphous iron oxide and less than 0.1% amorphous Al_2O_3 and SiO_2. They also detected significant quantities of quartz.

The Stokian Fall of the particles in the sludge was also studied. It was observed that the sand fraction (solids >40 μm) was unable to segregate from the fines fraction. They concluded that, in addition to normal hindrance to particle fall, complex interactions between the fines and sand must be present. This led them to investigate the theoretical influence of electrostatic double layer interactions.

Next, the suspension volume (the amount of water associated with each mineral) for each mineral in the sludge was calculated. When all of the individual characteristic mineral suspension volumes were added together, the total resulting volume was approximately the same as that of the actual sludge sample. This led Yong and Sethi to conclude that sludge stability was controlled mainly by the mineral particle interactions, and could be explained in terms of the effective interparticle pressures developed, and the Gouy double layer interaction of the mineral particles. Having developed this knowledge, they claimed that it would now be possible to develop a treatment scheme which would induce settling of the sludge solids.

By 1978, Kessick of the Alberta Research Council was also trying to determine the structure and properties of oil sand sludge. He initially proposed that sludge stability was dependent on the presence of residual bitumen as well as a clay-bound organic component (Kessick, 1979).

Kessick began his study by comparing the rheological and stability characteristics of oil sand sludge with those of a pure montmorillonite gel. A study of the dependence of gel strength on pH showed that montmorillonite retained its gel-like consistency throughout the entire pH range of 3 to 12. However, the viscosity of the sludge increased significantly at both high and low pH. He believed that this indicated an internal structure which changed with pH. He confirmed this point during a freeze-thaw test. The amount of freeze-thaw dewatering that occurred as a function of pH was profoundly different for the two samples. Greater amounts of water were released from the sludge at both high and low pH values. He concluded that montmorillonite was definitely not present in the sludge in sufficient amounts to control its dewatering and stability characteristics.

These results led Kessick to the hypothesis that sludge structure must be the result of a complex interaction between the clay and residual organic matter in the sludge. He believed that kaolinite and illite suspensions alone would simply settle out and not retain much water. After many failed attempts to model the sludge by dispersing pure kaolinite with bitumen under conditions similar to those of the Hot Water Extraction Process, Kessick concluded that the presence of organic matter closely associated with the clay fraction was necessary for gel formation. Clay particles containing this closely associated organic matter were known to be surface active and would impart stability to oil-in-water emulsions (van Olphen, 1976).

By the end of his study, Kessick concluded that in the absence of swelling clays (montmorillonite), three conditions were necessary for gel formation in oil sand sludge: 1) residual bitumen must be present; 2) a clay-bound organic component must also be present to impart surface activity to the clay particles; and 3) the clay particles must be well dispersed initially before subsequent structure formation would occur (Kessick, 1979).

By 1988, Suncor Inc. (GCOS was reorganized to Suncor Inc. in 1979),

Syncrude Canada Ltd., and numerous independent researchers had invested tens of millions of dollars attempting to solve the sludge stability problem. In 1989, the Sludge Fundamentals Consortium was formed to bring together and coordinate the efforts of industry, government agencies, and academic researchers. It was felt that this coordinated approach would be more effective in the development of science and engineering theories which would lead to the production of technology required to solve the sludge stability problem. At present, the main participants in the Sludge Fundamentals Consortium are the Alberta Oil Sands Technology and Research Authority, Alberta Energy, Alberta Research Council, Environment Canada, National Research Council, CANMET, Syncrude Canada Ltd., and Suncor Inc.

With funding from the Sludge Fundamentals Consortium, Sethi (1991) continued his research to determine the role of amorphous iron oxide in oil sand sludge stability. From previous results, Yong and Sethi (1978) documented that even though the presence of amorphous iron oxide in the fines fraction of sludge minerals was small (~4%) its contribution to the overall sludge volume was very large (~25%).

Sethi's study (1991) first showed that the amorphous iron oxide content and the percent fines in sludge minerals both decreased with depth. The average amount of amorphous iron oxide was calculated to be 4.08% of fines. Sethi also determined that the source of the amorphous iron oxide was the oil sand feed and not a product of the Hot Water Extraction Process.

Based on these new results and those from 1978, Sethi reinforced the belief that amorphous iron oxide and montmorillonite were the main components responsible for the stability and high water holding capacity of sludge, due to their high specific surface areas. He concluded that if montmorillonite could be transformed to iron rich chlorite by interlayering montmorillonite with crystalline iron oxide, the transformations would cause an overall reduction in the specific surface area and a

resultant reduction in the overall sludge volume (reduction of approximately 25-40%).

For many years, it was suggested that some sort of regular card house structure formation was present in oil sand sludge, thereby explaining its stability. To prove or disprove this hypothesis, Mikula et al. (1991) used cryogenic scanning electron microscopy to investigate sludge structure using a freeze fracture technique. Their results detected a cellular type structure arranged in domains of longer range ordering. This ordering was not observed in pure clay suspensions, thereby indicating that orientation of the sludge solids was occurring and could account for the stability of oil sand sludge.

The coordinated efforts of the Sludge Fundamentals Consortium are continuing with a relatively high level of success in many areas. As research continues and the knowledge base of the fundamentals of sludge structure is expanded, our ultimate goal of preventing and/or minimizing sludge formation will, in the near future, be reached.

Chapter 2

Theoretical Aspects

2.1 Terminology

Many specific terms will be used throughout this research paper which tend to have different definitions when applied for specific applications and disciplines. To ensure complete understanding, the following section is a list of terms and their definitions as they apply to this research.

Colloid: A suspension in which the dispersed phase consists of particles so small (~ 1 - 1000 nm) that gravitational forces are negligible and interactions are dominated by short-range forces, such as van der Waals forces and surface charges. The dispersed phase is also influenced by Brownian motion (Brinker and Scherer, 1990).

Sol: A colloidal suspension of solid particles in a liquid medium (Brinker and Scherer, 1990).

Gel: A dispersion of colloidal clay particles that form a solid skeletal network enclosing a continuous liquid phase (Brinker and Scherer, 1990).

Aggregation: The term used for all the ways in which colloidal particles are linked together (Iler, 1979).

Flocculation: The reversible process where the particles of a dispersion adhere to one another, but do not collapse on one another (Iler, 1979). There is minimal change in the overall surface area. An initially formed, rather open aggregate is called a floc, and the process of its formation is called flocculation.

Coagulation: The irreversible process where the particles in a dispersion collapse on one another, resulting in a significant reduction in the overall surface area (Iler, 1979). The resulting coagulum is very dense with little water trapped between the flocs. Normally, the particles cannot be redispersed.

2.2 Colloidal Clay Minerals

There are two basic types of clay minerals: amorphous and crystalline. The distinct properties of amorphous clays are very difficult to determine, especially when combined with other types of matter. Crystalline clays are very well understood and, in most cases, their properties can be easily identified.

Crystalline clay minerals are composed of small plate-like particles. Each clay platelet is made up of one or more unit layers, stacked like a deck of cards. The crystalline structure of the unit layers consists of sheets of tetrahedrally coordinated silica (oxygen linked to silicon) in combination with sheets of octahedral alumina or magnesia (hydroxyls or oxygen linked to aluminum or magnesium) (Swartzen-Allen and Matijevic, 1974). The distance between a certain plane in the unit layer and the corresponding plane in the next unit layer is called the basal spacing.

Kaolinite, the main colloidal clay present in oil sand sludge, is a two-layer clay with one octahedral and one tetrahedral layer. The unit layer is composed of one

sheet of silica and one sheet of alumina. Kaolinite has a basal spacing of 7.1 Å. The structure of a kaolinite unit layer is illustrated in Figure 2.1.

Electrokinetic studies of colloidal clay dispersions in aqueous media indicate that, at all pH values above two or three, the clay particles carry a net negative charge distributed over the basal surfaces (Swartzen-Allen and Matijevic, 1974). The net negative charge of colloidal kaolinite clay particles can be a result of isomorphic substitution, lattice imperfections, broken bonds at the edges of the particles and exposed structural hydroxyl ions. However, previous studies (van Olphen, 1963) indicate that isomorphic substitution appears to be the principal source of the net negative charge on the clay particles. When isomorphic substitution occurs, the constituent metal ions of the clay lattice are replaced isomorphically by cations of a lower charge. In the case of kaolinite, aluminum may be replacing silicon in the surface tetrahedral layer, thereby producing a net negative charge on the particle surface.

2.3 Stability of Colloidal Clay Sols

The stability of colloidal clay sols is determined by the net force acting between particles in the dispersion. If the net force is attractive, the particles will come together and form clusters or aggregates and the dispersion will be unstable. If the net force is repulsive, the system will be stable and all the particles will move around as individual entities. However, colloidal systems are complicated by the fact that the net force between two particles can be attractive at certain distances but repulsive at others. This results in the creation of energy barriers surrounding the particles (Van de Ven, 1989).

There are several different forces that determine the stability of colloidal dispersions. In general, since the electrons surrounding a nucleus do not form a spatially and temporally uniform screen, every atom reacts like a fluctuating dipole

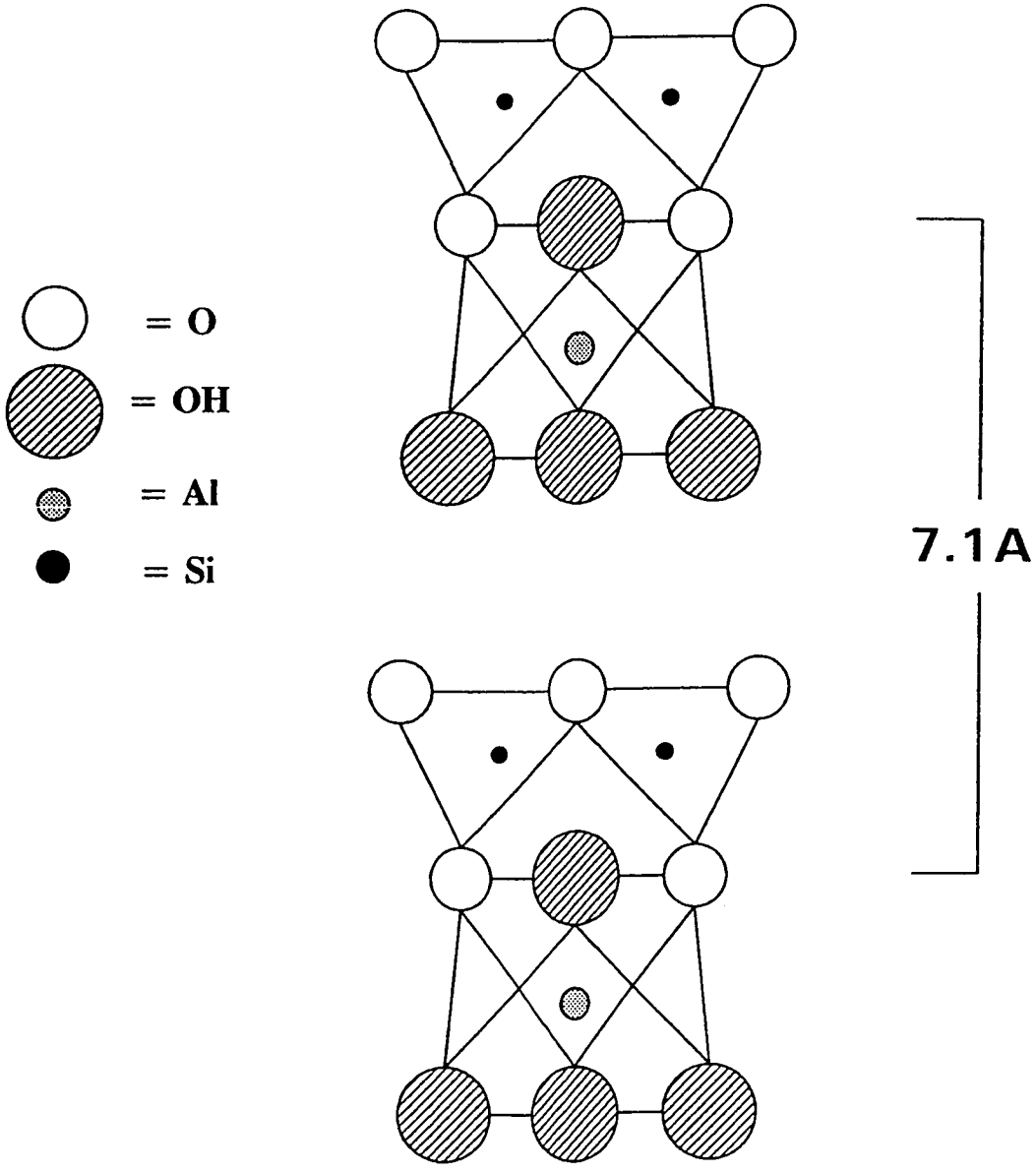

Figure 2.1: Schematic Structure of Kaolinite Clay.

(Brinker and Scherer, 1990). These fluctuations create a force of attraction between atoms, known as the van der Waals force or dispersion energy. The van der Waals force is proportional to the polarizabilities of the atoms and is inversely proportional to the sixth power of their separation distance ($V_A \propto -1/h^6$). The force results from three types of interactions (Brinker and Scherer, 1990): permanent dipole-permanent-dipole (Keesom forces), permanent dipole-induced dipole (Debye forces), and transitory dipole-transitory dipole (London forces). Thus, when atoms are far apart, the movement of their electrons is unrelated but as they come closer together the electrons are distributed so as to minimize the energy of the system.

The van der Waals attraction force, V_A, becomes important for particles of colloidal dimension as it is approximately additive. The total attraction between particles containing a large number of atoms is equal to the sum of all the attractive forces between every atom of one particle and every atom of the other particle. It also represents the attractive force tending to cause aggregation of the colloids. The attractive force between two infinite plates separated by distance h, is given by the expression (Everett, 1988):

$$V_A = - A / 12\pi h^2$$

where A, the Hamaker constant, (ranging from 10^{-19} to 10^{-20} J) is a material property which depends on both the properties of the particle and those of the medium. The dependence of force on distance has changed from V_A being proportional to $-1/h^6$ for atoms, to V_A being proportional to $-1/h^2$ for plates (recalling that the clay particles in oil sand sludge are composed of platelets).

The van der Waals attraction force is not the only force present in a colloidal dispersion. The next type of force that must be considered is the electrostatic repulsive force. The theory that describes the stabilization of colloids by electrostatic repulsion is called the Derjaguin, Landau, Verwey, and Overbeek Theory, or DLVO theory (Verwey and Overbeek, 1948, Derjaguin and Landau, 1941). This theory explains that the net force between particles in a dispersion is the sum of the van der

Waals attraction force and the electrostatic repulsion force created by charges adsorbed on the particles. Because a colloidal dispersion as a whole is electrically neutral, the DLVO theory explains that there must be an equivalent amount of ions of opposite charge in solution to balance the particle charge. These oppositely charged ions are found preferentially in the neighbourhood of the suspended colloidal particles and form a diffuse electrostatic double layer around each colloidal particle. These accumulated ions of opposite charge are called counter-ions.

Figure 2.2 is a schematic diagram reflecting the DLVO theory. It shows the net effect of adding the van der Waals attraction force and the electrostatic double layer repulsion force. Near the particle surface is the deep primary minimum in potential energy produced by the van der Waals attraction; farther away is a maximum, or repulsive barrier, produced by the electrostatic double layer. If the repulsive barrier is greater than approximately 10kT, where k is Boltzmann's constant ($1.38 * 10^{-23}$ J/molecule/K) and T is absolute temperature, then the collisions between particles produced by Brownian motion will not be able to overcome the barrier and, as a result, aggregation of the particles will be prevented (Brinker and Scherer, 1990). However, if the concentration of counter-ions in the solution is increased, then the electrostatic double layer will be compressed, because the same number of charges are required to balance the surface charge on the particle and they are now available in a smaller volume surrounding the particle. Since the attractive force is unchanged while the range of the repulsion potential is reduced, a secondary minimum appears in the DLVO potential diagram. If the counter-ion concentration is increased further, at some point the net interparticle potential will become attractive and, theoretically, the colloidal suspension should immediately coagulate.

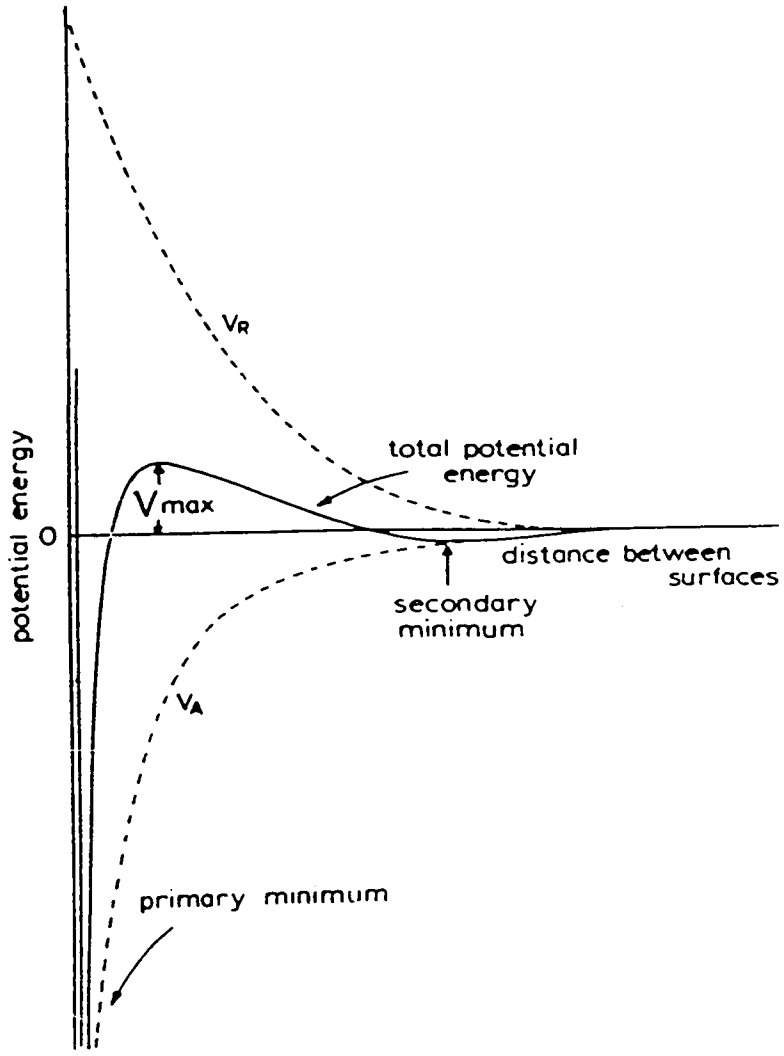

Figure 2.2: Schematic Diagram of the DLVO Theory

2.4 Repulsive Hydration Forces

For many years, it was believed that the attractive van der Waals force and the repulsive electrostatic double layer force were the only forces operating between solid surfaces in liquid media. However, recent experiments have revealed that another type of complex repulsive short-range (less than a few nanometres or molecular diameters) force can also influence particles in liquid media (Israelachvili, 1992). This additional force appears to change with distance, varying between attraction and

repulsion, with a regular reoccurrence that is equal to the average dimension of the liquid molecules (Israelachvili, 1992). The force appears to arise from the confining effect that two surfaces can have on the interlayering liquid molecules. The properties of these molecularly thin liquid films are no longer the same as they were in the bulk solution. Properties such as density and viscosity appear to change to those of a solid or a liquid crystal.

The forces occurring in water and in electrolyte solutions are more complex than those occurring in nonpolar liquids. There are many aqueous systems where the DLVO theory fails due to the presence of the above additional short-range force. Between hydrophilic surfaces, this force is commonly referred to as the hydration or structural force. This repulsive hydration force is believed to arise from strong hydrogen-bonding surface groups, such as hydrated ions or hydroxyl OH^- groups, which modify the hydrogen-bonding network of liquid water adjacent to them (Israelachvili, 1992).

In 1980, a series of experiments were conducted to determine the factors that influenced the hydration force in clay systems (Pashley, 1981). It was determined that in dilute electrolyte solutions, the clay systems obeyed the DLVO theory. However, at higher salt concentrations specific to each electrolyte, hydrated cations bound to the negatively charged clay surface, resulting in a repulsive hydration force (an additional hydration force appeared to be superimposed on the DLVO interaction curve). The studies showed that the strength and range of the hydration force increased with the known hydration numbers of the cations in the order $Mg^{2+} > Ca^{2+} > Li^+ \sim Na^+ > K^+ > Cs^+$ (Israelachvili, 1992).

Another interesting observation from Pashley's studies was that the hydration force had both an oscillation (fluctuated between attractive and repulsive) and a monotonic (uniform) component. These effects are shown in Figure 2.3. The hydration force between the clay platelets had a net repulsive force down to particle

separations of approximately 4 nm. However, the hydration force was not always monotonic below 2 nm and would exhibit oscillations of mean periodicity of 0.25 $\pm$ 0.03 nm. This distance is roughly equal to the diameter of the water molecule (Pashley, 1981). The clay platelets repelled each other with increasing strength down to separations of 2 nm; however, below 2 nm the clay platelets became stacked into stable aggregates with water interlayers of typical thickness 0.25 and 0.55 nm.

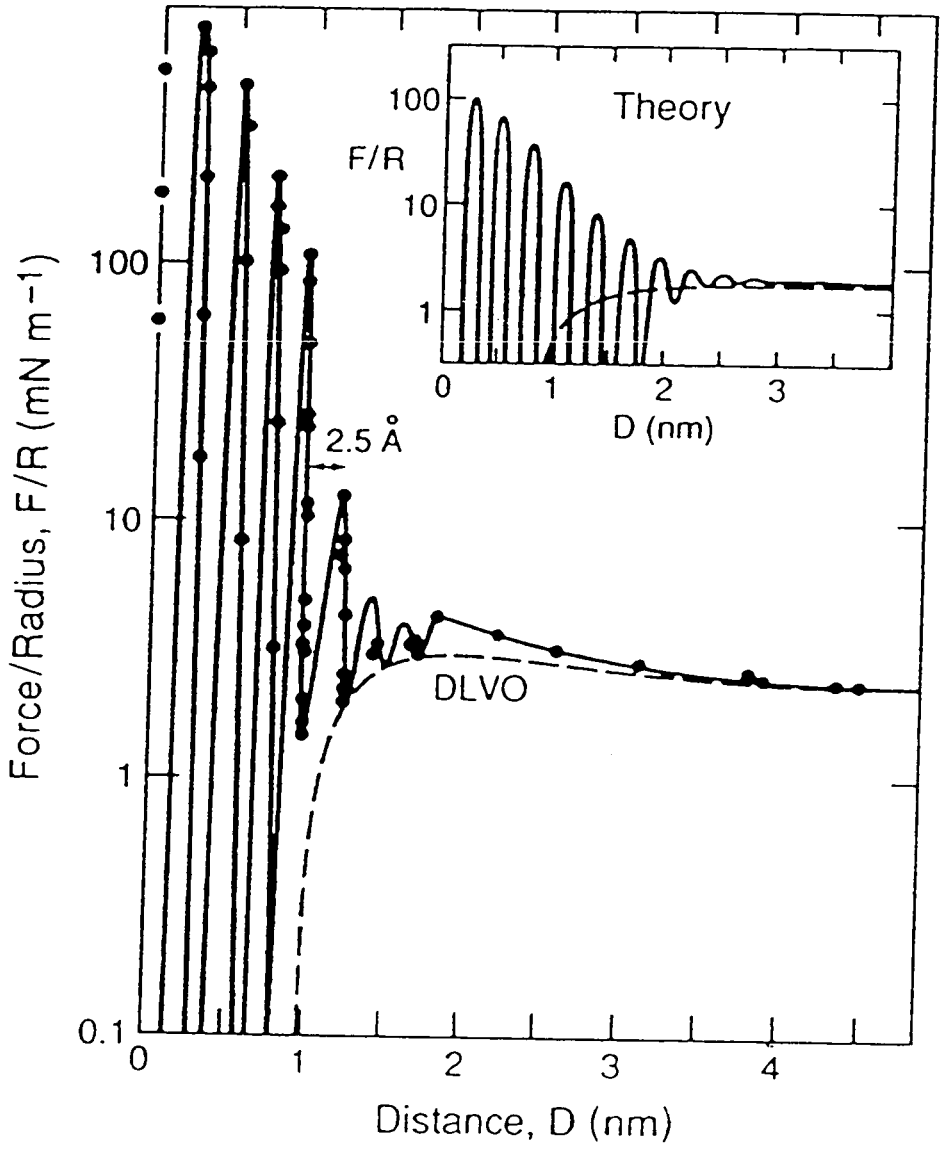

Figure 2.3: Schematic Diagram of Additional Hydration Force Superimposed on the DLVO Interaction Curve

The experiments by Pashley also showed that the hydration force can be modified by exchanging ions of a different hydration number on the clay surfaces. This effect may have important practical applications in controlling the stability of colloidal dispersions.

Much research has proven that colloidal particles can be coagulated by increasing the electrolyte concentration. This effect was traditionally attributed to the decreased screening of the electrostatic double layer repulsion between the particles. However, there have also been many examples that could not be explained by this simple theory. These colloidal systems were stable even at very high electrolyte concentrations. This effect is now being attributed to the increased hydration repulsion experienced by certain surfaces when they bind highly hydrated ions at high electrolyte concentrations (Israelachvili, 1992).

2.5 Repulsive Steric Forces

Besides the repulsive hydration force, the effect of a steric barrier has also been proven to prevent colloidal clay particles from coagulating. A thick adsorbed layer of organic compounds (polymers) on the clay surfaces can prevent the particles from entering the primary minimum. To provide an effective steric barrier, the adsorbed layer must meet the following requirements (Tadros, 1982):

1) the surface of the particle should be completely covered to prevent the organic polymer chains from attaching to both particles, thus causing what is called bridging flocculation;

2) the polymer should be firmly anchored to the surface so that it cannot be displaced during a Brownian collision;

3) the layer must be thick enough (typically >3nm) to keep the point of closest approach outside the range of the van der Waals attraction forces; and,

4) the nonanchored portion of the polymer must be well solvated by the liquid.

Figure 2.4 shows a schematic diagram of a steric barrier.

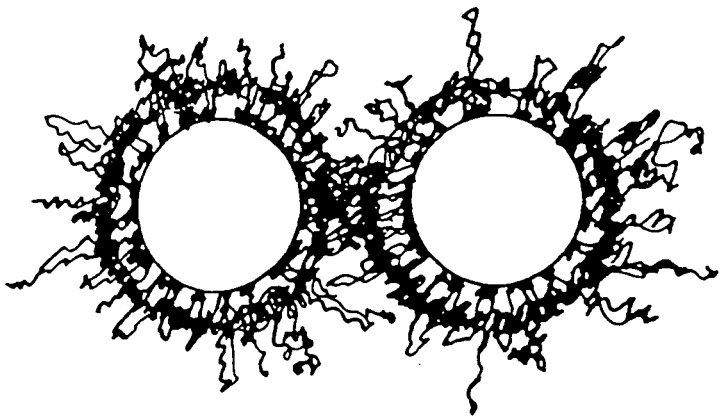

Figure 2.4: Schematic Illustration of a Steric Barrier

2.6 Clay Surface and Edge Charges

As mentioned earlier, the clay lattice carries a net negative charge because of isomorphic substitution, where certain electropositive elements are replaced by elements of a lower valency. This net negative lattice charge is compensated by cations which are located on the unit layer surfaces. In aqueous media, these compensating cations have a tendency to diffuse away from the clay layer surface since their concentration is normally lower in the bulk solution. At the same time, they are also attracted to the negatively charged clay lattice. These opposing forces cause the creation of an atmospheric distribution of the compensating cations in a diffuse electrical double layer on the exterior layer surfaces of the clay particle.

The compensating cations act as the counter-ions of the double layer and are exchangeable for other cations. The ability of these cations to be exchanged for other cations is referred to as the cation exchange capacity (CEC) and is an important property of clay.

Another important fact about clay layer surfaces is that the electric double layer on the layer surface has a constant charge. This charge is determined by the

type and degree of the isomorphic substitution; therefore, the layer surface charge density is independent of the presence of electrolytes in solution.

In addition to the electric double layer of the flat unit layer surface, the double layer of the edge surface is also important. The atomic structure of clay platelet edges is very different from that of the unit layer surfaces. It has been proven that part of the edge surface at which the octahedral sheet is broken, normally carries a positive double layer in acid solutions - with Al ions acting as potential-determining ions, and negative double layer in alkaline solutions - with the hydroxyl ion acting as potential-determining ions (van Olphen, 1963). The part of the edge surface at which the tetrahedral sheet is broken causes silica surfaces to be exposed. Silica surfaces normally have a negative double layer under most conditions. However, in the presence of small amounts of aluminum ions in suspension, the charge can become positive. Previous studies (van Olphen, 1963) have shown that it is possible that the tetrahedrally coordinated silica sheets can be preferentially broken at sites where aluminum ions have replaced silicon, resulting in a surface being exposed which is comparable with an alumina surface, rather than a silica surface. Therefore in summary, even though the net electric charge of the clay particle is always negative, the effect of the edge double layer cannot be neglected.

2.7 Gel Formation

As mentioned earlier in reference to this research, a gel is defined as a dispersion of colloidal clay particles that form a solid skeletal network enclosing a continuous liquid phase. As well, the gel is established by some type of equilibrium between the attractive force and repulsive forces. The particles are linked together in branched chains that fill the whole volume of the sol. The continuity of the solid structure increases the viscosity of the sol and gives elasticity to the gel. The gel also exhibits thixotropic behaviour; the phenomenon observed when the gel, having been destroyed by shaking or stirring, reappears when the disturbing influence is removed.

The gelation process can be pictured as a series of basic steps. First, clusters are formed by aggregation of the colloidal clay particles. Eventually, these clusters begin to collide with each other, causing links to be formed between the clusters. Eventually a single giant cluster, called a spanning cluster, is created. At this point, the suspension is considered to be completely gelled. The last link, leading to the formation of the overall spanning cluster, is no different from the initial links that were formed, with the exception that the last link is the one responsible for completion of the continuous solid network. The giant spanning cluster reaches across the entire vessel that contains it, so the sol does not pour when the vessel is tipped (Brinker and Scherer, 1990). Also, at the moment the gel forms, many clusters are still present in the sol phase, entangled in but not attached to the spanning cluster; with time, they progressively become connected to the network causing an increase in the stiffness (viscosity) of the gel.

2.8 Modes of Particle Association

To understand the interactions between the clay particles in the gelation process, it is necessary to determine how the particles associate with each other. Particle associations can occur in three different modes: face-to-face; edge-to-face; and edge-to-edge. The electrical interaction energy for the three modes is governed by three different combinations of the two double layers (unit layer and edge) (van Olphen, 1963). The various modes of particle association are shown schematically in Figure 2.5.

The type of structures formed in clay suspensions depends upon the mode of particle association. A face-to-face association can produce a thick, dense, and very compact stacked structure. Conversely, if the clay particles are joined edge-to-face, a three-dimensional, card-house structure is formed, resulting in voluminous aggregates and, at relatively high solids concentrations, in gels (having the ability to hold large amounts of water). Edge-to-edge association can produce ribbons or lamellae which

eventually interact, also resulting in the formation of a voluminous three-dimensional structure.

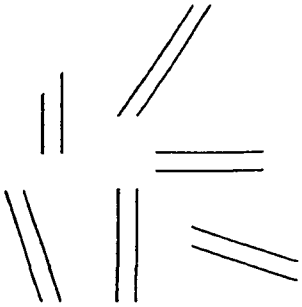

Face-to-Face

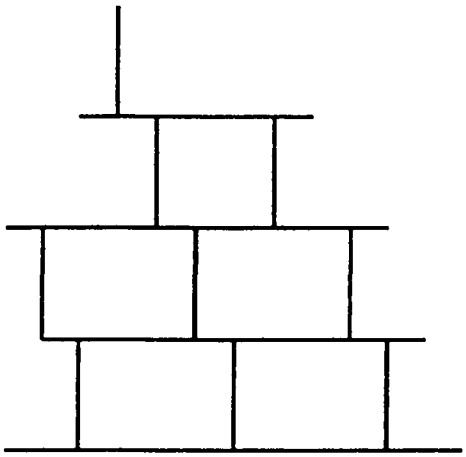

Edge-to-Face
(Card House)

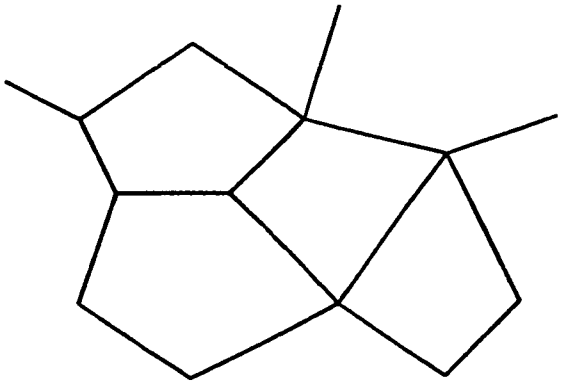

Edge-to-Edge

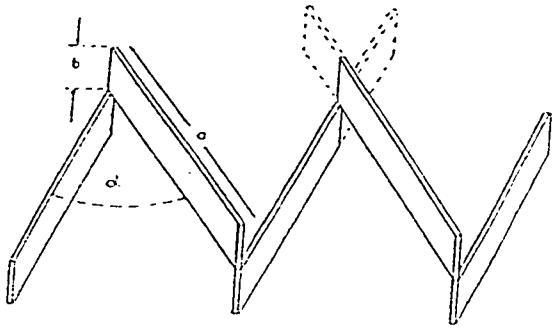

Ribbon-like

Figure 2.5: Various Modes of Particle Association

2.9 Coagulation

By definition, coagulation is the process whereby colloidal particles in suspension collapse on one another. This results in a dense sediment (coagulum) settling out and allows a clear, particle-free supernatant liquid to be released. However, coagulation will only occur if the surface charge of the colloidal particles is reduced or the effect of this charge is overcome. According to the DLVO theory, the

effect of the surface charge can be overcome by: 1) the addition of ions, which will be taken up by or will react with the colloidal clay particle (the addition of strong acids or bases to change pH); or 2) the addition of electrolytes (counter-ions) which will reduce the double layer thickness. The effectiveness of a counter-ion in reducing the double layer is strongly dependent on the valency of the ion. This effect was first observed by Schulze in 1882 and in 1890 he formulated the Schulze-Hardy rule (van Olphen, 1963). It states that the coagulative power of a salt is determined by the valency of one of its ions. This ruling ion is either the negative or the positive ion, according to whether the net charge of the colloidal particles is negative or positive. The coagulating ion is always of the opposite electrical sign to the particle. Therefore, the higher the valency of ions of opposite charge, the greater their coagulating power, and consequently, the lower the concentration needed to induce coagulation.

2.10 Nuclear Magnetic Resonance Theory

In general, nuclear magnetic resonance (NMR) uses the nucleus of certain atoms as a probe to measure the electronic distribution in its vicinity. The nuclei of certain atoms have a spin (magnetic moment) and this causes the nuclei to behave like tiny bar magnets. When a magnetic field is applied, some will line up with the magnetic field and some will line up against it. So, in order to go from one orientation to another, it is necessary to supply electromagnetic radiation of energy and frequency that corresponds to this difference in orientation. The frequency depends on the strength of the magnetic field. When suitable nuclei are placed in the magnetic field, the radiation frequency is kept constant and the strength of the magnetic field is varied, until at a certain value of the field strength the energy required to change the orientation matches the energy of radiation and, at this point, absorption occurs. At this value, a signal will be observed. A NMR spectrum will show a signal for each kind of proton in a molecule.

Chapter 3

Methodology

3.1 Overview of Experimental Methods

At the onset of this research project, there were preliminary indications that oil sand sludge consisted of colloidal clay particles which could be responsible for structure formation within the sludge. Therefore, the first requirement of this research was to develop a separation scheme which would effectively segregate the colloidal clay particles from the bulk of the sludge. The preliminary phase of the separation scheme divided the sludge into four distinct layers; one of which contained the colloidal clay particles. The other three layers were also studied to determine their role in the structure formation process. The following steps of the separation scheme involved further division of the colloidal layer by particle size. Three sub-fractions, having distinct particle sizes, were discovered.

Next, the sub-fractions were analyzed using a variety of techniques. It was determined that the sub-fractions were mainly composed of crystalline kaolinite and mica. However, significant amounts of poorly-crystalline inorganic components and strongly bound organic matter were also detected. The effect of the different sub-fractions, the poorly-crystalline inorganic components, the strongly bound organic

matter, and coarse solids, on the structure formation process in oil sand sludge, was monitored quantitatively by deuterium nuclear magnetic resonance.

Concurrently, it was determined that the aqueous media of the sludge solids consisted of a relatively high concentration of electrolytes. The final set of experiments studied the effect of a decrease and increase in electrolyte concentration on the structure formation process.

3.2 Deuterium Nuclear Magnetic Resonance

The deuterium nuclear magnetic resonance (^{2}H NMR) technique was used extensively to study the structure formation process of the colloidal clay particles. The following section is a brief description of this effective and accurate technique.

Over the last ten years, nuclear magnetic resonance (NMR) techniques have shown considerable promise in understanding clay-water interactions at a molecular level (Ripmeester et al., 1992). The NMR technique was first used after the discovery of thixotropic gels from a suspension of ultrafine ($< 0.4\ \mu$m) clay particles. The fact that NMR could be applied to these clay particles indicated that the particles were anisotropic, charged, and were not associated with any paramagnetic species. This led to the decision to use the ^{2}H NMR technique to study the interactions between the water and colloidal clay particle surfaces, with the ultrafine clay particles originating from Syncrude and Suncor oil sand sludge.

Earlier ^{2}H NMR work (Woessner and Snowden, 1969) concentrated on clay-water systems with relatively high solids content. Recent studies (Grandjean and Laszlo, 1990) have shown that the NMR technique is also sensitive enough to study relatively dilute systems ($\leq$ 1.0 wt%). This sensitivity is due to the fact that, upon application of the NMR magnetic field, parallel stacks (tactoids) of the charged clay platelets orient themselves collectively with respect to the magnetic field and, in turn,

orient the water molecules which are closest to the clay surfaces. These water molecules move rapidly back and forth between the bulk water in the suspension and the charged clay surface. This forces the rotating dipole of the water molecule to align its positively charged end towards the negatively charged clay platelet (Grandjean and Laszlo, 1989). This ordering of the dipole can be monitored by measuring the quadrupolar splittings of the deuterium nuclear magnetic resonance signal for deuterons in water molecules (Wong and Hakala, 1985 and Hakala and Wong, 1986). The quadrupolar splittings, however, can only be detected if the water molecules reside in an anisotropic environment. Because the water molecules move very quickly between the surface of the clay particles and the bulk water, the residual splitting is directly proportional to the mole fraction of the oriented water at the periphery of the particles (Grandjean and Laszlo, 1989).

Chapter 4

Properties of Materials

4.1 Oil Sand Sludge

The sludge samples, representative of the oil sand sludge present in the tailings ponds, were supplied by Suncor Research Ltd. The sludge samples were retrieved from the Suncor tailings ponds using a barge with a winch and were collected in a weighted steel cylinder (approximately 15 cm diameter x 45 cm height). The sampler was washed thoroughly with water and diesel oil to remove residual sludge and bitumen, and the sampler interior was sterilized by rinsing with diluted commercial bleach. To ensure that anaerobic conditions were maintained, a pressure-regulated pinch valve was attached to a gas line which provided oxygen-free nitrogen. The sampler was lowered into the tailings pond to a pre-determined depth using a cable calibrated in feet. Sludge entered the cylinder when the outer pressure exerted by the sludge equalled or overcame the inner pressure exerted by the nitrogen gas. After collection, the sampler was winched back and washed free of excess sludge and bitumen clinging to the outside.

4.2 Pond Water

The Suncor pond water was supplied by Energy, Mines, and Resources Canada. An elemental analysis is shown in Table 5.1. The pH of the pond water

was approximately 8.4.

4.3 Chemicals

- Deuterium oxide was supplied by MSD Isotopes, a division of Merck Frosst Canada Inc. It had a minimum isotopic purity of 99.9 atom% D.

- Toluene was supplied by BDH Inc.

- Tiron, 4,5-dihydroxy-1,3-benzene-disulfonic acid (disodium salt), $C_6H_4Na_2O_8S_2$ (Sigma No. D-7389) was supplied by the Sigma Chemical Co.

- Aluminum chloride ($AlCl_3$), sodium chloride (NaCl), and calcium chloride ($CaCl_2$) were supplied by Anachemia Co. of Montreal, Quebec.

Chapter 5

Experimental Aspects

5.1 Sample Preparation

5.1.1 Preliminary Sludge Fractionation

At the onset of this research project, there were preliminary indications that oil sand sludge contained ultrafine ($<0.4\ \mu m$) clay particles which could be responsible for the structure formation within the sludge. During a series of precursory sludge fractionation studies, it was discovered that the sludge did indeed consist of gel forming components of colloidal size which also exhibited the property of thixotropy. This thixotropic property was successfully utilized to separate the gel forming ultrafine clay particles from the bulk of the sludge to study them more closely. Mechanical agitation of the sludge samples was applied to break the loose three-dimensional gel network, thereby allowing other entrapped components to be released (ie. coarse solids, bitumen). However, if the settling rate of the coarse solids was slower than the time required to reform the gel network, the sludge structure would reform visually unchanged. Using this new information as a basis, the following fractionation procedure was developed to prepare the sludge samples for thorough analysis.

The oil sand sludge was agitated for 15 minutes using a high intensity Spex mixer (Spex Industries, Scotch Plains, N.J.) and then centrifuged (IEC Centrifuges,

Model CRU-5000) at 200 g (where "g" is acceleration due to gravity) for 10 minutes. This treatment scheme caused the sludge sample to separate into four distinct layers. From bottom to top they were:

1) a light coloured sediment containing residual coarse solids (RS);

2) a dark layer of organic rich solids (ORS);

3) an aqueous colloidal suspension layer (fraction containing the gel forming constituents); and

4) a bitumen layer (B) containing some associated solids (BS).

The preliminary separation scheme is shown in Figure 5.1.

A portion of each fraction was dried and the carbon content of each was determined using a LECO CR12 carbon analyzer (all bitumen was removed prior to analysis). The insoluble carbon content (IOCC) was obtained by subtracting the carbonate carbon from the total carbon. The carbonate carbon content was analyzed titrimetrically after acid digestion using a Carbon Dioxide Coulometer Model 5011. This analysis was performed by the Measurement Sciences Division of NRC.

5.1.2 Colloidal Suspension Layer Sub-Fractionation

Following the preliminary separation scheme, the aqueous colloidal suspension layer was separated according to particle size. To achieve this separation, the layer was centrifuged into four sub-fractions. The entire layer was centrifuged at 200 g for one hour. The solids that did not settle under these conditions were centrifuged for a further two hours at 500 g. Again, any solids that did not settle at 500 g were subjected to centrifugation at 1500 g for two hours. Finally, any remaining solids not settled out were ultra-centrifuged (Sorvall Ultra-Centrifuges by Du Pont, Model OTD 65B) at 91500 g for 30 minutes[1].

---

[1] Initially, the forces of 200 g, 500 g and 1500 g were based on the operating conditions of the centrifuge: 200 g (~1000 rpm) is the lowest force that can be applied by the centrifuge for extended periods of time; 1500 g (~3000 rpm) is the highest force achievable by the centrifuge; and 500 g (~2000 rpm) was chosen as an

At this point, the four sub-fractions were still in a highly flocculated form owing to the presence of naturally occurring electrolytes in the pond water. To effectively separate the sub-fractions according to particle size, pond water was exchanged for distilled water. Distilled water was added to the solids separated into the four sub-fractions and they were mechanically agitated for 15 minutes. Following this treatment, each sub-fraction was ultra-centrifuged at 91500 g for 30 minutes. The released water was discarded and additional distilled water was added to the sedimented portion. After repeating this procedure three times, most of the natural electrolytes were washed out of the samples, thereby leaving the ultrafine particles in a less-flocculated form.

Following the last washing, additional distilled water was added to each sub-fraction and they were again mechanically agitated for 15 minutes. The above centrifugation process was repeated. Each suspension in distilled water was separated into four sub-fractions by sequential centrifugation at the indicated increasing forces (200 g, 500 g, 1500 g, and 91500 g). All of the solids which settled at 200 g were combined, all of the solids which settled at 500 g were combined, all which settled at 1500 g, and all which settled at 91500 g were combined. These sub-fractions were designated A-200, A-500, A-1500, and A-91500, respectively. Figure 5.2 (Parts 1 and 2) shows the colloidal layer separation scheme.

Finally, pond water was substituted for the distilled water so the particles would be in an aqueous media identical to that of the tailings pond. As with the distilled water washing procedure, the samples were diluted with pond water, mechanically agitated for 15 minutes and ultra-centrifuged at 91500 g for 30 minutes. This was repeated three times. An elemental analysis of the different wash waters

---

intermediate force. After two hours at 1500 g, a small fraction of the solids were unsettled so the ultra-centrifuge had to be used. 91500 g is the centrifugal force at which all of the colloidal solids in an aqueous media of pond water will settle.

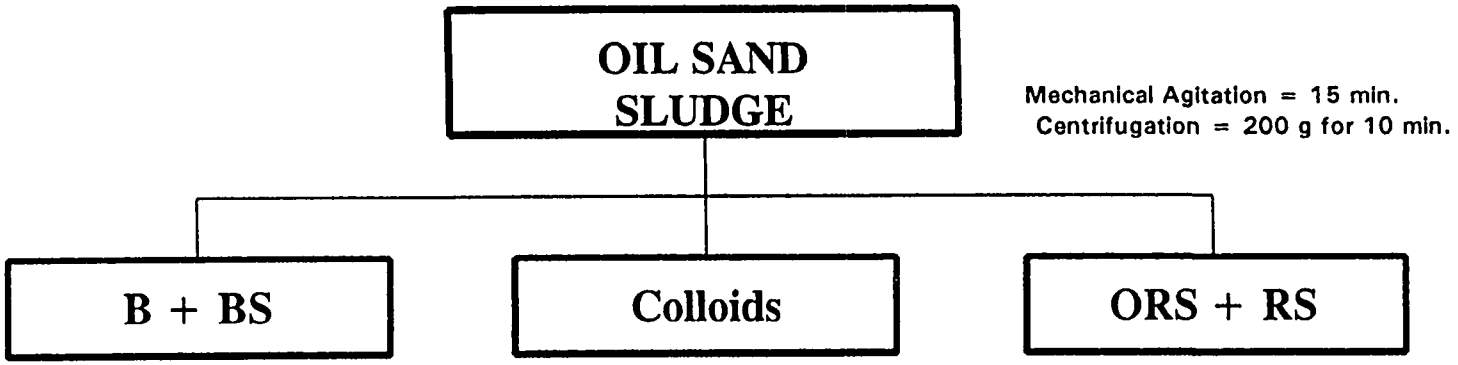

Figure 5.1:Preliminary Sludge Fractionation Scheme

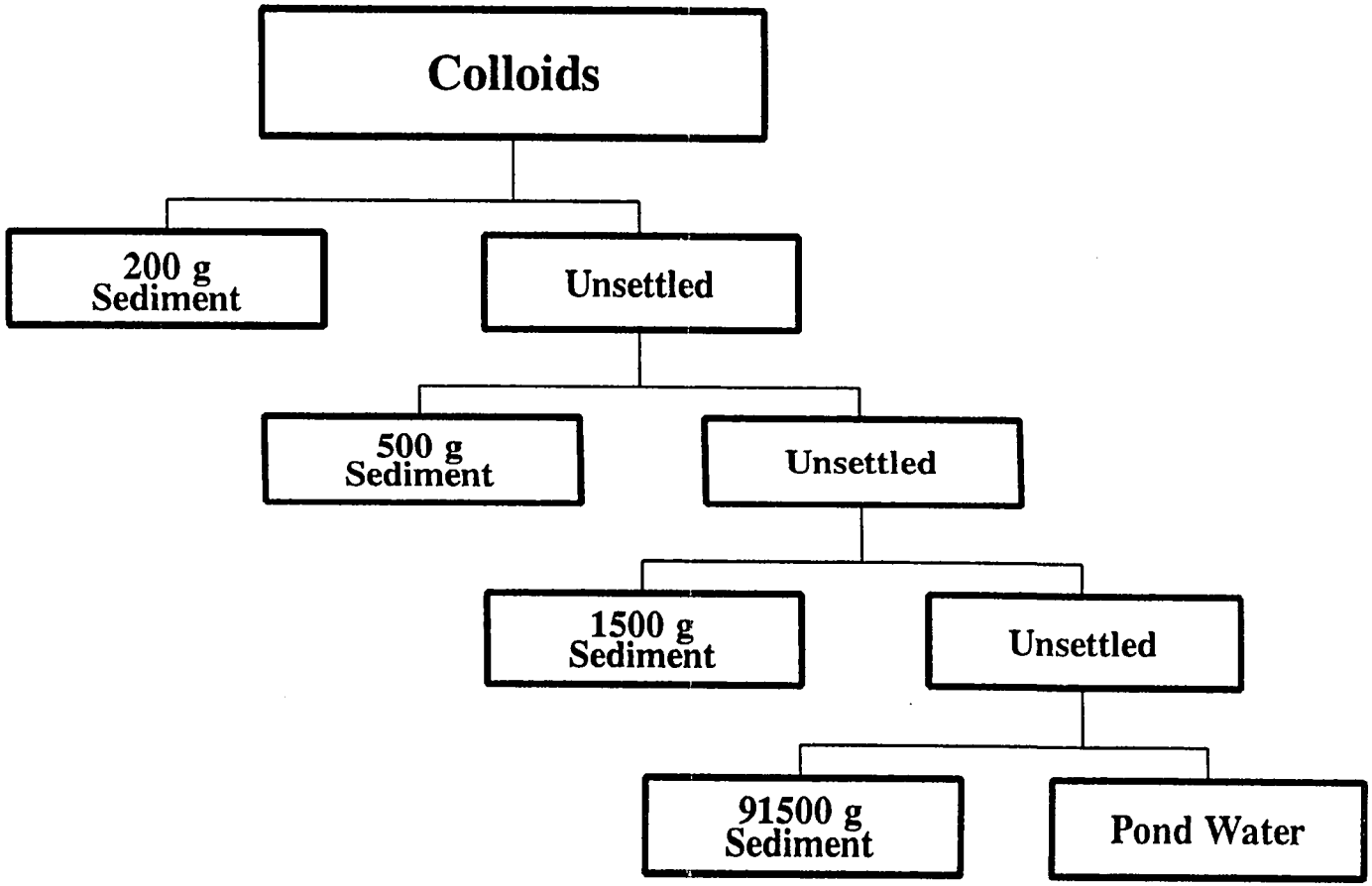

Figure 5.2: Colloidal Layer Separation Scheme (Part One)

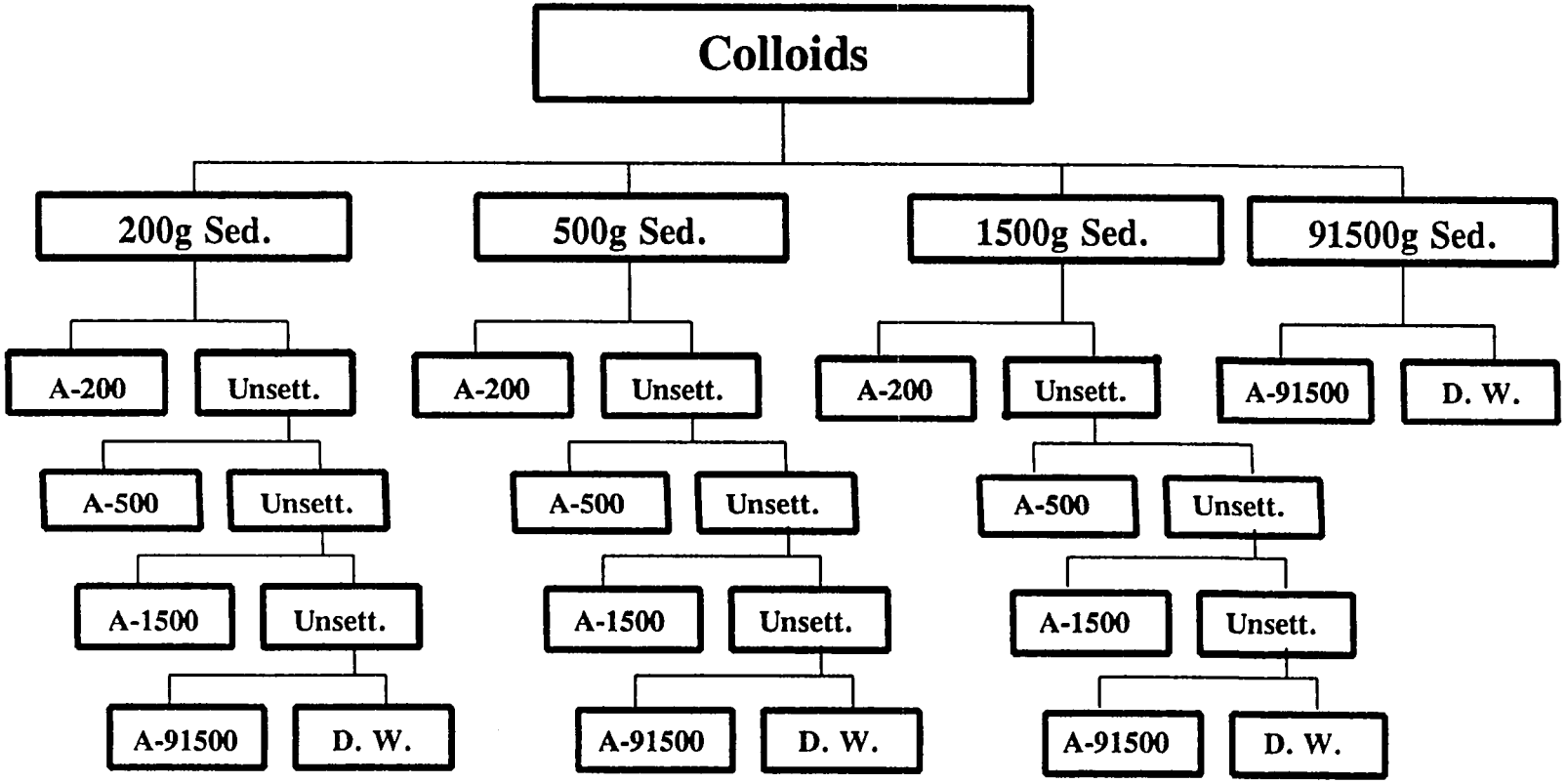

Figure 5.2: Colloidal Layer Separation Scheme (Part Two)

was conducted using X-ray florescence to ensure that the final aqueous media of the particles was identical to that of the pond water. The results presented in Table 5.1 show that the washing procedure is, indeed, reversible and satisfactory, as the elemental analysis of the final wash is almost identical to that of the pond water.

The morphology of each sub-fraction was examined by transmission electron microscopy (TEM). For the TEM examination, a drop of the suspended sample, after sonification for 1 minute, was deposited on a carbon coated copper grid. After 1 minute, the liquid was blotted to leave only a thin layer which was then allowed to dry. The grid was then examined with a Carl Zeiss transmission electron microscope Model 902, operated at 80 kV. These TEM examinations were performed by the Environmental Protection Sciences Division of NRC.

Table 5.1: Elemental Analysis of Wash Waters, ppm.

Water	Na	Mg	Ca	Al	Si	B
Suncor	430	**7.0**	**5.4**	**4.7**	**12.0**	**4.1**
Dist. Water 1st Wash	410	5.8	9.5	1.2	2.8	4.2
2nd Wash	72	0.4	1.1	0.7	1.5	1.3
3rd Wash	48	0.3	1.1	0.5	2.3	1.1
Pond Water 1st Wash	260	4.5	7.2	1.9	2.2	1.4
2nd Wash	350	5.1	8.3	1.6	2.0	2.1
3rd Wash	**420**	**5.6**	**9.6**	**2.6**	**3.0**	**2.9**

5.2 Procedure to Study the Effect of Particle Size on the Gelation Process

The colloidal sub-fractions were studied using ^2H NMR. Concurrently, the ^2H NMR technique was able to quantitatively monitor the effect of particle size on the sol to gel transformation (aggregation process) that occurs in oil sand sludge. Suspensions of different concentrations were prepared from each concentrated sub-fraction using pond water. Approximately 0.83 wt% D_2O was added to each diluted sample (25 mg of D_2O was added to 3.0 g of sample).

Next, the ^2H NMR spectra were recorded on either a Bruker MSL-300 NMR spectrometer (magnetic field of 7.1 T) at a frequency of 46.07 MHz or a Bruker AM-400 NMR spectrometer (magnetic field of 9.4 T) at a frequency of 61.4 MHz. In this experiment, 8 transients were acquired in 16K points, with a spectral width of 1000 Hz. Before the initial NMR spectrum was recorded, each sample was vigorously shaken by hand then immediately inserted into the magnetic field. The time of this measurement was designated as "Zero Time" and the maximum attainable splitting, D_o, was observed. Following this, the sample was removed from the magnetic field and then reinserted after 30 min, 1 hr, 4 hr, 23 hr, 48 hr, 5 days, 9 days, and lastly, 14 days. The spectrum was recorded after each reinsertion.

5.3 Procedure to Verify Effectiveness of Separation Scheme and Applicability of ^2H NMR Technique

To verify that the colloidal layer separation scheme was not altering the ultrafine clay particles in any way, and that the ^2H NMR technique was sensitive enough to accurately monitor the sol to gel transformation process, a comparison study was performed.

The aqueous colloidal suspension layer was separated out from the bulk of the sludge and further fractionated using the rigorous separation scheme described in

Section 5.1. Following this, the four sub-fractions (A-200, A-500, A-1500, and A-91500) were recombined in the same ratio in which they were present in the original aqueous colloidal suspension layer and suspensions of different concentrations were prepared using pond water.

The sol to gel transformation of the recombined aqueous colloidal suspension layer was studied using ^{2}H NMR as a probe over a period of two weeks. The same procedure as described in Section 5.2 was followed.

Concurrently, the sol to gel transformation process of an original (untreated) aqueous colloidal suspension layer was studied. Dilutions were prepared from the concentrated original fraction and the same procedure as described above was followed. The results of the two studies were compared to determine how the rigorous separation scheme had affected the sub-fractions, as well as the accuracy of the ^{2}H NMR technique.

5.4 Procedure to Study the Mutual Effect of the Gel Forming Colloidal Solids on Gel Forming Propensity

During the sol to gel transformation, a variety of mechanisms and interactions influence the gel forming ultrafine clay particles. Section 5.2 examined the sol to gel transformation of the individual sub-fractions. These studies showed that the A-200 sub-fraction is of colloidal size, but does not contribute to the gel forming propensity of oil sand sludge. As well, further examination of the A-1500 sub-fraction showed that it is not a distinct sub-fraction, but actually a flocculated mixture of A-500 and A-91500 particles (42 wt% and 58 wt%, respectively). These studies concluded that A-500 was a relatively weak gel former and that A-91500 was a strong gel former. From these results, it can be concluded that gel formation in oil sand sludge is primarily caused by the A-500 and A-91500 sub-fractions. Results from the total sludge mass balance show that these two sub-fractions constitute only 8.1 wt% of the

sludge solids. Because of this, the presence of any additional interactions between A-500 and A-91500 was investigated by observing the sol to gel transformation of A-500/A-91500 mixtures. It was hypothesized that gel formation by A-500 and A-91500 was promoted by synergistic interactions. Therefore, to determine whether gel formation is a synergistic, antagonistic, or simply an additive property, the following experimental procedure was developed.

Three mixtures of the A-500 and A-91500 sub-fractions were prepared:

1) 25 wt% A-500 and 75 wt% A-91500;
2) 50 wt% A-500 and 50 wt% A-91500; and
3) 75 wt% A-500 and 25 wt% A-91500.

A series of concentrations were prepared from each mixture using pond water. Approximately 0.83 wt% D_2O was added to each diluted sample. The sol to gel transformation was studied for each sample using ^2H NMR as a probe over a period of two weeks. The same procedure as described in Section 5.2 was followed.

5.5 Procedure to Determine the Effect of Coarse Particles on Gel Formation

It has been shown that there are gel forming particles present in oil sand sludge. However, in actual sludge the gel forming particles do not exist alone but in the presence of coarse solids. Therefore, to study the effect of coarse solids on the sol to gel transformation, mixtures of A-500, A-91500, and A-(500/91500) with A-200 were prepared. (The A-(500/91500) sub-fraction was a mixture of A-500 and A-91500 in the exact ratio in which they occur in the original oil sand sludge.) The mixtures prepared were:

1) 25 wt% A-200 with 75 wt% A-500;
2) 50 wt% A-200 with 50 wt% A-500;
3) 75 wt% A-200 with 25 wt% A-500;
4) 25 wt% A-200 with 75 wt% A-91500;

5) 50 wt% A-200 with 50 wt% A-91500;

6) 75 wt% A-200 with 25 wt% A-91500;

7) 25 wt% A-200 with 75 wt% A-(500/91500);

8) 50 wt% A-200 with 50 wt% A-(500/91500); and

9) 75 wt% A-200 with 25 wt% A-(500/91500).

A series of concentrations, using pond water, were prepared from each mixture. Approximately 0.83 wt% D_2O was added to each diluted sample. The sol to gel transformation was then studied using ^2H NMR as a probe over a period of two weeks. The same procedure as described in Section 5.2 was followed.

5.6 Procedure to Determine the Effect of Poorly-Crystalline Components on Gel Forming Propensity

The XRD examination performed on the colloidal clay sub-fractions showed that the degree of molecular disorder (poorly-crystalline character) increased with a decrease in particle size. In addition, the results from Section 5.2, where the effect of particle size on gel formation was studied, showed that gel forming propensity also increased with a decrease in particle size. It was then deduced that the poorly crystalline components may be a major influence on the gel forming propensity of the sludge.

To study the effect of poorly-crystalline components on gel forming propensity, the Tiron Dissolution Method, originally developed by Biermans and Baert (1977), was used to remove the poorly-crystalline components from the gel forming ultrafine solids. In this investigation, a modification of the original procedure (developed by Kodama and Ross (1991)) was used. The method was as follows: 31.42g of Tiron was dissolved in 800 ml of distilled water in a plastic beaker. The resulting solution was clear yellow in colour and had a pH of 4.5. A Na_2CO_3 solution was prepared by dissolving 5.3g anhydrous Na_2CO_3 in 100 ml of

distilled water. This was stirred into the Tiron solution, raising the pH to 7.4 and causing the solution to turn green in colour. Finally, 4M NaOH was added to the Tiron solution until the pH was raised to 10.5.

The extraction procedure proposed by Kodama and Ross utilized 25 mg of dry specimen with 30 ml of Tiron solution (larger samples may be used in the same solid to solution ratio). As drying the colloidal clay sub-fractions would alter their properties, wet specimens were used, ensuring that the same solids to solution ratio was maintained.

The sub-fraction used for the extraction procedure was A-91500. The sub-fraction and Tiron solution were placed in a 150 ml Corex glass bottle. Corex glass has four to six times the strength of conventional glass and has excellent chemical resistance and durability. Corex can also withstand very strong acids and bases. By utilizing this type of bottle, we were ensured that no contamination of the sample from the glass container would occur during the extraction process.

The bottle was placed in a constant temperature bath at 80 °C for one hour. During the extraction process, the bottle was occasionally shaken by hand. After the one hour extraction process, the bottle was cooled in an ice bath. Once cooled, the bottle was shaken and the contents were centrifuged at 91500 g for 30 minutes. To ensure that all of the solids settled at this speed, the supernatant (containing the extracted, poorly-crystalline inorganic components) was separated from the sediment and the supernatant was centrifuged once again at the maximum force achievable with the ultra-centrifuge (300,000 g) for 30 minutes. As no additional sediment settled, 91500 g was deemed sufficient to achieve complete solids separation.

To study the effect of poorly-crystalline components on the sol to gel transformation, ^{2}H NMR was used. However, before the treated sediment could be studied, it was necessary to wash the sample free of Tiron solution with distilled

water. The sample was diluted with distilled water, mechanically agitated for 15 minutes, then ultra-centrifuged to settle the solids. This procedure was repeated until the pH was lowered to that of distilled water. At this point, the distilled water was replaced with pond water. Finally, the sol to gel transformation of the treated A-91500 sub-fraction was monitored using ^2H NMR. The procedure described in Section 5.2 was followed.

5.7 Procedure to Study the Effect of Surface Active Solids

Previous studies (Section 5.1) of the ultrafine clay sub-fractions identified the presence of a substantial amount of strongly bound organic matter, capable of imparting intermediate wettability characteristics to clay particle surfaces. Clay particles, contaminated with highly hydrophobic organics, may also be capable of forming structures through an immiscible phase wetting mechanism (Kotlyar et al., 1991). To identify the properties of these solids and to determine their role in the gelation process, the following experimental procedure was conducted.

Based on wettability, the A-500 and A-91500 sub-fractions were separated into hydrophilic solids (aqueous solids, AS) and surface active solids (SAS). From A-500, the sub-fractions were designated AS-500 and SAS-500, and from A-91500, the sub-fractions were designated AS-91500 and SAS-91500.

To perform this separation, toluene and pond water (1:10 ratio by weight) were added to each sub-fraction and the mixture was mechanically agitated for 5 minutes. This allowed the SAS to be emulsified with the toluene. The SAS could then be removed from the AS using mild centrifugation at 200 g for 10 minutes. This centrifugation forced the SAS to float on top of the AS and the SAS could easily be skimmed off with a metal spatula.

The AS-500 and AS-91500 samples were prepared for thorough analysis by

first washing out any traces of toluene. The AS solids were separated from the dispersion using ultra-centrifugation. The contaminated pond water was substituted for distilled water and the mixture was mechanically agitated for 15 minutes. This procedure was repeated three times. After the third washing the distilled water was substituted for pond water and the procedure was, once again, repeated three times.

The carbon content of the AS and SAS solid fractions was determined using a LECO CR12 carbon analyzer. The insoluble organic carbon content (IOCC) was obtained by subtracting the carbonate carbon from the total carbon. The carbonate carbon content was analyzed titrimetrically using a Carbon Dioxide Coulometer Model 5011 after acid digestion. The metals content was analyzed semi-quantitatively using DC arc emission spectrometry. This analysis was performed by the Measurement Sciences Division of NRC.

X-ray diffraction (XRD) analysis was performed on powder specimens of the AS and SAS samples to determine the main mineral composition and to detect any smectite minerals which may be present. A procedure called random mounting was used for mineral (crystalline) composition analysis. For the procedure, approximately 100 - 250 mg of air dried sample was gently packed in a Plexiglass sample holder. For detection of smectite mineral, a procedure called preferred orientation was used. For this, 30 mg of air dried sample was suspended in 1 ml of 2% aqueous glycerol solution, pipetted onto a glass slide (30 mm x 25 mm) and allowed to air dry. The two types of samples were then analyzed using a Scintag PAD II diffractometer with Co radiation and a graphite monochromator. Mineral composition of the samples was determined quantitatively by comparing their XRD peak intensities with those of standards. This analysis was performed by Land Resources Research Institute.

The morphology of the clay particles was investigated by transmission electron microscopy (TEM). For the TEM observations, the same procedure as described in Section 5.1.2 was followed.

X-ray photoelectron spectroscopy (XPS) analyses were also made. For these measurements, drops of each SAS and AS suspension were spread over a clean glass slide and allowed to air dry. The dried solids were then scraped off the glass with a razor blade and pressed onto a piece of Indium foil. The XPS spectra were recorded using a PHI 5500 Instrument (PHI Electronics, Minn., USA) using Al Kα source of x-rays. The pressure inside the instrument during analysis was always below $8x10^{-9}$ torr. An electron flood gun was used to neutralize the charge present at the surface of the sample, during the recording of the spectrum. High resolution spectra were obtained at a pass energy of 29.6 eV while survey spectra were recorded at a pass energy of 156 eV. Several repetitions were made to ensure accuracy of the results. From these spectra, the atomic fraction of the element, i, was calculated using the formula:

$$C_i = (I_i/S_i)/\Sigma(I_i/S_i)$$

where I_i is the area under a spectral peak and S_i is the sensitivity factor. Values of 0.296, 0.711, 0.262, 0.870, 0.213, and 1.791 were used as the sensitivity factors for C1s, O1s, Ki2p, K2p, Al2s, and Fe2p3, respectively. This XPS analysis was conducted by the Environmental Protection Sciences Division of NRC.

Finally, the sol to gel transformation of AS-500 and AS-91500 was monitored using ^2H NMR[2]. A series of concentrations, using pond water, was prepared from each AS sub-fraction and approximately 0.83 wt% of D_2O was added to each sample. The same procedure as described in Section 5.2 was followed.

5.8 Procedure to Study the Effect of Water Chemistry

Knowledge accumulated thus far has allowed us to conclude that ultrafine clay particles, capable of forming a highly porous, three-dimensional gel network, are the

---

[2] The SAS-500 and SAS-91500 sub-fractions could not be studied by NMR due to their final state after the emulsification process. The process forced the SAS ultrafine clay particles to form complex aggregates that could not be redispersed.

main components responsible for structure formation in oil sand sludge. Also, it has been observed that the gel forming propensity of ultrafine clay particles is increased by the presence of a substantial amount of strongly bound organic matter, which is capable of imparting intermediate wettability characteristics to the clay particle surfaces. However, as the ultrafine clay particles, with the strongly bound organic matter, are an integral part of oil sand sludge and cannot be avoided, it was hypothesized that sludge structure formation may be prevented by changing the water chemistry.

The electrolyte concentration of the tailings pond water is relatively high, as was shown in Table 5.1. At this concentration, the electrostatic double layer of the clay particles has been reduced enough to cause gelation, but not to such an extent to cause coagulation. The following experiments were developed to understand the effect of water chemistry on the behaviour of the ultrafine clay particles.

5.8.1 Sol to Gel Transformation in Distilled Water

The aqueous media of the ultrafine clay particles (pond water) was replaced with distilled water. The natural electrolytes were washed out of the A-500 and A-91500 sub-fractions by diluting each sub-fraction with distilled water by a factor of 10. They were then mechanically agitated for 15 minutes and the particles were separated from the water phase using ultra-centrifugation. This process was repeated three times.

A series of concentrations were prepared from the concentrated A-500 and A-91500 sub-fractions, using distilled water. The effect of reduced electrolyte concentration on the gelation process was studied by following the sol to gel transformation using ^{2}H NMR. The same procedure as described in Section 5.2 was followed.

5.8.2 Gel to Coagulum Transformation of A-91500

Results from the above distilled water study proved that proper water chemistry is essential for gel formation. In distilled water, the sol to gel transformation was significantly reduced. As a result, it was hypothesized that an increase in electrolyte concentration (over that of pond water) should force coagulation to occur. The coagulation process would cause the particles to come together and settle as a dense, close-packed sediment, releasing a large fraction of the entrapped water.

Application of an electrolyte at an optimal concentration, which would force a gel to coagulum transformation, could be an effective method to destabilize (remediate) oil sand sludge. The purpose of the next set of experiments was to study a variety of electrolytes and their effect on sludge stability.

A gel to coagulum transformation study was initiated by determining the effect of three electrolytes on the sedimentation behaviour of a relatively well defined component; the A-91500 sub-fraction was chosen. The electrolytes selected were: NaCl, $CaCl_2$, and $AlCl_3$. The electrolyte solutions, each having an ionic strength of 0.6 eq/L, were added to the concentrated A-91500 sub-fraction until the final concentration was 2.0 wt%. After preparation, the samples were sealed with plastic film to prevent water evaporation and manually shaken to distribute the electrolyte solution uniformly throughout the suspension. The sedimentation rate was recorded over a period of two weeks.

Finally, the role of the cation on the gel to coagulum transformation was investigated. According to the Schulze-Hardy rule, the valency of the cation should have a significant effect on the coagulation process of the negatively charged clay particles.

Chapter 6

Results and Discussion

6.1 Attributes of Sludge Fractions

The composition of the oil sand sludge, as determined by the classical technique using Soxhlet extractors with Dean and Stark separators, (Syncrude, 1979) was determined to be 31.2 wt% solids, 3.5 wt% bitumen, and 65.3 wt% water.

The thixotropic property of oil sand sludge has been effectively used to separate the colloidal clay particles from the bulk of the sludge. Applying mild centrifugation, following mechanical agitation, enhanced the settling rate of the coarse solids and allowed the sludge to be separated into four distinct layers (Figure 6.1). From bottom to top they were:

1) a light coloured sediment containing residual coarse solids (RS);
2) a dark layer of organic rich solids (ORS);
3) an aqueous colloidal suspension layer; and
4) a bitumen layer (B) containing some associated solids (BS).

The solids content, distribution, and quantity of each layer are presented in Table 6.1. The insoluble organic carbon content and iron content of the four sludge fractions (bitumen free) are shown in Table 6.2.

Figure 6.1: Separation of Oil Sand Sludge by Mechanical Agitation Followed by Centrifugation. (Sample on the left is the original.)

Table 6.1: Solids Content, Distribution, and Quantity of Each Sludge Layer.

Fraction	Wt% of Sludge	Solids Distribution by Layer, wt% (Dry Basis)	Solids Content of Each Layer wt%
B + BS	6.8	8.7	41.4
RS	31.2	70.2	62.0
ORS	8.1	7.5	52.3
Colloidal Solids	53.9	13.6	7.5

Table 6.2: Insoluble Organic Carbon (IOCC) and Iron Content of Sludge Fractions.

Fraction	IOCC, [a] %	Fe, %
B + BS	25.1	N.A.[b]
RS	0.3	1.1
ORS	14.5	13.8
Colloidal Solids	4.9	1.5

[a] IOCC was used as a measure of the amount of strongly bound organic matter (SOM).

[b] not available.

6.1.1 Residual Coarse Solids Layer

The residual coarse solids (RS) fraction is a heterogeneous mixture of coarse ($\geq$ 1 μm) water wet particles. It has a high sedimentation velocity relative to the rest of the sludge solids. The high sedimentation velocity allows the formation of a distinct separate layer consisting of clean sand, silt, and clay. These solids appear to be physically trapped in the sludge without contributing to the sludge structure.

6.1.2 Organic Rich Coarse Solids Layer

The organic rich coarse solids (ORS) fraction has a similar size to that of the RS fraction, but it concentrates in a layer above RS due to its lower sedimentation velocity. The lower sedimentation velocity of the ORS solids is due to a higher amount of strongly bound organic matter relative to the RS fraction. The strongly bound organic matter causes the ORS fraction to have a lower density and, therefore, a slower settling rate.

The bulk iron content of this fraction is very high, even though the particle surfaces have been shown to be almost devoid of iron. Most of the iron bearing minerals are present in the form of complexes with the organic matter, and occur largely as the binding agent in dense aggregates of fine quartz particles, kaolinite, and mica flakes (Kotlyar et al., 1990). The strongly bound organic matter is commonly identified with surface modifiers capable of rendering the mineral surfaces hydrophobic (Darcovich et al., 1989). This factor could account for the high ability of the ORS fraction to retain bitumen.

6.1.3 Aqueous Colloidal Suspension Layer

A very important initial observation was made from the aqueous colloidal suspension layer (A). After setting for several hours, a gelation process had commenced, causing the consistency of the fraction to resemble that of the original sludge sample. This observation led to the identification of the aqueous colloidal suspension layer as the fraction which contained the components responsible for the stability and non-settling properties of oil sand sludge.

The particles in the aqueous colloidal suspension layer are anisotropic and ultrafine, having a particle size range of 0.01 to 0.5 μm. X-ray diffraction showed that the main inorganic components present in this layer are kaolinite and mica, with smectite-type minerals present in trace amounts. The results also showed that the degree of molecular disorder (poorly-crystalline character) increased with a corresponding decrease in particle size. The iron content of these solids was shown to be relatively low.

In aqueous suspension, these clay particles of ultrafine dimensions (especially those $\leq$ 0.2 μm) behave differently than coarser solids of the same mineral. Also, experimentation has proven that submicron kaolinite is negatively charged and is capable of both sol and gel formation (Searle and Grimshaw, 1958). These factors led to further investigation into the hypothesis that the ultrafine clay particles may be

a major factor in the stability and non-settling characteristics of oil sand sludge.

6.1.4 Bitumen Layer

Inefficiencies in the Hot Water Extraction Process caused small amounts of bitumen (B), with associated hydrophobic solids (BS), to be released to the tailings pond stream. The oil wetted BS solids do not appear to participate in the sludge structure formation, but can reduce separation efficiency in the primary separation vessel by increasing the density of bitumen.

6.2 Properties of Colloidal Layer Sub-Fractions

Investigation into the gel forming properties and propensity of the aqueous colloidal suspension layer began by separating the fraction, using distilled water, to determine the amounts and distribution of different particle sizes. The colloidal suspension layer was separated into four sub-fractions which were designated A-200, A-500, A-1500, and A-91500. Figures 6.2, 6.3, and 6.4 show the distribution of particle sizes in each of the sub-fractions before the pond water was substituted for distilled water. Figure 6.5 shows the solids distribution of the sub-fractions within the colloidal layer and Figure 6.6 shows the total solids distribution of each fraction in the sludge. Additional data on the particle size distribution of each sub-fraction is given in Appendix A.

Samples of each sub-fraction underwent TEM examination. The results showed that the sub-fractions were platelets of ultrafine particles. Visual observations showed that the morphology of the majority of the particles was irregular. The average particle size of each sub-fraction was calculated from the TEM photos. When rounded off, they were determined to be:

A-200 = 500 nm;

A-500 = 200 nm;

A-1500 = 100 nm; and

Solids Distribution of A-200
(Before electrolytes were washed out)

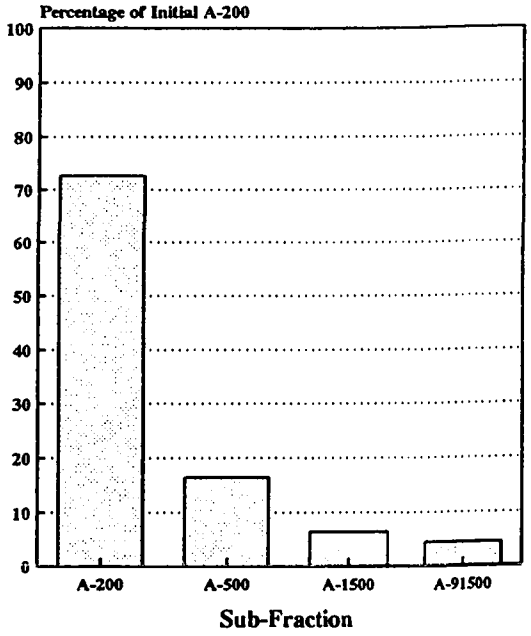

Figure 6.2

Solids Distribution of A-500
(Before electrolytes were washed out)

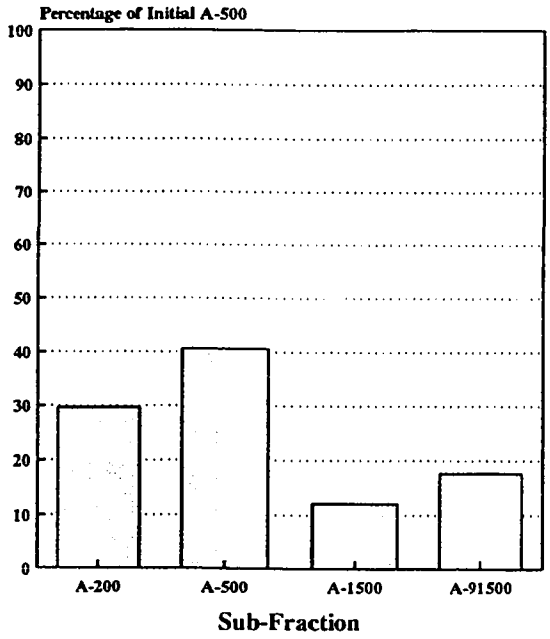

Figure 6.3

Solids Distribution of A-1500
(Before electrolytes were washed out)

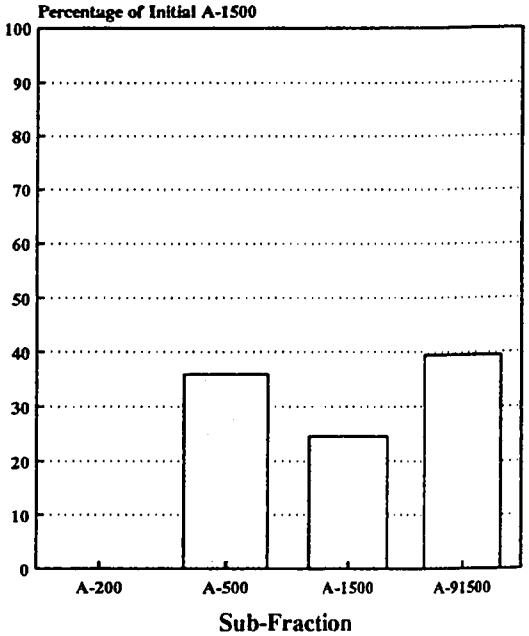

Figure 6.4

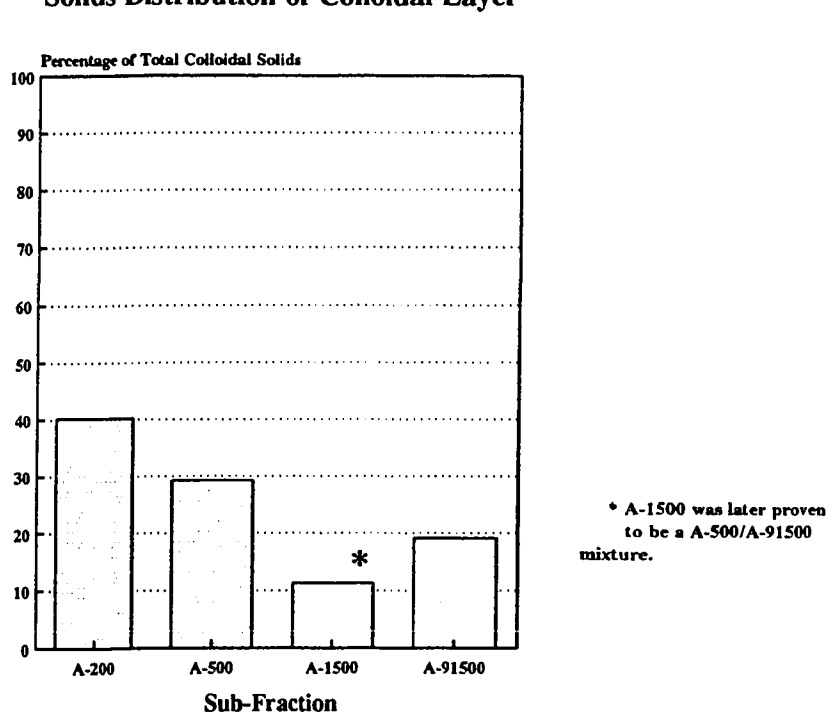

Figure 6.5: Solids Distribution of Colloidal Layer

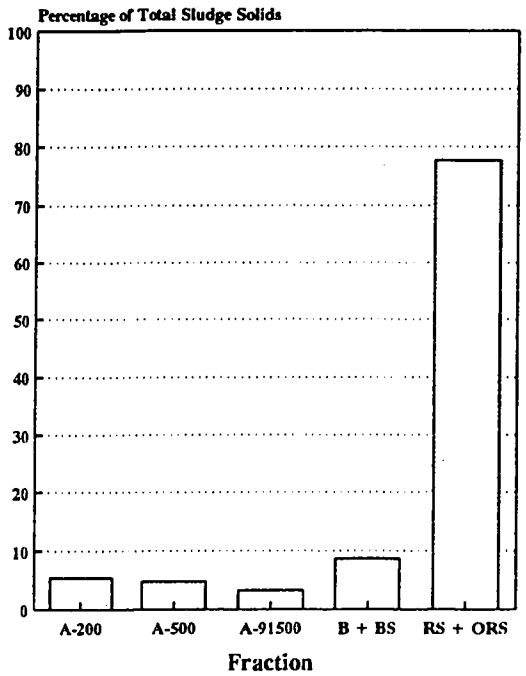

Figure 6.6: Solids Distribution of Sludge

A-91500 = 10 to 50 nm.

One interesting visual observation relating particle size and colour was made concerning the four sub-fractions. Even though the composition of all four sub-fractions was identical, their physical appearance differed significantly. The A-200 sub-fraction, having the largest particle size, was light greyish-white in colour, the A-500 sub-fraction was greyish-brown in colour, the A-1500 sub-fraction was brown in colour, and the A-91500 sub-fraction, having the smallest particle size, was almost black.

A rule concerning the relationship between particle size and colour was formulated by Ostwald (Hartman, 1934). It states that as the particle size of a substance increases, its colour will shift towards the blue end of the light spectrum. For example, a surface which is perfectly smooth and 100 percent reflecting is theoretically invisible (clear). If this surface is broken slightly, the mass will appear white as a result of light being scattered from the irregular surfaces. Upon progressive subdivision, the colour of the mass will eventually proceed to black. One common example is yellow gold. As yellow gold is progressively subdivided, its colour changes to reddish brown and eventually to black. For the A-91500 sub-fraction, it is believed that light was reflected back and forth among the broken crystal surfaces until it was completely absorbed, resulting in its black appearance.

6.3 Nuclear Magnetic Resonance Observations

The ^{2}H NMR technique was a very effective tool to obtain information on the ultrafine clay particles and the sol to gel transformation that occurs in oil sand sludge. This technique measures the residual splitting of the deuterium peak. The splitting is a result of a rapid exchange of deuterium molecules between the bulk water in the suspension and the bound water on the ultrafine clay platelet surfaces. As the gel network is gradually formed, the exchange process is inhibited resulting in a decrease

in the residual splitting. Several initial observations from the NMR results allowed many characteristics of the ultrafine clay particles to be understood:

1) The residual splitting recorded immediately after the sol was shaken was the measurement at which aggregation was absent.

2) The initial residual splitting of the sols increased with an increase in concentration (Figure 6.7).

3) As the sol to gel transformation progressed, the ultrafine clay particles lost their ability to be orientated by the magnetic field and this was reflected in a decrease in the residual splitting. The sol to gel transformation could be studied as a function of time by observing the decrease from the initial value (Figure 6.8).

4) A sol which was allowed to gel outside the magnetic field did not show a splitting signal. This indicated that the clay platelets could not be orientated by the magnetic field, as they were bound in the gel network.

5) The sol to gel transformation process was observed to be completely reversible. After the gel network was formed, it could be broken by manual agitation and the residual splitting would return to the value measured previously at zero time. Also, the gel network would be completely reformed after the same amount of time as required initially.

The NMR splitting data tables for all of the following experiments is presented in Appendix B. All NMR splitting measurements were repeated at least two times to ensure accuracy of the results. The difference between the repeated measurements was consistently less than 2 Hz.

6.4 Effect of Particle Size

The effect of particle size on gel formation in oil sand sludge was studied by closely monitoring the sol to gel transformation of the A-200, A-500, A-1500, and A-91500 sub-fractions in pond water using ^2H NMR. Immediately after the samples were manually shaken (at zero time), the A-500, A-1500, and A-91500 sub-fractions

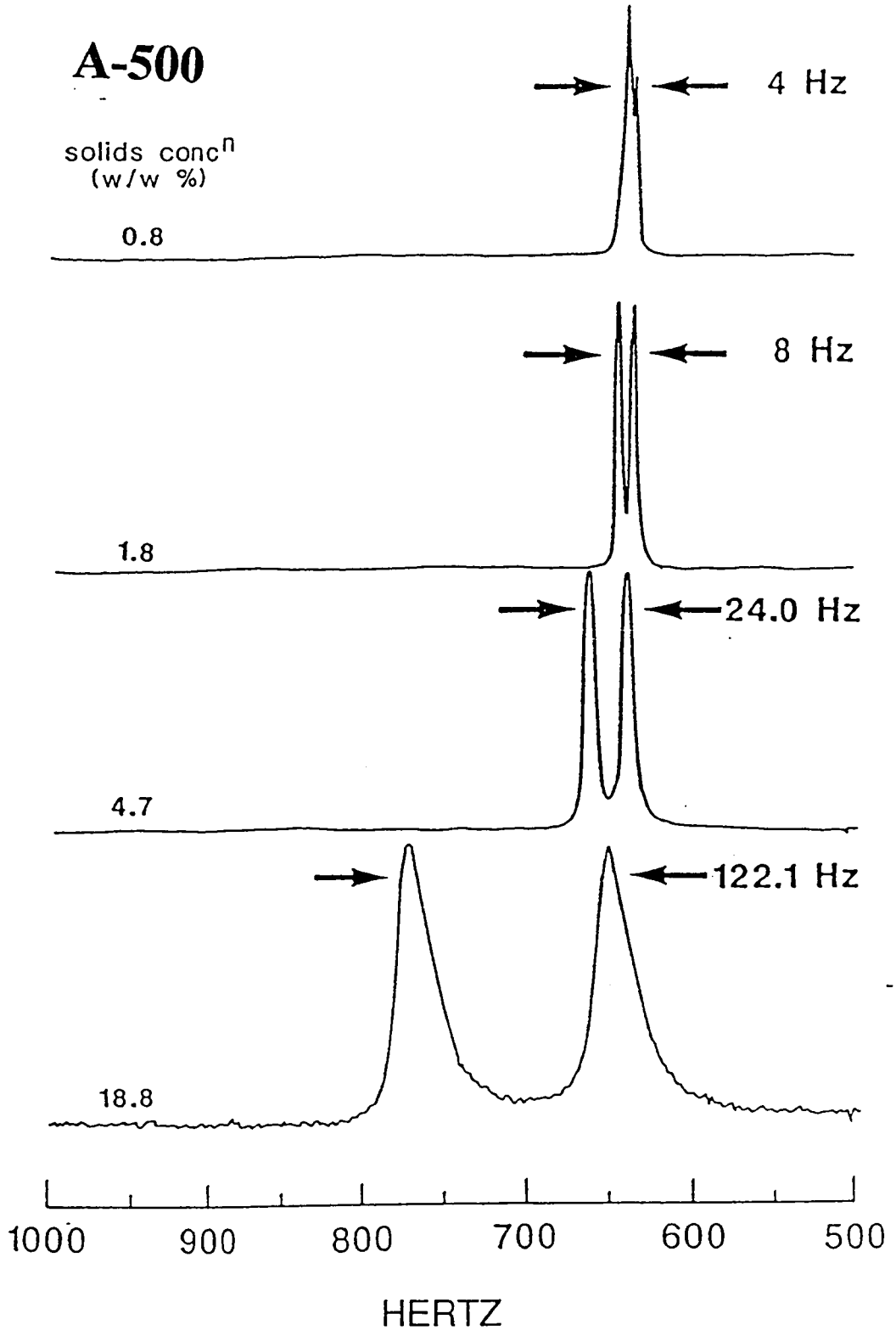

Figure 6.7: Deuterium Resonance Splitting Increase with an Increase in Concentration (at Zero Time).

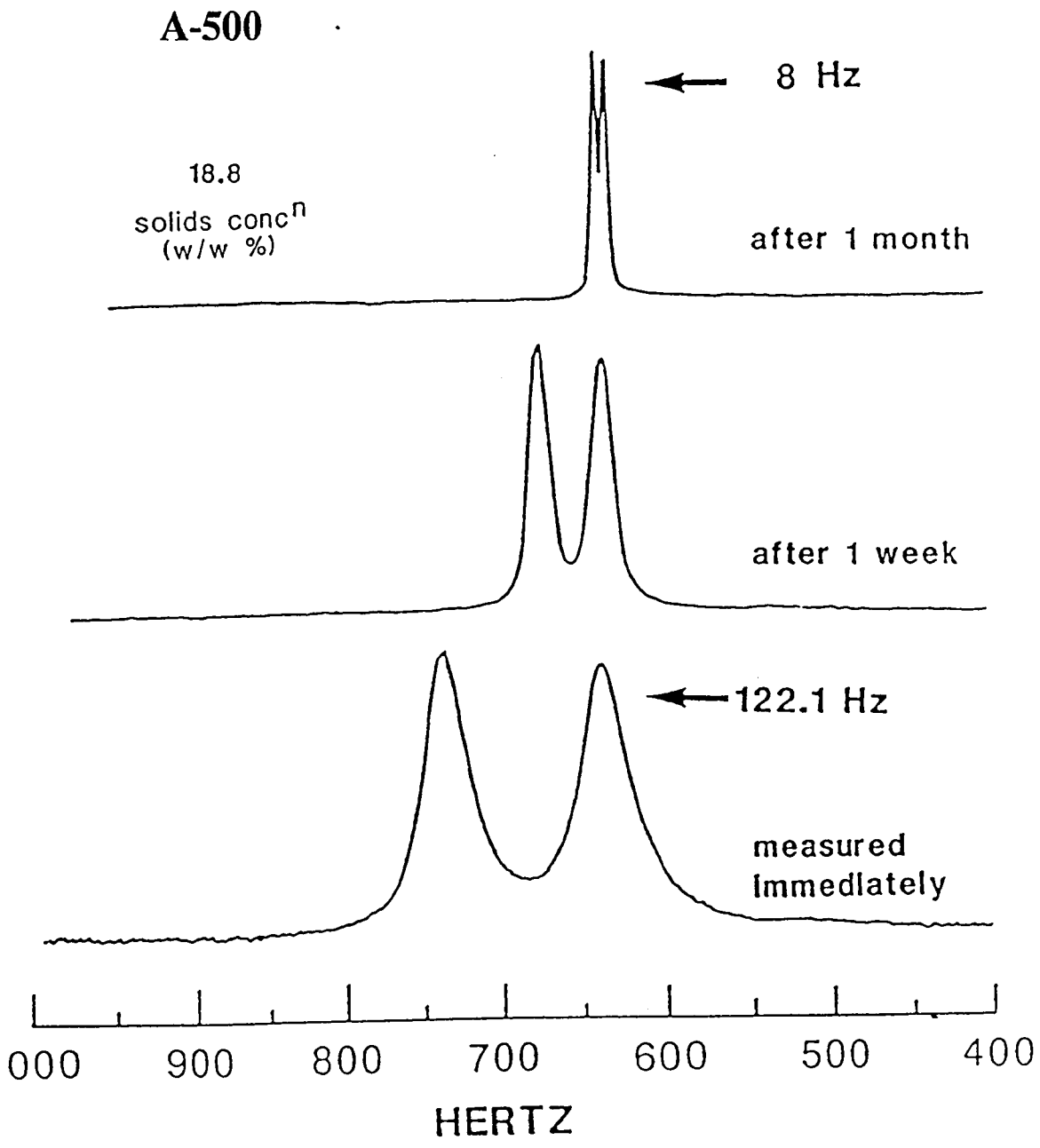

Figure 6.8: Time Dependence of Deuterium Resonance Splitting.

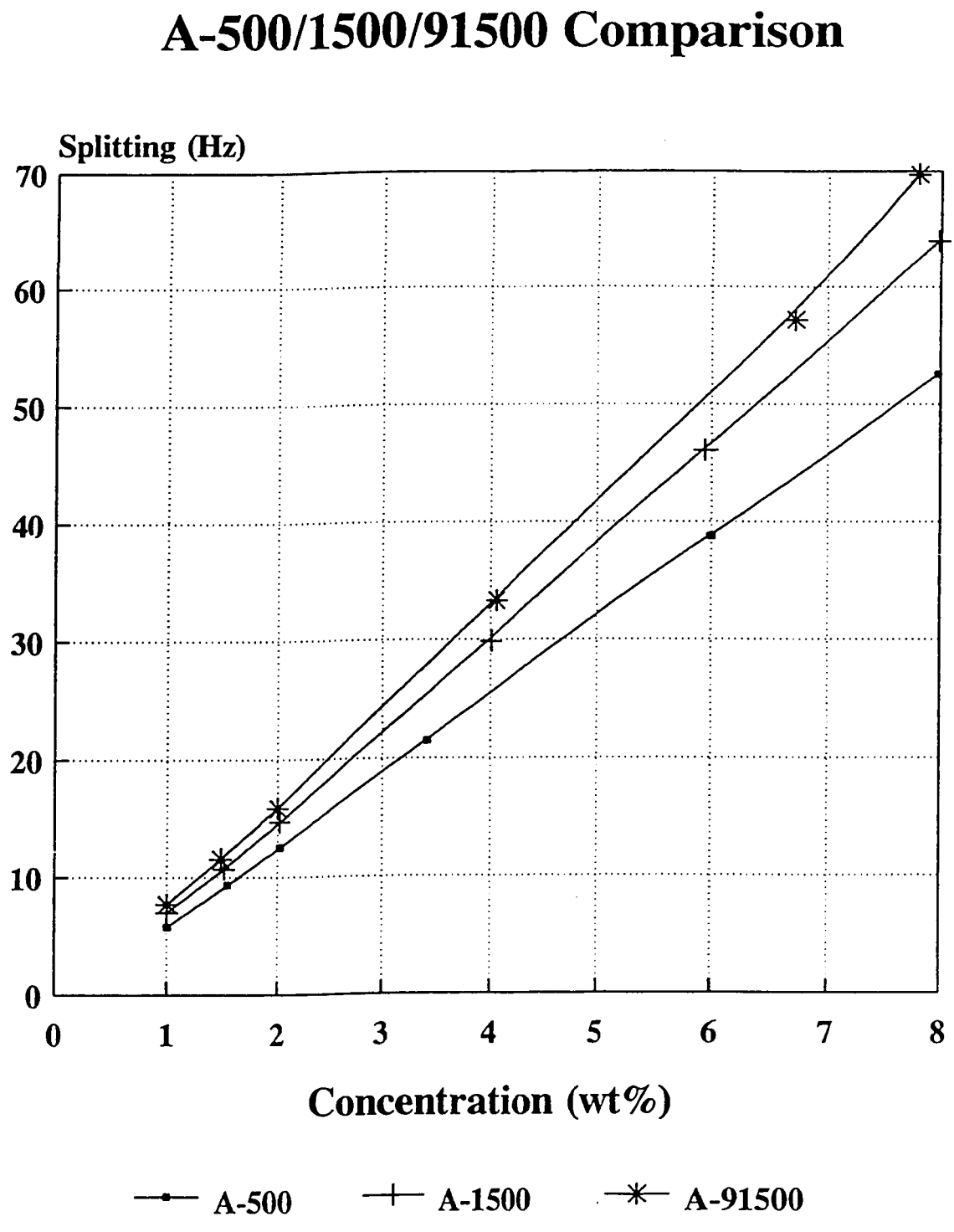

Figure 6.9: Splitting vs. Concentration
at Zero Time.

showed the characteristic doublet splitting. Figure 6.9 shows that at zero time there was a linear dependence of splitting on concentration throughout the entire concentration range, for all of the sub-fractions. As the concentration was increased, the residual splitting also increased. Also, the slope for A-91500 was greater than the slope for A-500, confirming that the original building blocks for the A-91500 sub-fraction are smaller than those for the A-500 sub-fraction. The reason for this is, that at a particular concentration, more surface area is available for exchange with A-91500, which has the smallest particles; therefore, a larger residual splitting signal is observed.

Figure 6.10 shows the concentration dependence of residual splitting for the A-500 sub-fraction at different time periods. For concentrations less or equal to 2.0 wt%, the splitting increased linearly with concentration throughout the considered time period (up to 2 weeks). From Figure 6.11, which shows the time dependence of splitting, it can be seen that there are virtually no differences in splitting for concentrations less or equal to 2.0 wt% as a function of time. These observations indicate that for the considered time period and for concentrations less or equal to 2.0 wt%, the A-500 sol was stable (no aggregation had occurred).

From Figures 6.10 and 6.11, it can be seen that for A-500 concentrations greater than 2.0 wt%, the linear relationship (stability) held for several hours after being shaken (at zero time). However, after 23 hours for the highest concentration (8.0 wt%), the aggregation process began. This is indicated by a deviation from linearity (splitting had decreased 6 Hz to 47 Hz, from 53 Hz). Such a significant change is an indication of cluster formation (gel network formation), causing reduced mobility of the ultrafine clay particles.

Figures 6.12 and 6.13 show the concentration and time dependence of splitting for the A-91500 sub-fraction. These figures show that at the highest concentration (8.0 wt%) aggregation had begun after only 30 minutes. After only 48 hours, the 4.0

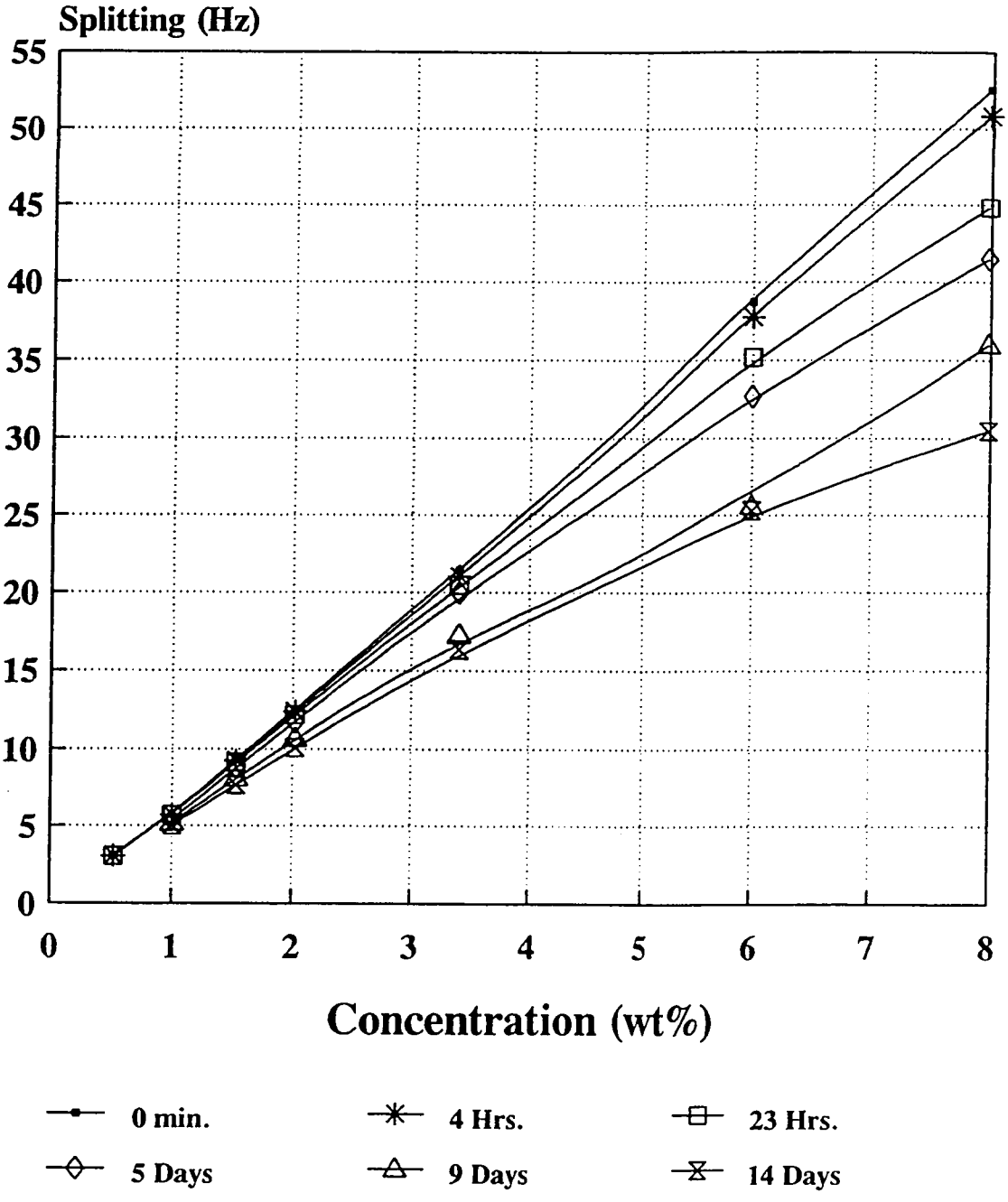

Figure 6.10: Splitting vs. Concentration for A-500.

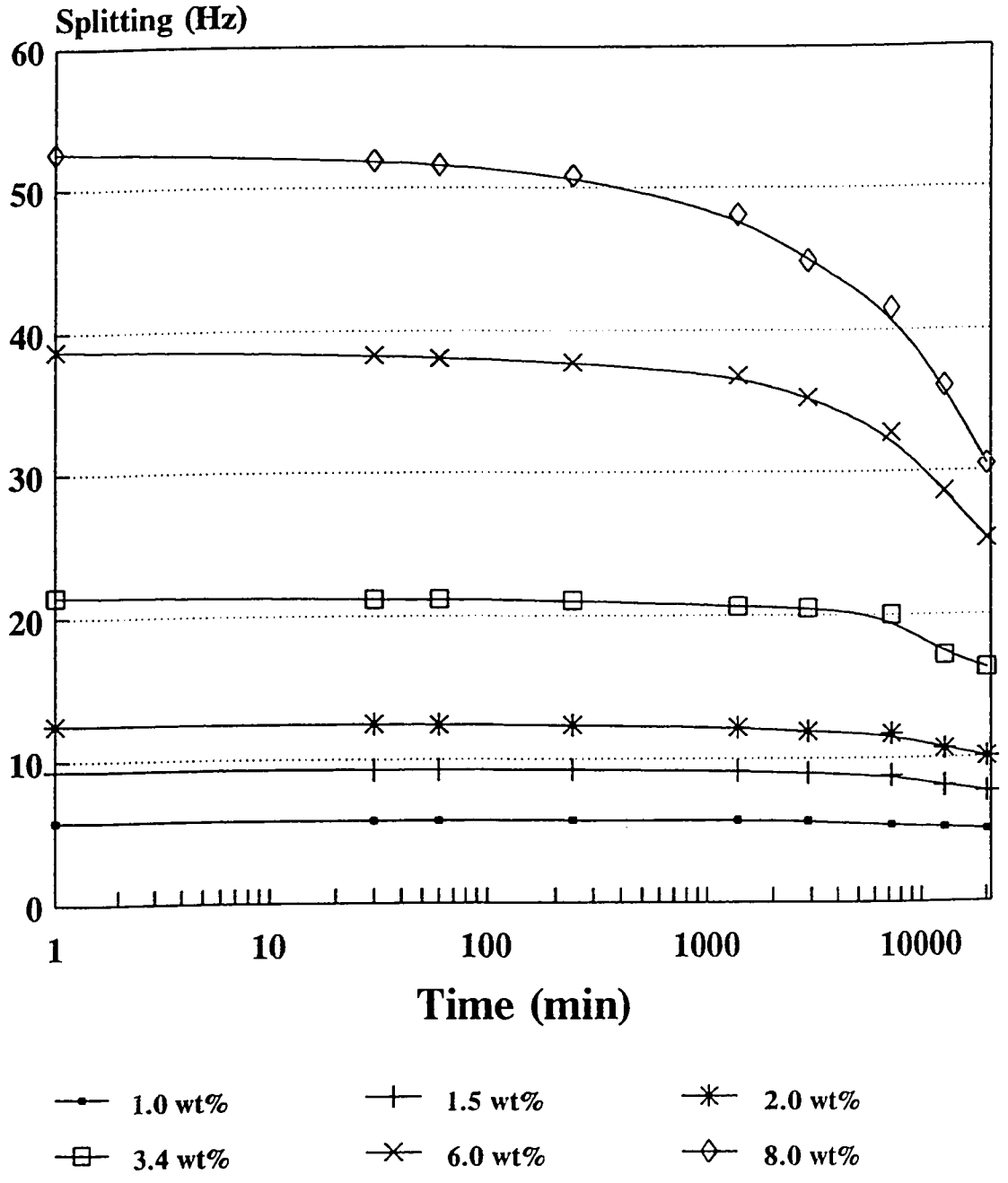

Figure 6.11: Splitting vs. Time for A-500.

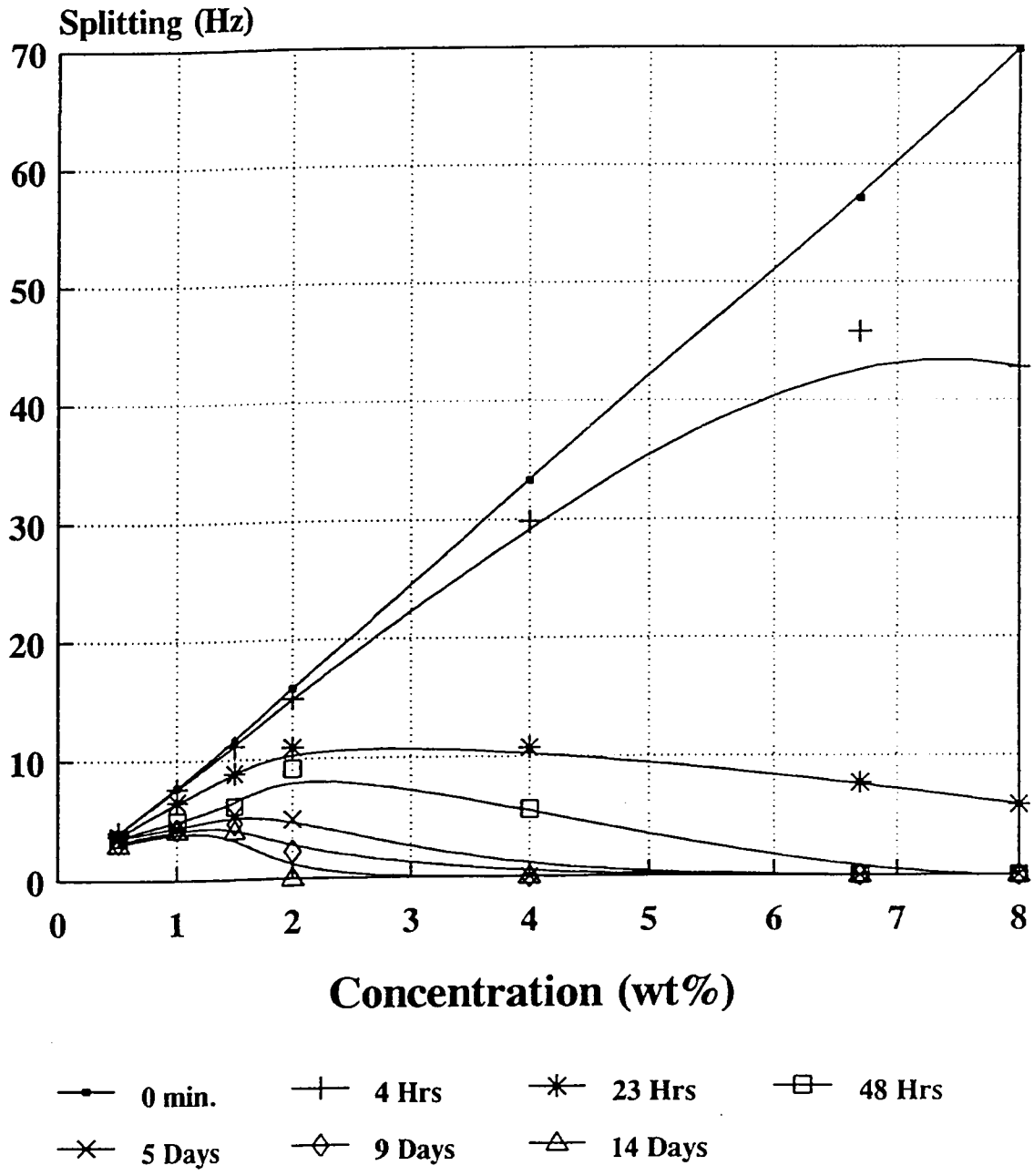

Figure 6.12: Splitting vs. Concentration for A-91500.

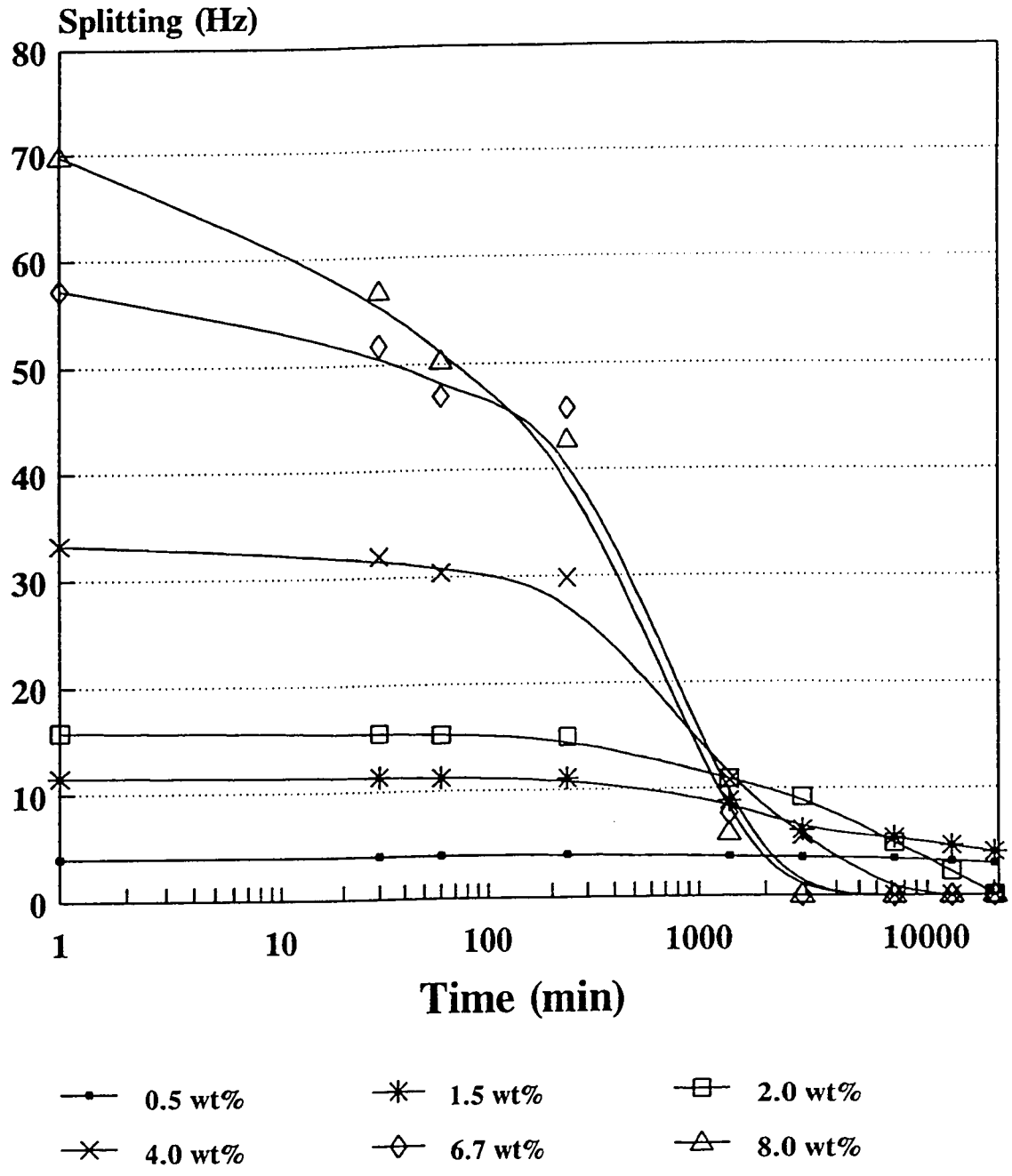

Figure 6.13: Splitting vs. Time for A-91500.

wt% sample was almost completely gelled.

The percent change in splitting [(D_o - D_v) / D_o * 100], or percent losses, was used as a parameter to quantitatively monitor the degree of aggregation (growth of the gel network) over time. Results presented in Figures 6.14 and 6.15, for suspensions of A-500 and A-91500, show the time dependence of the degree of aggregation (% losses). The degree of aggregation was not prominent for the A-500 sub-fraction. As shown in Figure 6.14, little aggregation, if any, had occurred during the first 4 hours (the suspensions are present in the form of a sol). This is indicated by a value of zero for the degree of aggregation (% losses = 0; therefore, there has been no loss of mobility by the ultrafine clay particles). As time progressed, the particles began to lose mobility resulting in an increase in the degree of aggregation. However, after 2 weeks for the 8.0 wt% concentration, approximately 42% of the dispersed solids had aggregated. The sol to gel transformation process for the A-500 sub-fraction is relatively slow. It can be concluded that the A-500 ultrafine clay particles are relatively weak gel formers.

Figure 6.15 shows the sol to gel transformation process for the A-91500 sub-fraction. The degree of aggregation over time is much more pronounced than for A-500. After only 23 hours for the 8.0 wt% sample, the degree of aggregation was 100%, indicating that the ultrafine clay particles had lost their ability to be oriented in the magnetic field. The gel network had been formed and the sample was in the form of a stiff gel. These results indicate that the A-91500 ultrafine clay particles are strong gel formers.

The A-200 sub-fraction did not show a residual splitting signal at any concentration or after any time period. Visual observations also showed that it did not appear to form a gel. After a prolonged time period, the A-200 sub-fraction had settled, even though it was of colloidal size (500 nm). These results allow us to conclude that A-200 does not appear to contribute to the gel forming propensity of oil

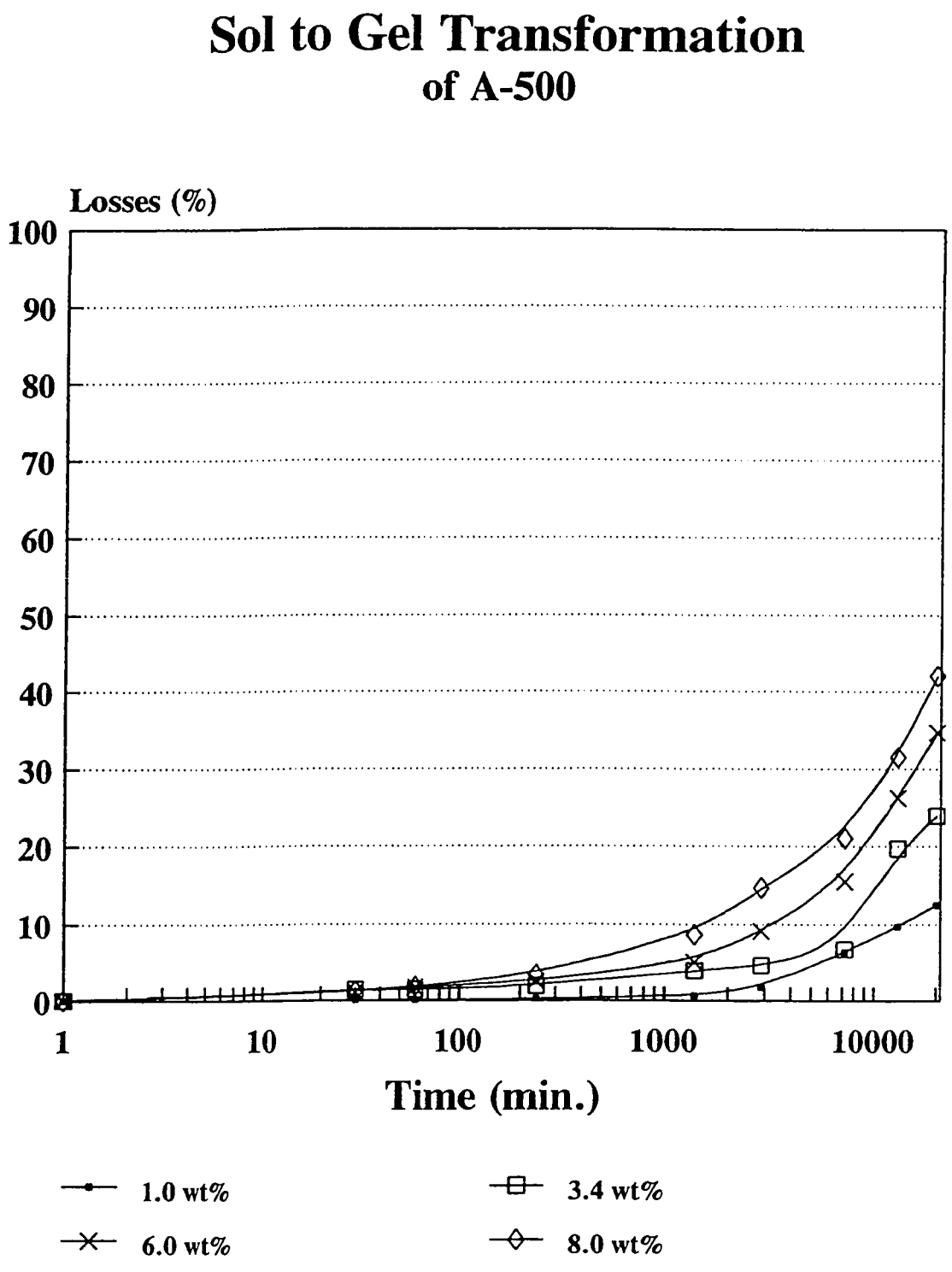

Figure 6.14: Losses vs. Time for A-500.

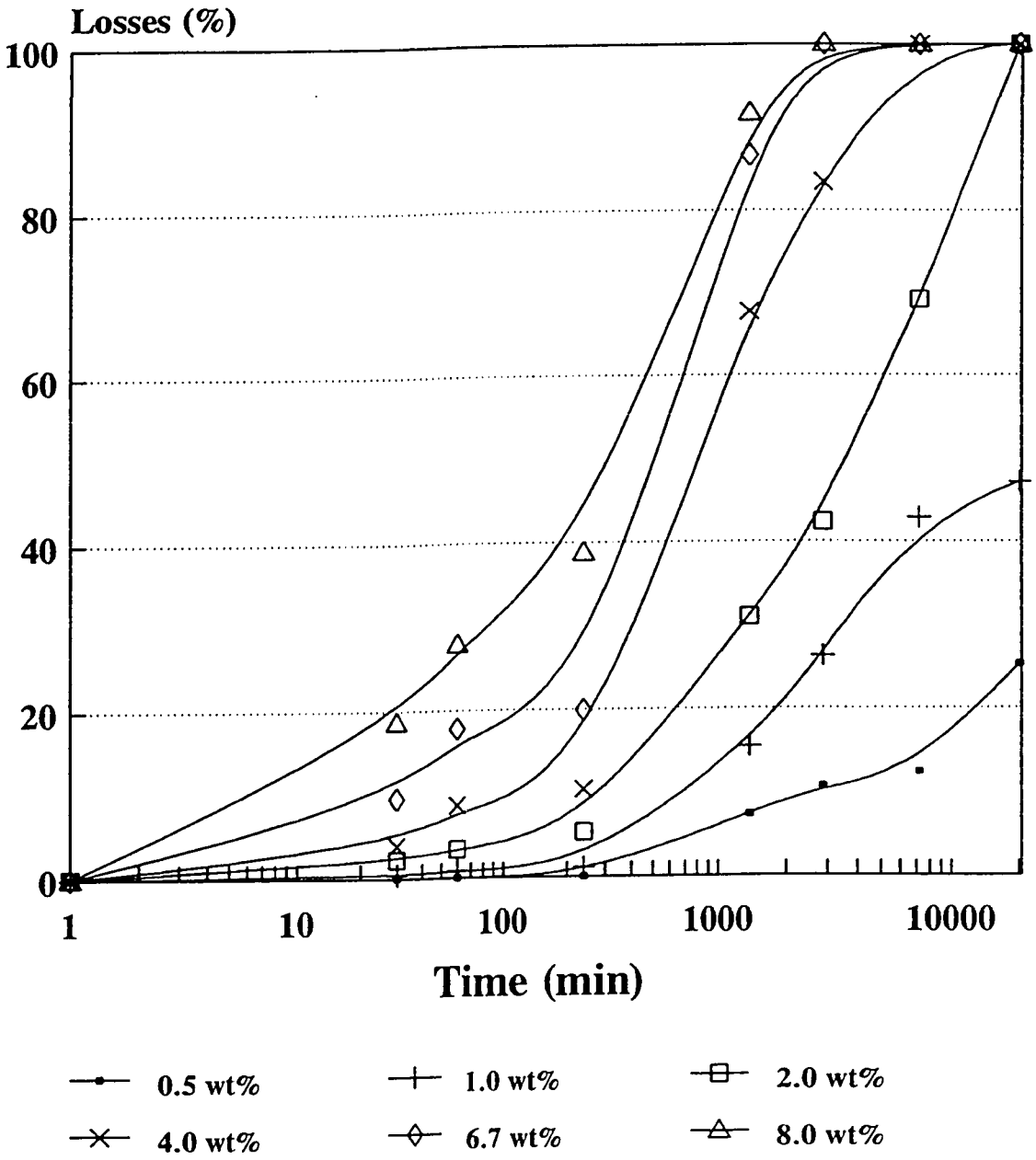

Figure 6.15: Losses vs. Time for A-91500.

sand sludge.

In summary, particle size has a significant effect on the sol to gel transformation process. The gel forming propensity increases as particle size decreases. The ultrafine clay particles with approximate diameters of 50 nm (A-91500) have a strong gel forming propensity. Particles with diameters in the range of 200 to 300 nm (A-500) have a weak gel forming propensity. Particles with diameters greater than 400 nm (A-200) do not appear to contribute to the gel forming propensity of sludge at all.

The observation that small particles gel more rapidly than larger particles of the same material can be attributed to three influences. The first influence may be that of Brownian motion. Brownian motion is the result of thermal motion of water molecules surrounding the particles. The water molecules are continuously colliding with the particles, forcing them to move in all different directions. In kinetic equilibrium, the average translational kinetic energy of the particles is equal to that of the water molecules (van Olphen, 1963):

$$[\tfrac{1}{2}\ m\ v^2]_{particle} = [\tfrac{1}{2}\ m\ v^2]_{water\ molecules}.$$

The average velocity of the particles decreases with an increase in mass, resulting in less intense Brownian motion for larger particles. In relation to sol to gel transformation, the velocity of larger particles is less than that of smaller particles, therefore, the force of collision, leading to gel formation is lower.

Studies conducted by van Olphen (1963), Parfitt (1981) and others have also shown that smaller particles gel faster than larger particles. They were able to prove that there is less of a repulsive force between small particles than between larger particles carrying an identical double layer. This is due to the larger interaction surface area on the larger particles. By comparing small and large particles with identical double layers, they were able to show that the repulsive-potential curves, for the interaction of unit surface areas of the particles, were identical (van Olphen,

1963). However, the total particle repulsive force was less for the smaller particles, thereby allowing the smaller particles to gel faster than larger particles.

The third influence is related to the fact that, since the gelation process involves the collision of particles, the gelation rate will depend more on the number of particles per unit volume in suspension than on concentration. For example, a 2.0 wt% suspension of A-91500 will have more particles available for gelling interactions than a 2.0 wt% suspension of A-500 particles. Therefore, a A-91500 suspension would gel faster than a A-500 suspension.

6.5 Characterization of the Gel Forming Propensity of Sludge Sub-Fractions

To characterize the gel forming propensity of the ultrafine sub-fractions, the gel onset concentration (GOC) and critical gel concentration (CGC) were evaluated for each. The GOC describes the concentration at which a thickening of the suspension is first observed. The CGC is the lowest concentration at which a stiff gel is first observed. Two main methods to determine these values are rheology and visual observation. However, during this research, an alternate method was developed.

The GOC and CGC values were evaluated from the ^2H NMR data. The GOC was obtained from the intersection of the two tangents of the slopes produced by plotting the difference in the initial splitting and the splitting after 9 days, D_o-D_9, versus concentration (time periods less than 9 days gave scattered results and time periods greater than 9 days gave approximately the same values as those determined for 9 days). An example of this graphical method is shown in Figure 6.16. The CGC was indicated when a value of zero was first observed for the residual splitting signal for the lowest concentration (the time period varied for each sub-fraction). In all cases, these values corresponded closely to those predicted by the visual

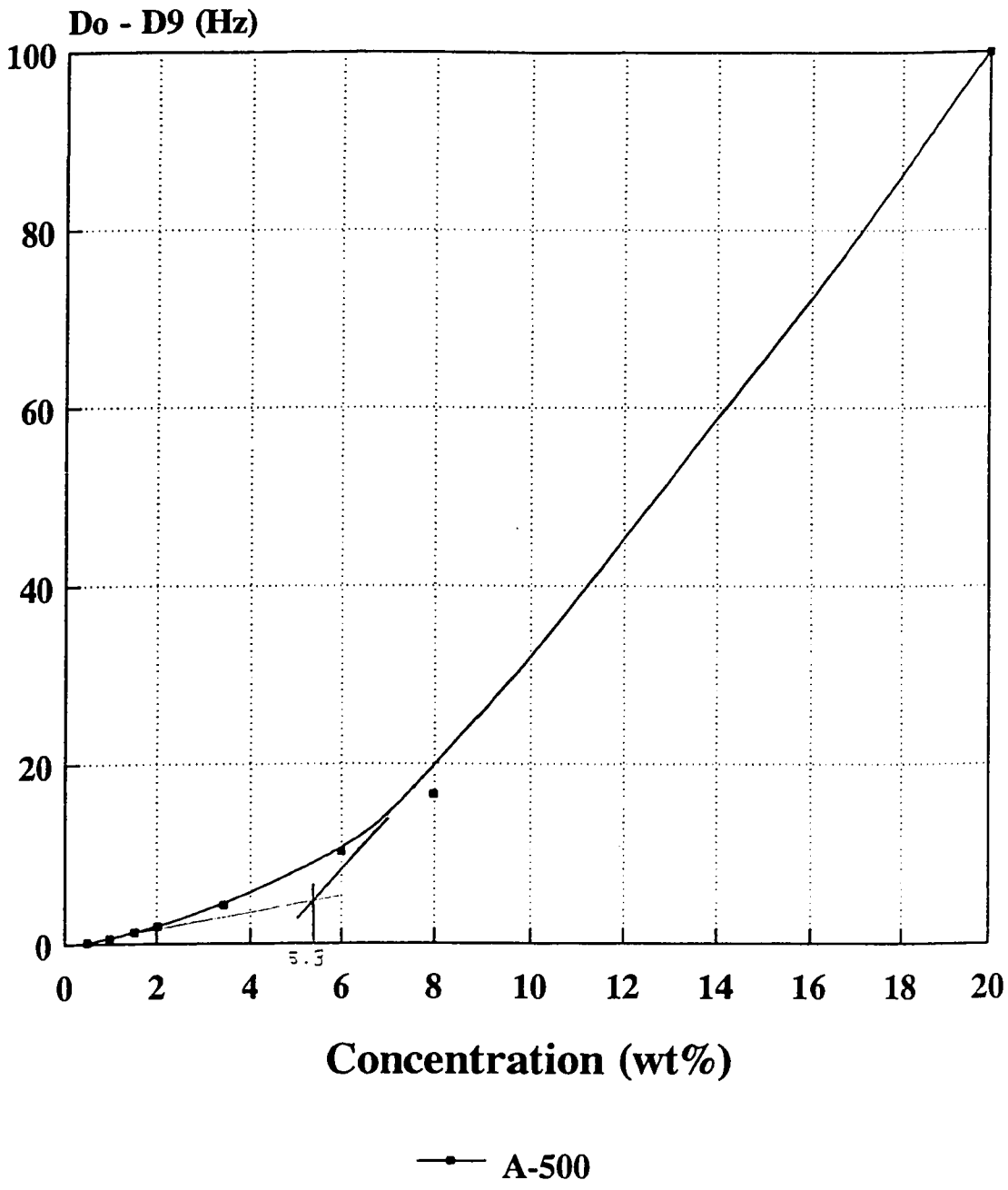

Figure 6.16: Gel Onset Concentration Determination for A-500

(GOC = 5.3)

observation method. The GOC and CGC for each sub-fraction are given in Table 6.3. This alternate, more convenient method allowed a direct comparison of all samples.

Table 6.3: GOC and CGC for Each Sub-Fraction:

Sub-Fraction	GOC	CGC	wt% of Colloidal Fraction
A-500	5.3	20.0	49.6
A-1500	3.4	10.0	19.2
A-91500	0.8	2.0	31.2
Gel Forming Fraction	3.4	8.0	100

The results shown in Table 6.3 also indicate that the GOC for the entire gel forming colloidal fraction is approximately the same as the concentration at which the gel forming solids are present in the bulk sludge sample (5.3 * 0.496 + 3.4 * 0.192 + 0.8 * 0.312 = 3.5). This observation reinforces the fact that these gel forming ultrafine solids alone could be responsible for the exceptionally high water holding capacity of oil sand sludge. It is proposed that these gel forming solids could be interacting in two separate processes: 1) by forming gels they are involved in creation of a three-dimensional, viscous structure; and 2) the presence of this structure could be providing a supporting medium for coarser particles. This may be allowing the coarser solids to form an auxiliary structure, similar to that recently observed by electron microscopy (Mikula et al., 1991).

6.6 Verification of Separation Scheme and ^2H NMR Technique

To verify that the rigorous colloidal layer separation scheme was not altering the ultrafine particles and that the ^2H NMR technique was sensitive enough to closely monitor the sol to gel transformation, the residual splitting for each of the solid

Comparison of Original vs. Recombined Colloidal Fraction

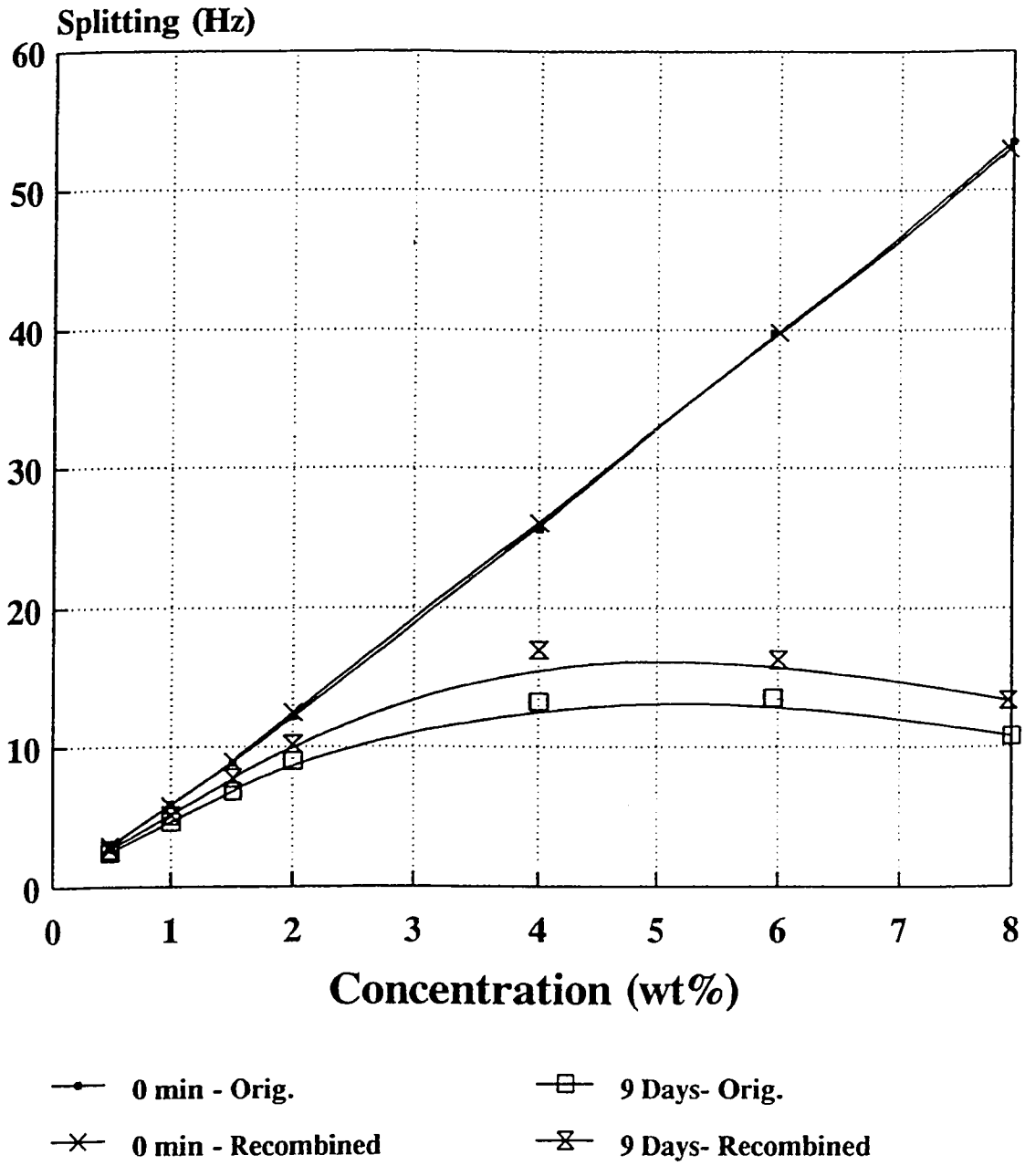

Figure 6.17: Splitting vs. Concentration for Original and Recombined Colloidal Fractions.

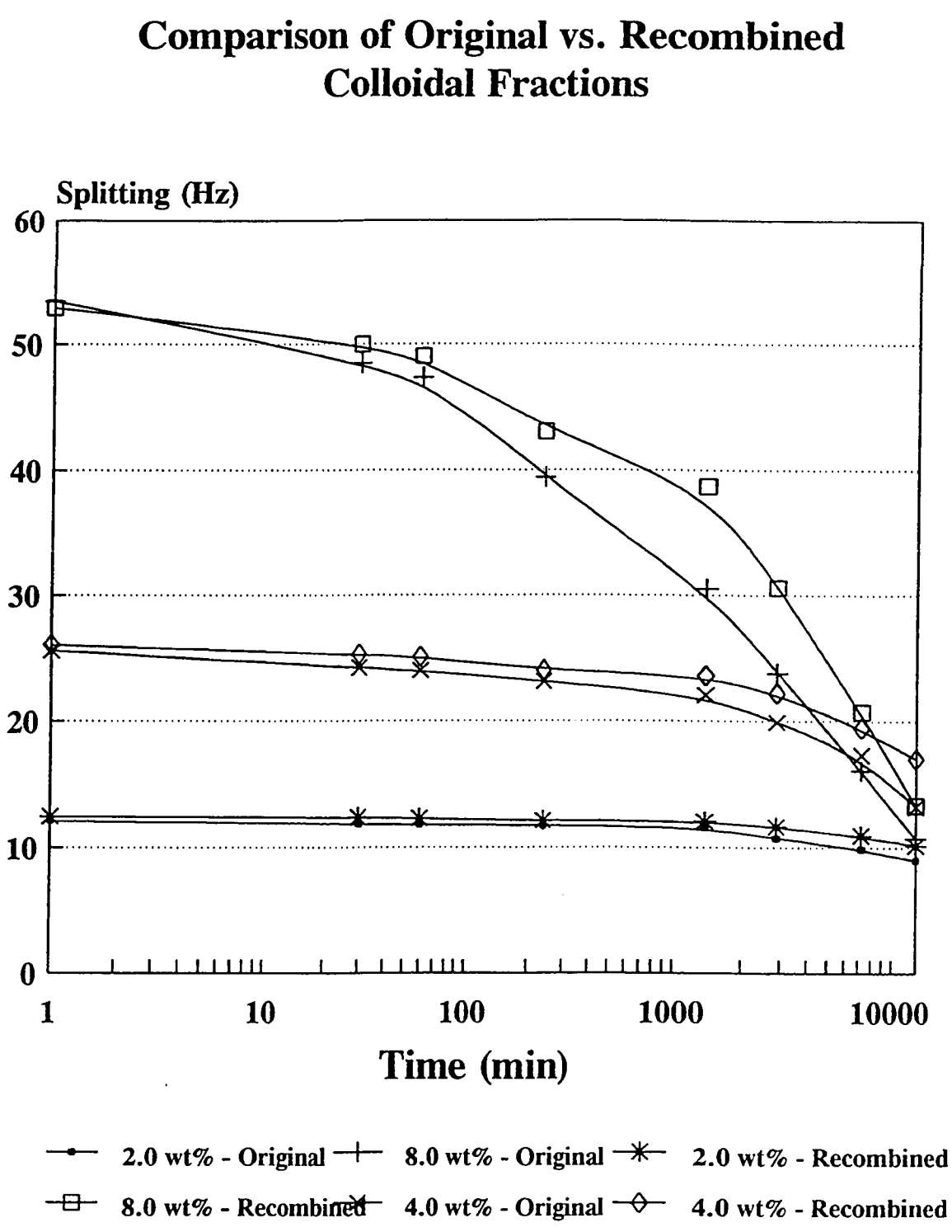

Figure 6.18: Splitting vs. Time
for Original and Recombined Colloidal Fractions.

concentrations was recorded over various time periods (up to 2 weeks) using both the original and recombined colloidal fractions. Figures 6.17 and 6.18 show a comparison of the actual splittings over different concentrations and time periods. It can be seen that there is little difference between the results obtained from the original fractions and the recombined fractions. Even after 9 days for the 8.0 wt% concentration, the difference between the measured splittings is only 3 Hz.

The GOC was also determined for both fractions. The NMR results shown in Figure 6.19 indicate that the GOC was 3.4 wt% for both the original and recombined colloidal fractions.

The results of this study prove that:

1) the extensive colloidal separation scheme did not affect the properties of the colloidal suspension of ultrafine clay particles;

2) the ^{2}H NMR technique was sensitive enough to accurately and effectively monitor the sol to gel transformation process within oil sand sludge; and

3) the ^{2}H NMR data can be used to determine the GOC.

6.7 Mutual Effect of Gel Forming Components

To determine whether gel formation is an additive, synergistic, or antagonistic property, the GOC was determined for each A-500/A-91500 mixture. Each GOC was then plotted against the weight percent of A-91500 in each mixture, as shown in Figure 6.20. Previous results showed that the GOC for the entire colloidal gel forming fraction was 3.4 wt%. This was compared to that indicated on Figure 6.20, where the relative contribution of A-500 and A-91500 is 57 wt% and 43 wt%, respectively. Figure 6.20 shows that for 43 wt% A-91500, the GOC would be 3.5 wt%, approximately the same value measured for the entire colloidal fraction. A GOC value less than 3.5 wt% would indicate that gel formation was a synergistic property and values greater than this would indicate an antagonistic property.

GOC Determination For Original and Recombined Colloidal Fractions

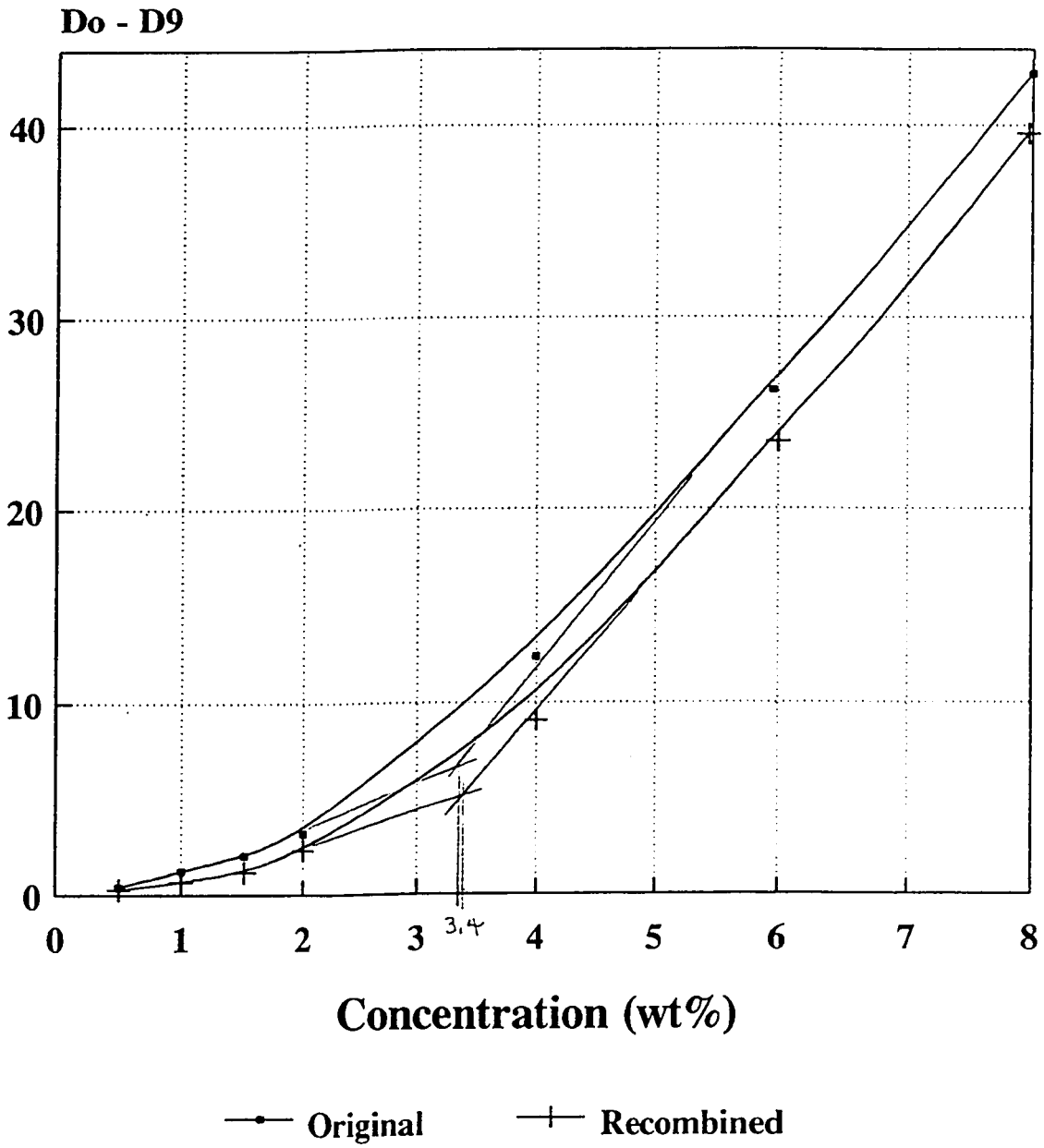

Figure 6.19: Change in Splitting vs. Concentration For Original and Recombined Colloidal Fractions.

(GOC = 3.4)

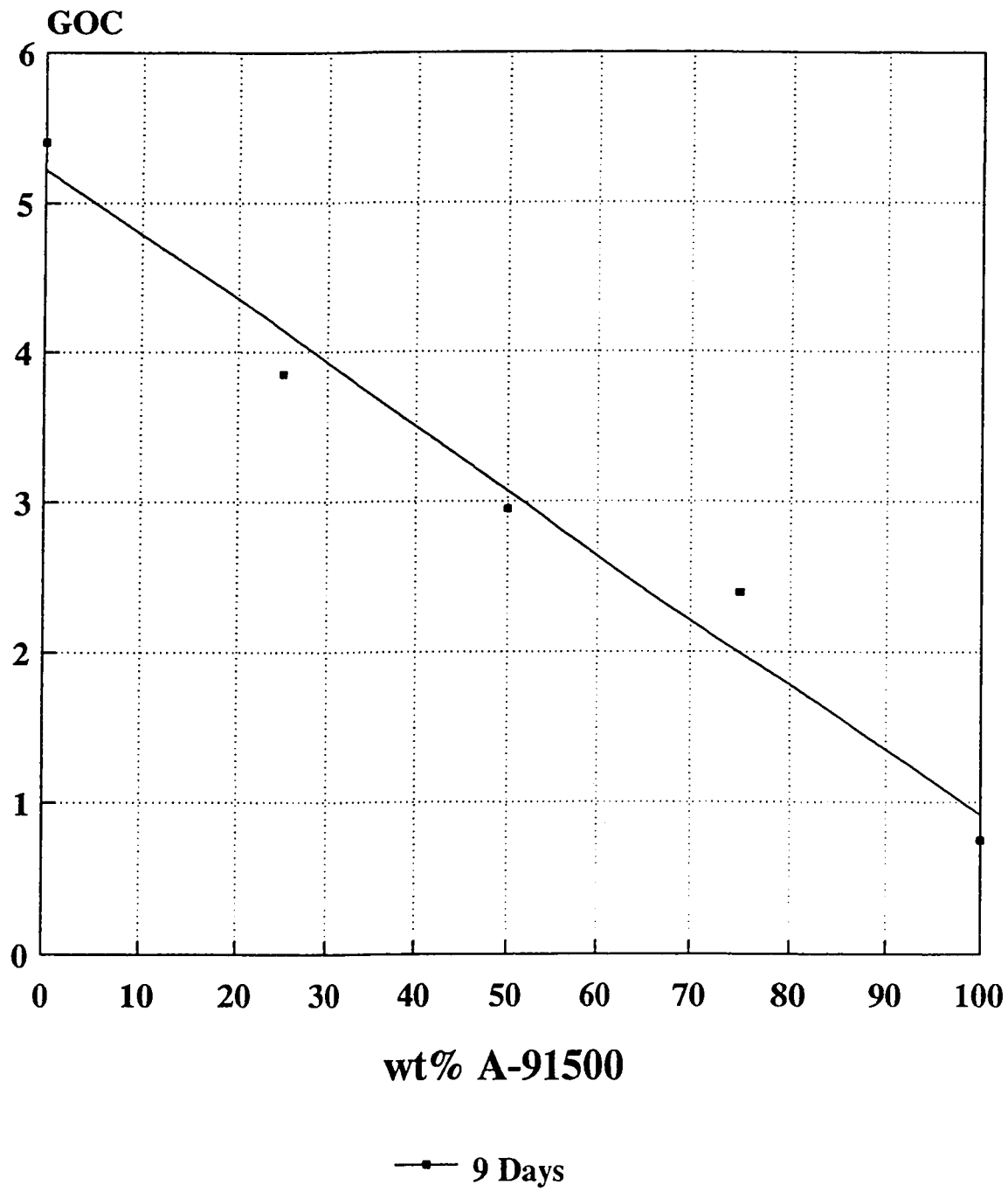

Figure 6.20: GOC vs. wt% A-91500

However, a value of 3.5 wt% demonstrates that gel formation is simply an additive property with no additional interactions occurring between the A-500 and A-91500 particles. Appendix C shows the GOC determinations for all of the sub-fractions and mixtures.

6.8 Effect of Coarse Solids

The sol to gel transformation of the A-200/A-500/A-91500 mixtures in pond water was studied using ^2H NMR. The residual splitting recorded immediately after the samples were shaken was the measurement at which aggregation was absent. An increase in solids concentration resulted in an increase in the amount of surface area that was able to orientate the immobilized water. This was reflected in a linear increase in the residual splitting, as depicted in Figure 6.21. The initial residual splitting values for the mixtures increased linearly over the entire range of concentrations. Figure 6.21 also shows that the slope for the pure A-91500 samples was greater than the slope for the mixtures, indicating that the dispersed particles in the pure samples were smaller that those of the mixtures (more overall surface area per unit concentration).

As the sol to gel transformation progressed, the ultrafine clay particles aggregated, resulting in a loss in their ability to be orientated by the magnetic field. As more particles became involved in the aggregation process, less surface area was available to orientate the immobilized water. Thus, any change in the aggregation state was translated into a change in the amount of immobilized water capable of fast exchange, and consequently, a corresponding decrease in the residual splitting.

However, the change in the aggregation state, where the clay particles become involved in the gelling network, is not the only process which can cause a reduction in the residual splitting. The presence of coarse solids, (particles which do not form gels) along with the gel forming particles within the suspension, can cause a reduction

A-200/A-91500 Mixtures

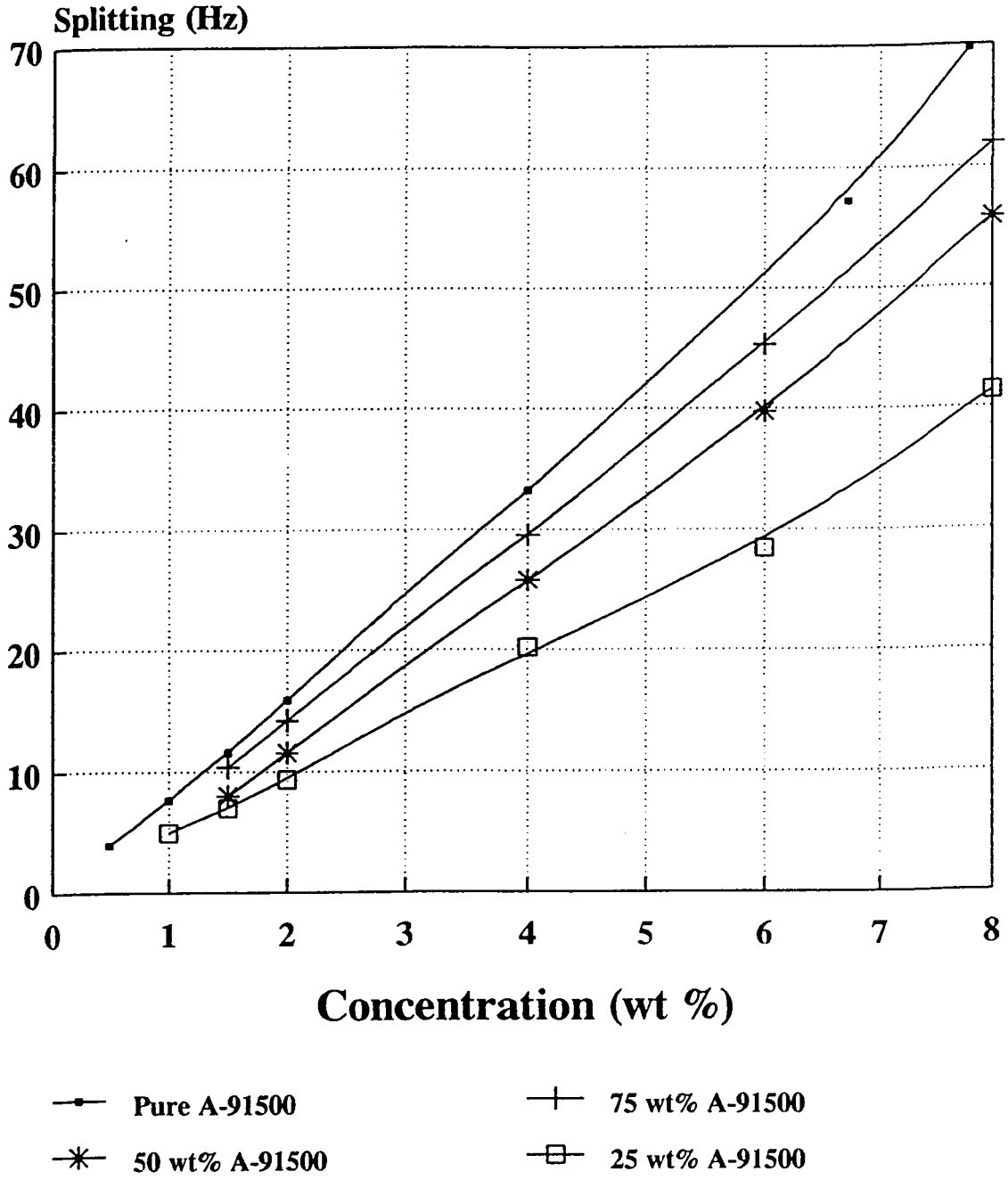

Figure 6.21: Splitting vs. Concentration at Zero Time For A-200/A-91500 Mixtures.

in residual splitting in two different ways:

1) If the ultrafine clay particles are relatively weak gel formers, such as A-500, the sedimentation velocity of coarse solids at low solids concentrations will be greater than the network-forming ability of the weak gel formers. Therefore, the coarse particles would settle out before the gel network is formed (the non-gelling particles will segregate from the gel formers). Over time, a reduction in the residual splitting would occur simply because the surface area, capable of ordering the immobilized water, has been physically removed (settled out) from the suspension.

2) If the ultrafine clay particles are strong gel formers, such as A-91500, the network-forming ability of these particles will be greater than the sedimentation velocity of the coarse solids. This would result in the coarse solids being entrapped in the gelling network before settling out. The residual splitting would decrease over time, as the sol to gel transformation process proceeds with the coarse particles physically trapped in the gelling network.

Figure 6.22 shows an example of the first situation. The change in splitting (D_o - D_f) after 5 days for two of A-200/A-500 mixtures is shown for a range of A-500 solids concentrations. This is then compared to the pure A-500 sub-fraction (weak gel former). The change in splitting was greater for mixtures than for pure samples, indicating that the A-200 particles were settling out. Visual observations showed that the sediment was light greyish-white in colour (A-200) and the suspension above it was greyish-brown in colour (A-500), confirming that the A-200 particles separated from the gel-formers.

Figure 6.23 shows an example of the second situation. At lower concentrations, there was little difference in the change in splitting for the mixtures compared to the pure A-91500. This indicates that the A-200 particles are being caught up in the gelling network. However, when the concentration of the A-200 particles was increased significantly, even A-91500, the best gel former, could not prevent A-200 from settling before the gel network was formed.

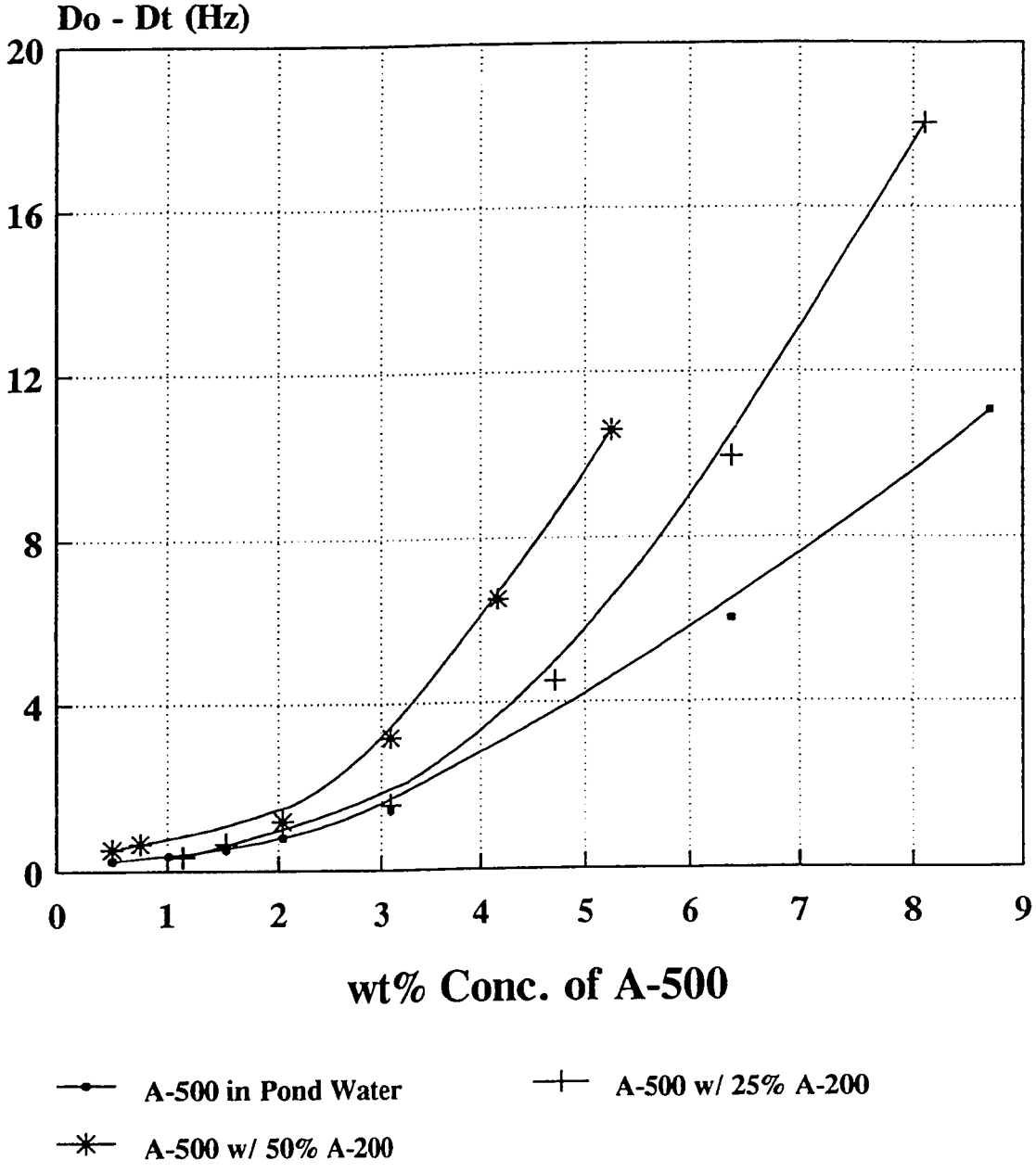

Figure 6.22: Change in Splitting vs. A-500 Concentration

A-200/A-91500 Mixtures
Difference in Splitting After 5 Days.

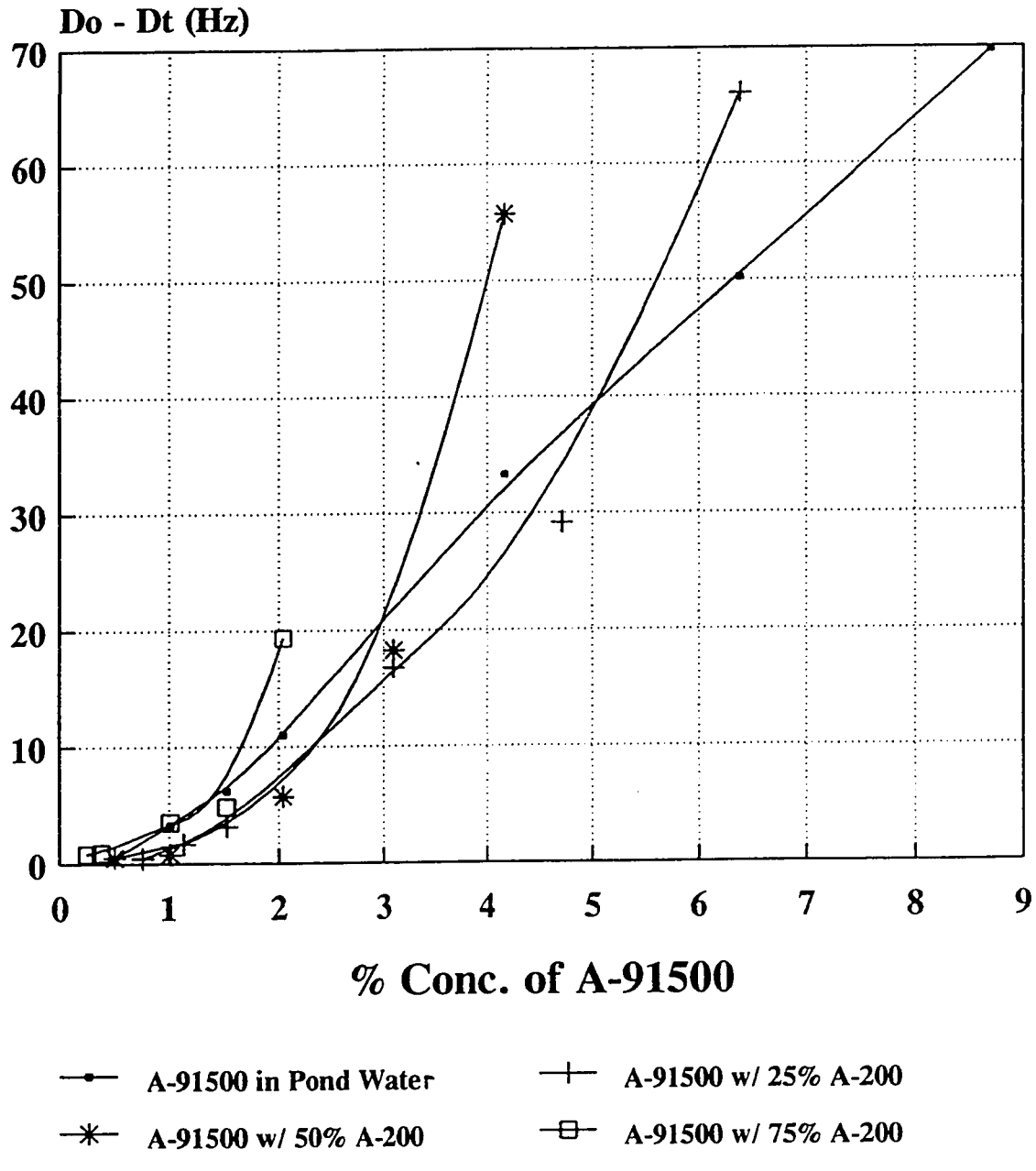

Figure 6.23: Change in Splitting vs. A-91500 Concentration.

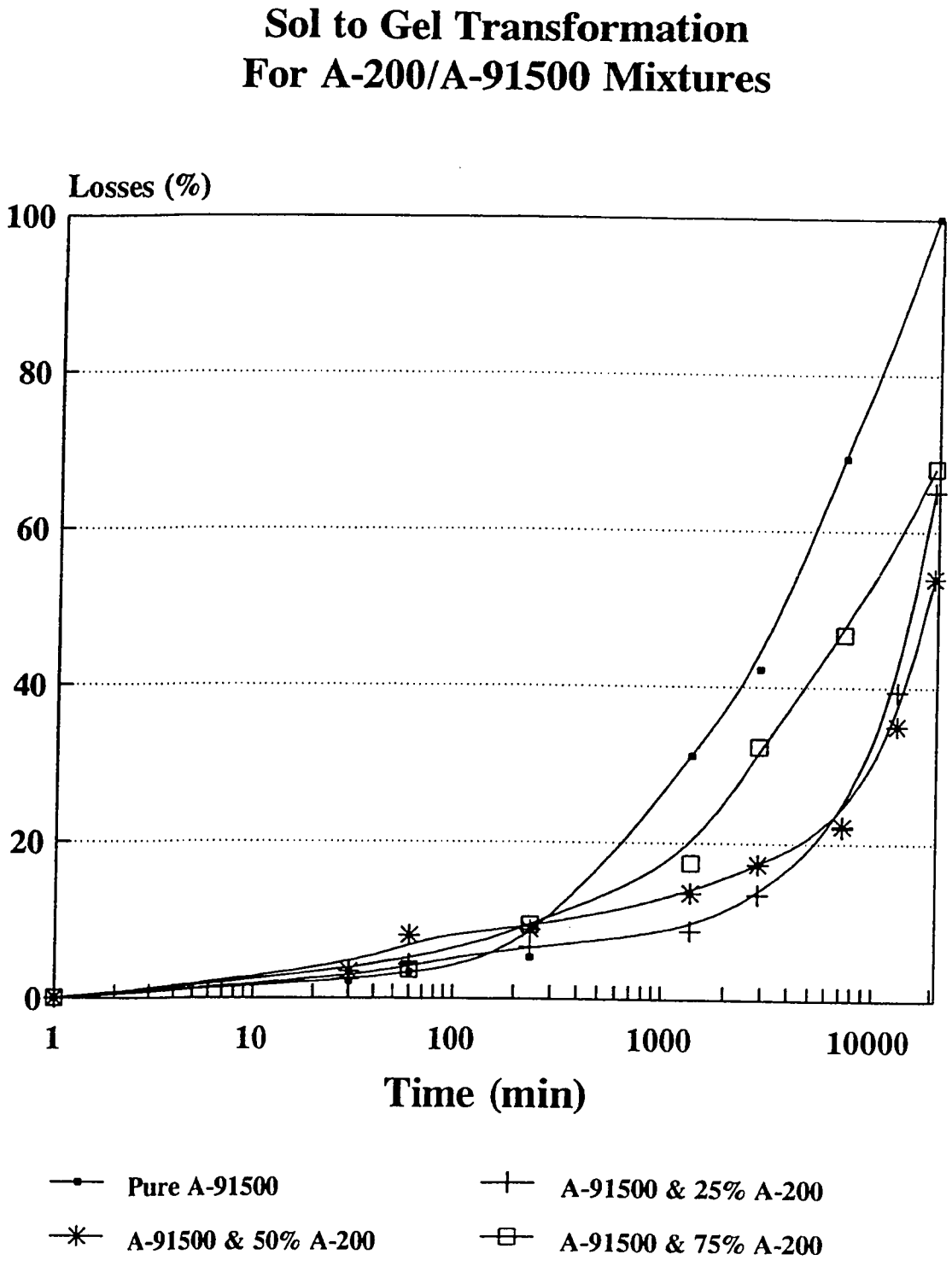

Figure 6.24: Losses vs. Time for 2.0 wt% A-91500.

The percent change in splitting [(D_o - D_t) / D_o * 100] over time was also studied to evaluate the effect of the A-200 coarse particles on the degree of aggregation. When the percent change in splitting was zero, no aggregation occurred (% losses = 0). Results presented in Figures 6.24 show the time dependence of the A-200/A-91500 mixtures with 2.0 wt% A-91500 on the degree of aggregation. During the first 4 hours, the degree of aggregation for the mixtures, as well as pure A-91500, was approximately zero. As time progressed, the degree of aggregation of pure A-91500 increased significantly over that of the mixtures. After 2 weeks, 100% of the dispersed solids in the pure A-91500 sample had aggregated (stiff gel formed). For the mixtures, only about 55% to 65% had aggregated. These results indicate that the presence of coarse solids appears to slow down, but not totally cease the rate of aggregation.

6.9 Effect of Poorly-Crystalline Components on Gel Forming Propensity

The poorly-crystalline inorganic components were extracted from the best gel forming ultrafine fraction, A-91500, using the Tiron Dissolution Method. It was determined that the poorly-crystalline inorganic components comprised 15 wt% of the total A-91500 solids. The sol to gel transformation of the treated sample was monitored using ^2H NMR. Figure 6.25 compares the degree of aggregation over time, for the Tiron treated sample with that of the untreated sample. It can be seen that there is not a significant difference between the two. The sol to gel transformation of the treated sample did proceed more slowly than the treated sample but not to a notable degree. It can be concluded that the poorly-crystalline inorganic components do not greatly affect the gel forming propensity of the ultrafine clay solids.

6.10 Effect of Surface Active Solids

Biwetted ultrafine solids (SAS), whose surfaces are associated with a large

Effect of Poorly-Crystalline Components

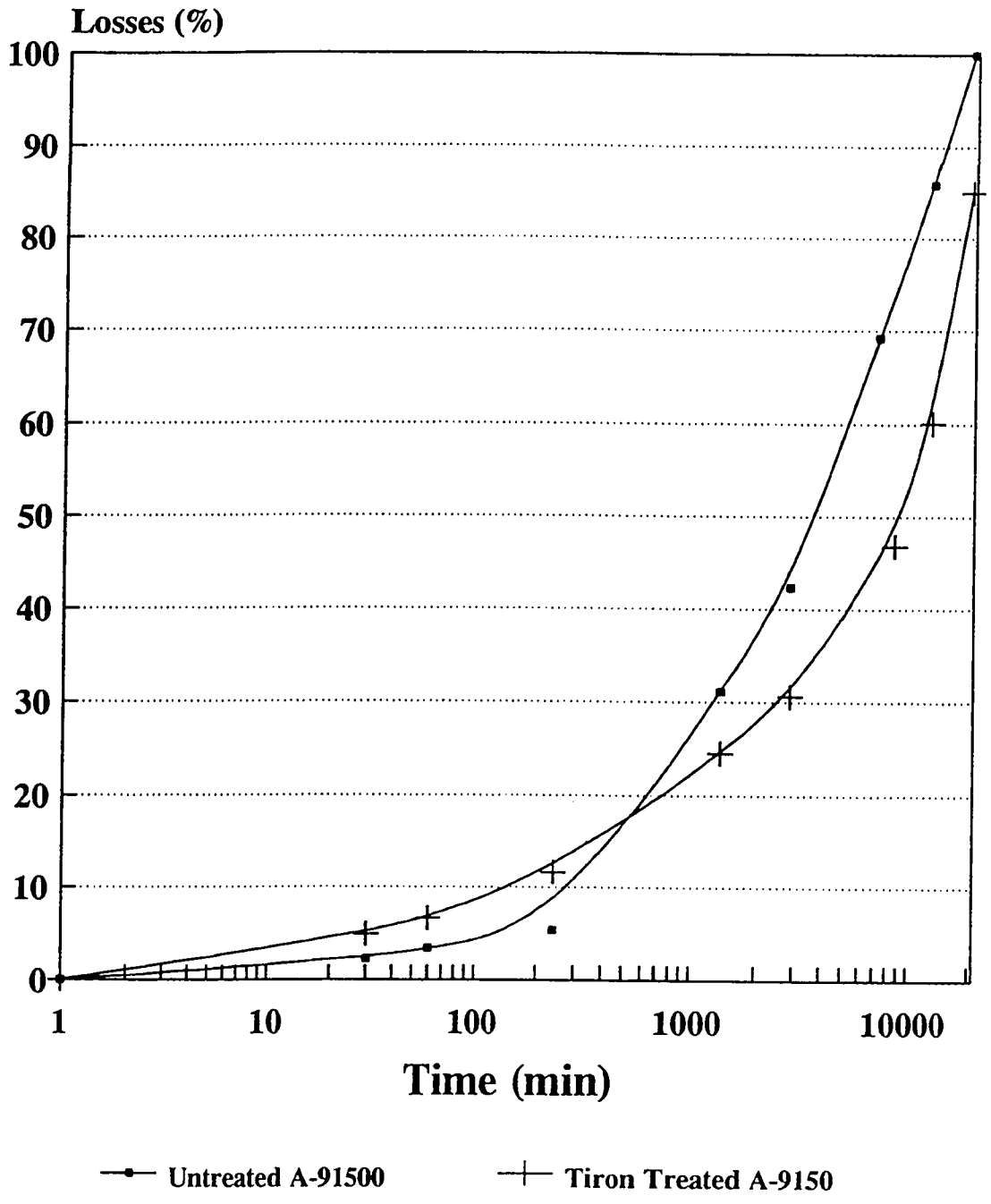

Figure 6.25: Losses vs. Time for Tiron Treated A-91500.

percentage of organic matter, were isolated from the aqueous colloidal sub-fractions by emulsification with toluene, followed by flotation. Owing to the presence of this organic matter, the SAS particles are surface active and, therefore, are capable of stabilizing bitumen emulsions. A micrograph of a bitumen solution in toluene emulsified in water through SAS stabilization is shown in Figure 6.26. As a result, the properties and role of the SAS in structure formation in oil sand sludge was studied using a variety of techniques. Figures 6.27, 6.28, and 6.29 show the distribution of particle sizes in each of the SAS sub-fractions before the pond water was substituted for distilled water. Figure 6.30 shows the overall solids distribution for each of the sludge fractions with SAS removed. Additional data on the particle size distributions of each sub-fraction is given in Appendix A.

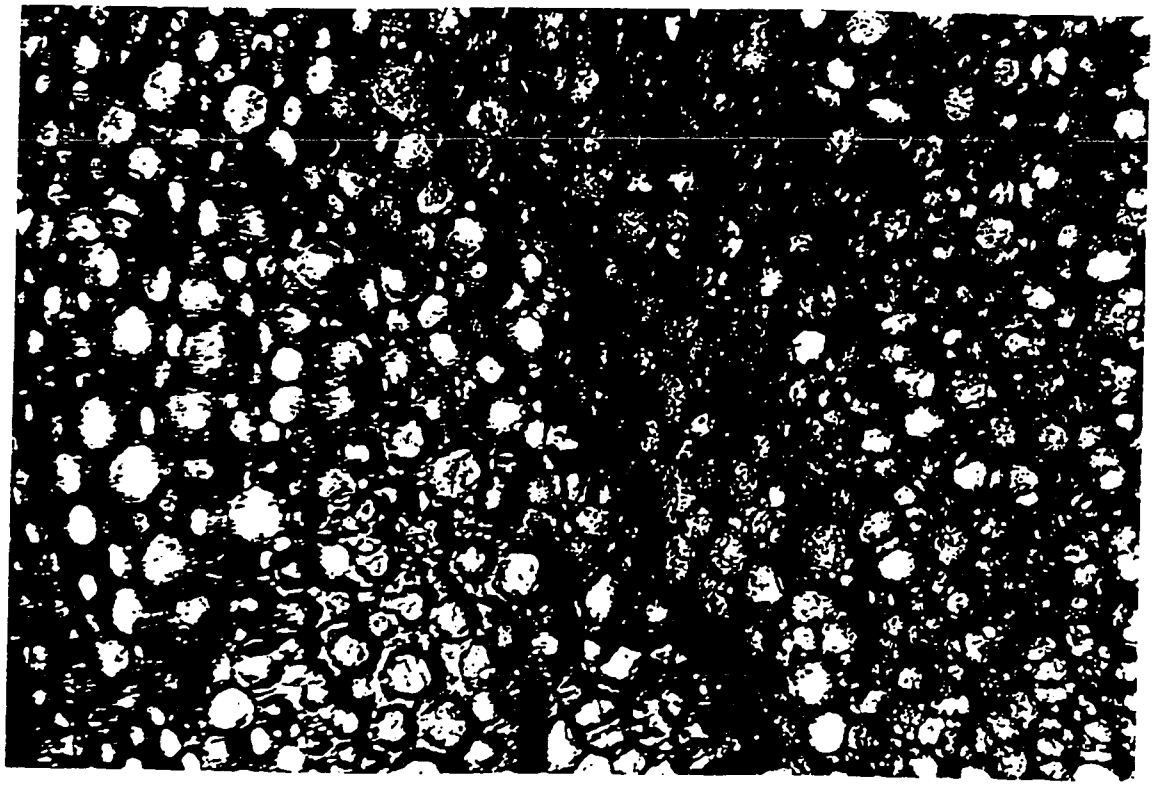

Figure 6.26: Bitumen Solution in Toluene Emulsified in Water Through SAS Stabilization.

6.10.1 Characterization of the Surface Active Solids

The mineralogical properties of the colloidal clay particles were examined

Solids Distribution of AS-200
(Before electrolytes were washed out)

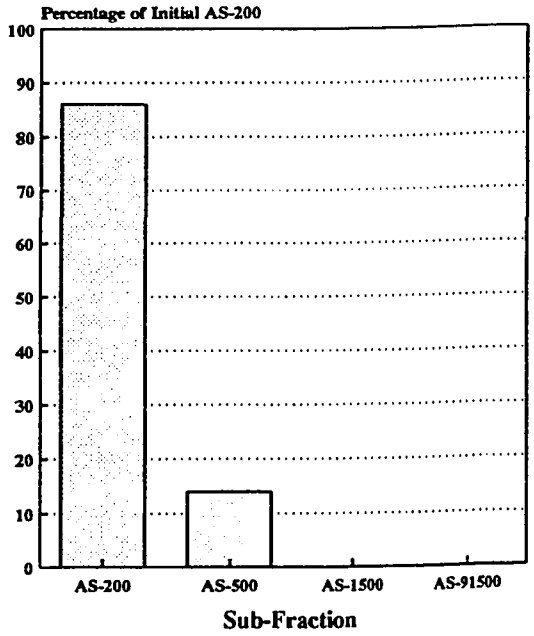

Figure 6.27

Solids Distribution of AS-500
(Before electrolytes were washed out)

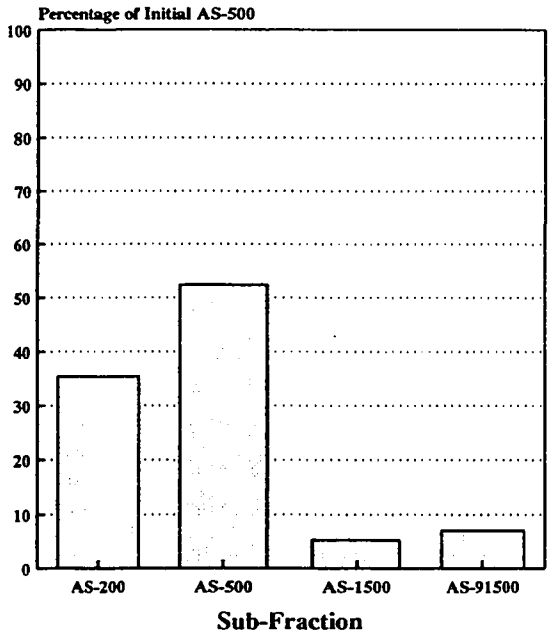

Figure 6.28

Solids Distribution of AS-1500
(Before electrolytes were washed out)

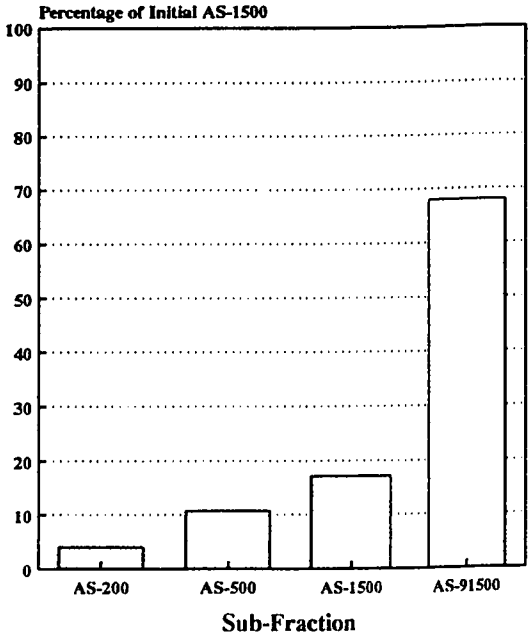

Figure 6.29

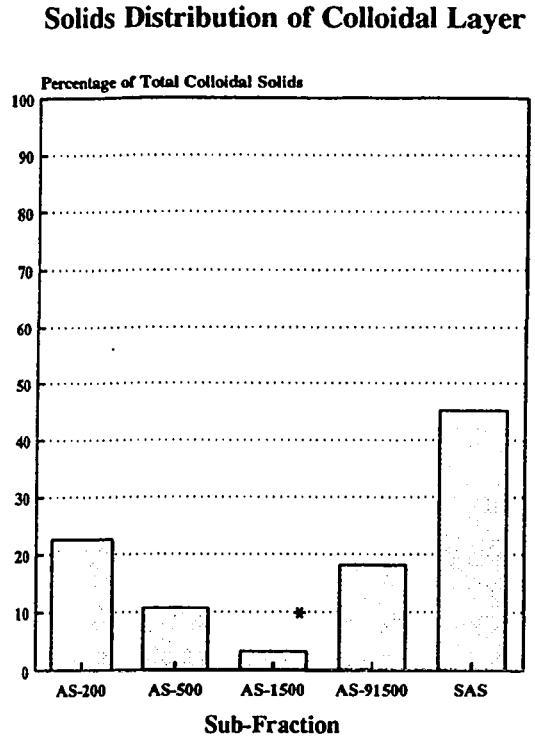

* AS-1500 was later proven to be a AS-500/AS-91500 mixture.

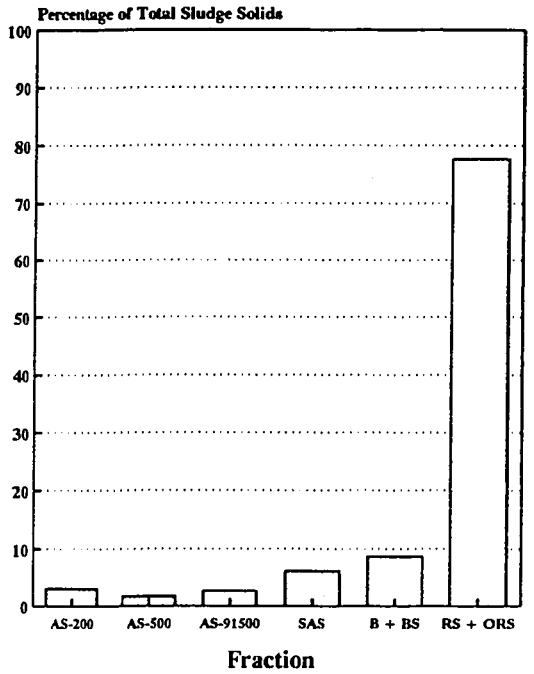

Figure 6.30: Solids Distribution of Sludge Solids.

using the XRD technique. The results showed that, for both the AS and SAS fractions, the main inorganic components were kaolinite and mica with smectite minerals present only in trace amounts. The results also showed that the poorly-crystalline character of each sub-fraction increased as particle size decreased. These results agree with those obtained from a ^{29}Si NMR study conducted by Kotlyar (1992).

TEM of the AS-500 and AS-91500 sub-fractions, as shown in Figure 6.31, indicate that the sub-fractions consist of platelets of ultrafine particles.

XPS survey spectra of the SAS-91500 and AS-91500 sub-fractions are shown in Figures 6.32 and 6.33. The spectra indicate surfaces with contributions from carbon, oxygen, aluminum, and silicon atoms. For both SAS and AS, iron was present in only trace amounts. The atomic concentrations (atomic %) of the main elements are tabulated in Table 6.4. The results from Table 6.4 show that the main difference between the SAS and AS solids was that carbon, which accounted for almost 40 atomic % of the SAS surface, as opposed to 10 atomic % for the AS surface.

Table 6.4: X-ray Photoelectron Spectroscopy of the SAS and AS Sub-Fractions.

Fraction	Atomic %				Si/Al
	C	O	Si	Al	
AS	10.0	54.0	17.3	11.5	1.5
SAS	39.7	42.9	10.2	6.3	1.6

Since the XPS technique only provides information about a surface layer having a thickness of approximately 75 Å, this technique cannot be used to differentiate between a uniform thin layer of organic matter covering the entire

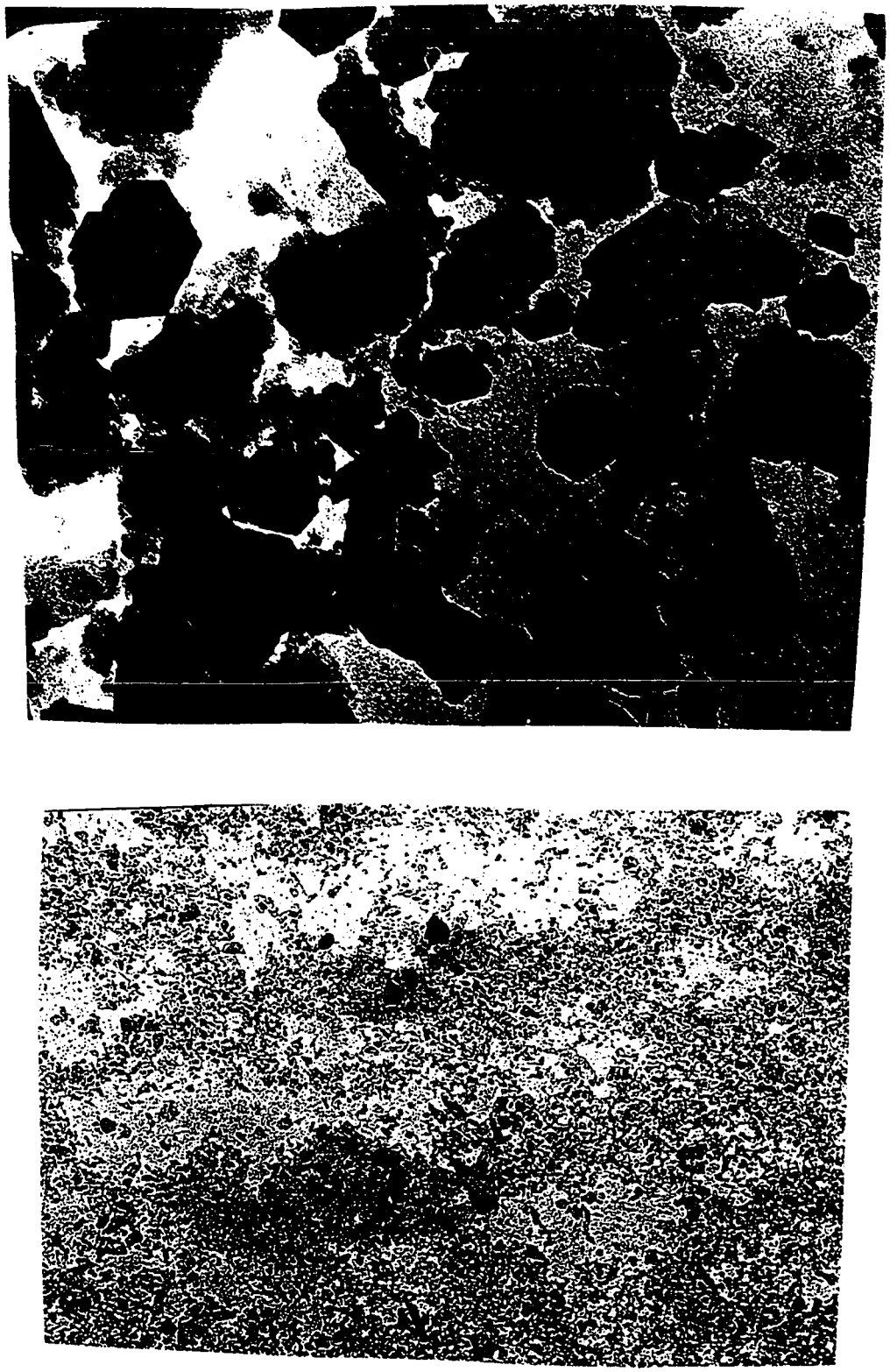

Figure 6.31: TEM of AS-500 and AS-91500 Solids.

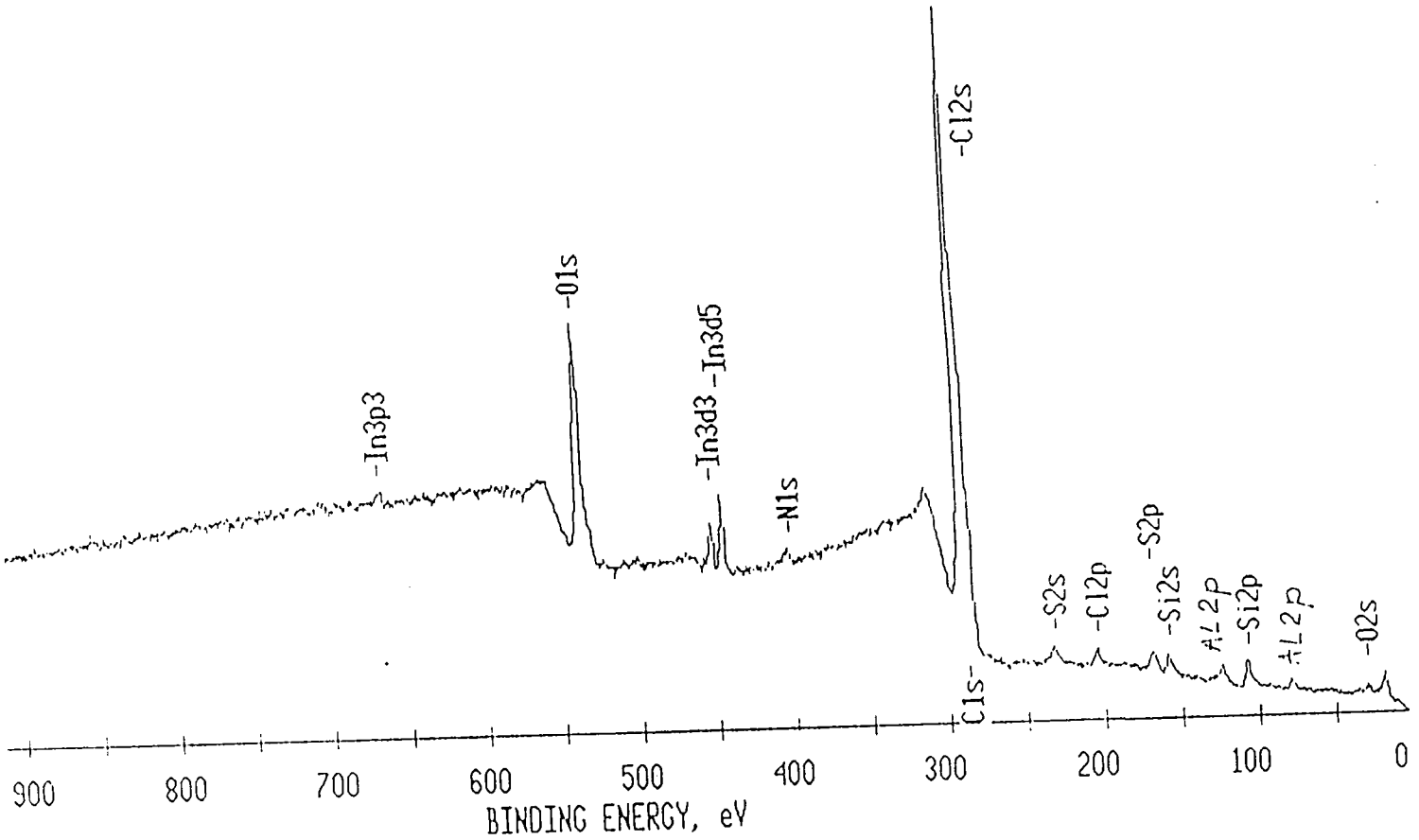

Figure 6.32: XPS Spectrum of SAS-91500.

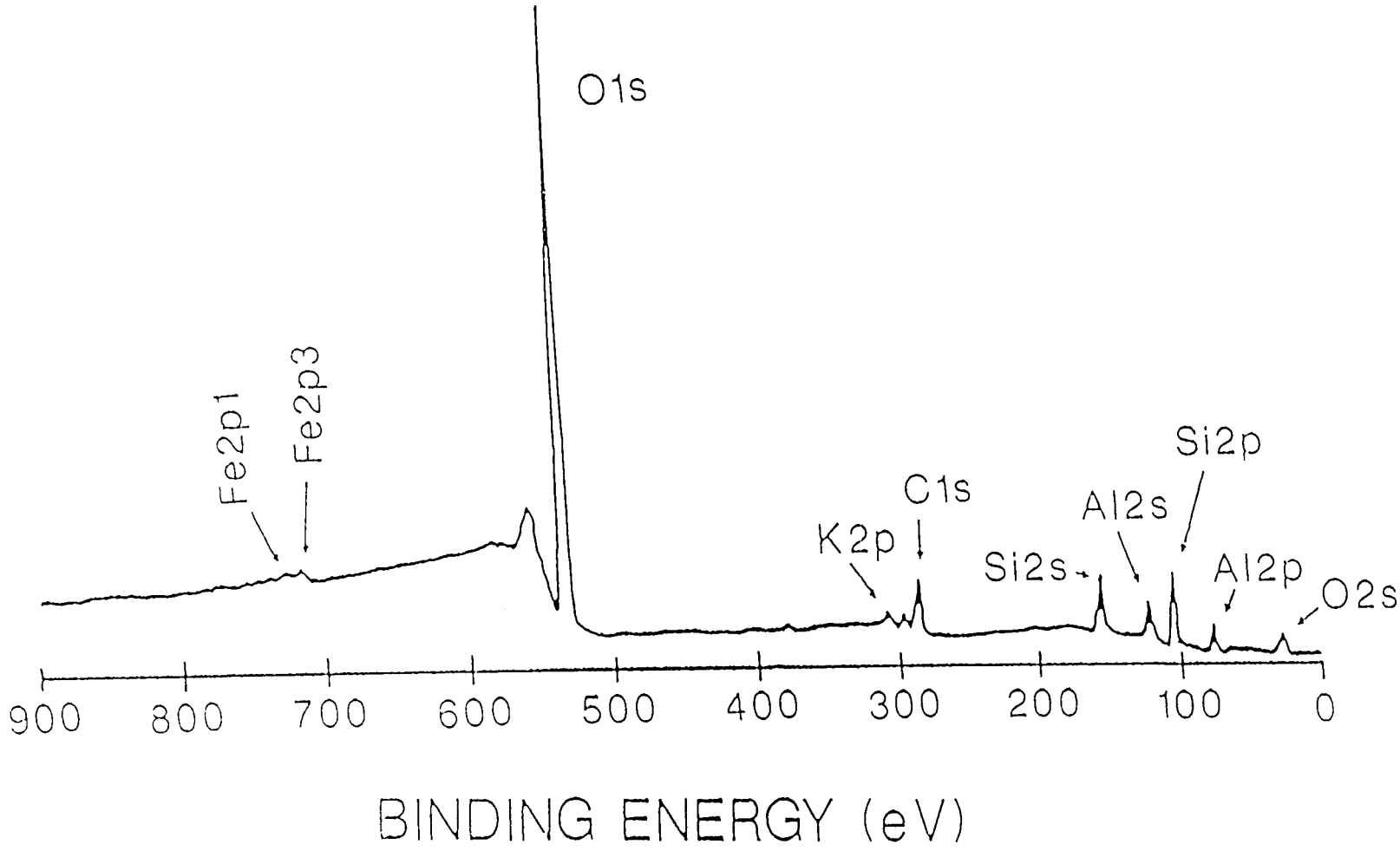

Figure 6.33: XPS Spectrum of AS-91500.

particle surface, or a patchy distribution of organic matter, where the clay minerals would be partially exposed at the surface. Information about this important aspect of sample characterization is obtainable with other techniques such as secondary ion mass spectrometry (SIMS).

The C1s peak envelope was deconvoluted into different chemical functionalities. The deconvoluted C1s peaks for SAS and AS are shown in Figures 6.34 and 6.35. The relative amounts of the functionalities were quantified and are listed in Table 6.5. However, due to the complex chemical nature of the material, the envelope is rather broad and the outline is relatively featureless. Consequently, many different deconvolutions could be generated from such an envelope. Interpretation of the deconvoluted spectra was done with caution.

Table 6.5: Results of C1s Deconvoluted for SAS and AS.

Fraction	% of Carbon				
	C-C	C-O	C=O	C=O O	$(CO_3)^{-2}$
AS	74.5	7.5	13.3	3.3	1.3
SAS	93.2	3.3	2.1	1.1	0.3

The main conclusion that was drawn from the deconvoluted spectra is related to the polarity of the organic matter. It can be inferred that the SAS organic matter displays a greater degree of hydrophobicity as the quantity of carbon atoms linked to oxygen atoms accounted for less than 7% of the total carbon signal, whereas it was approximately 25% for the AS. It appears that the organic matter on the surface of the SAS particles is orientated in such a manner that causes the external areas to be mainly hydrophobic. This difference could have important implications on the role that the SAS plays in sludge structure-forming behaviour.

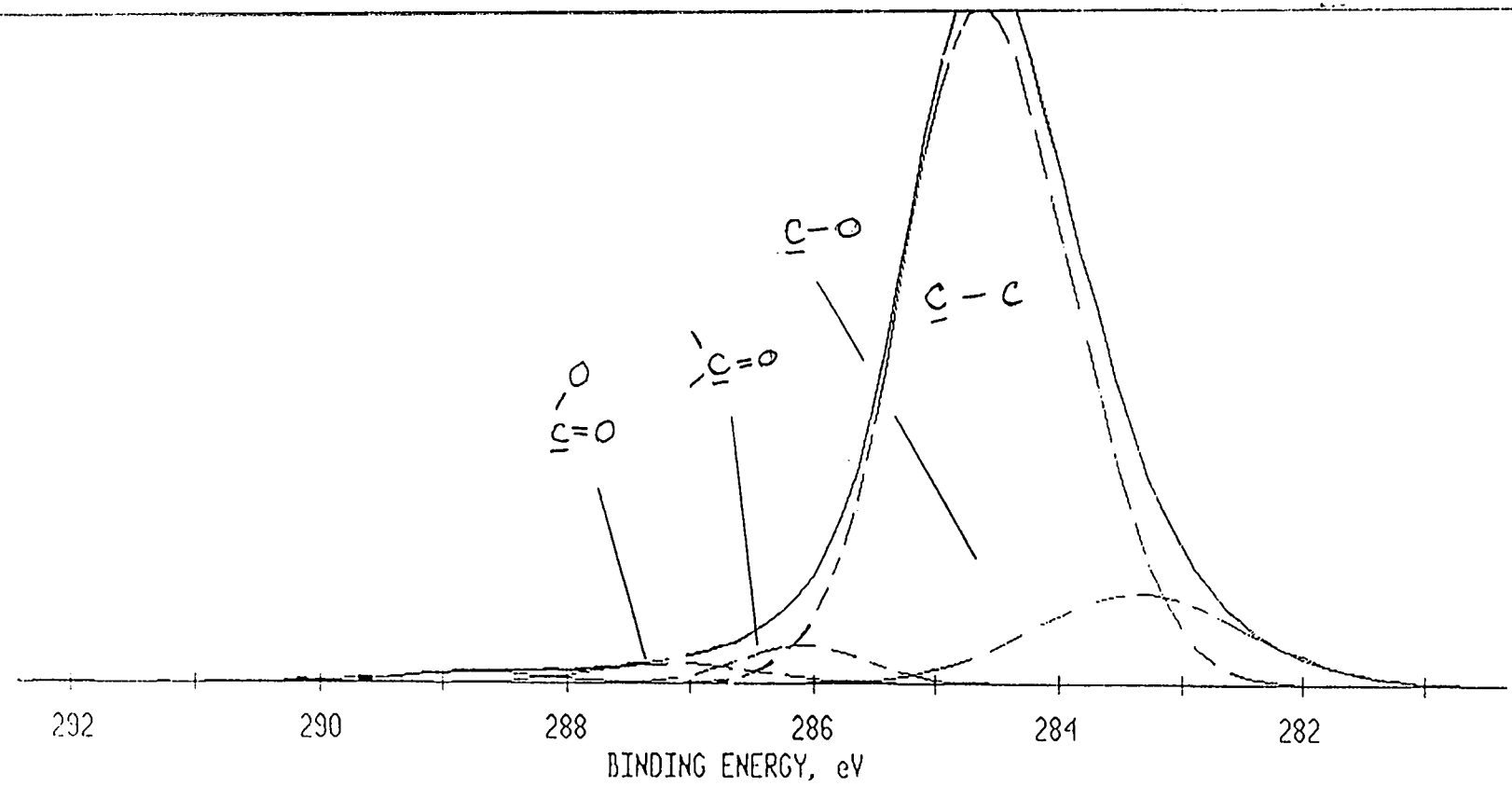

Figure 6.34: Deconvolution of Carbon XPS Peak for SAS.

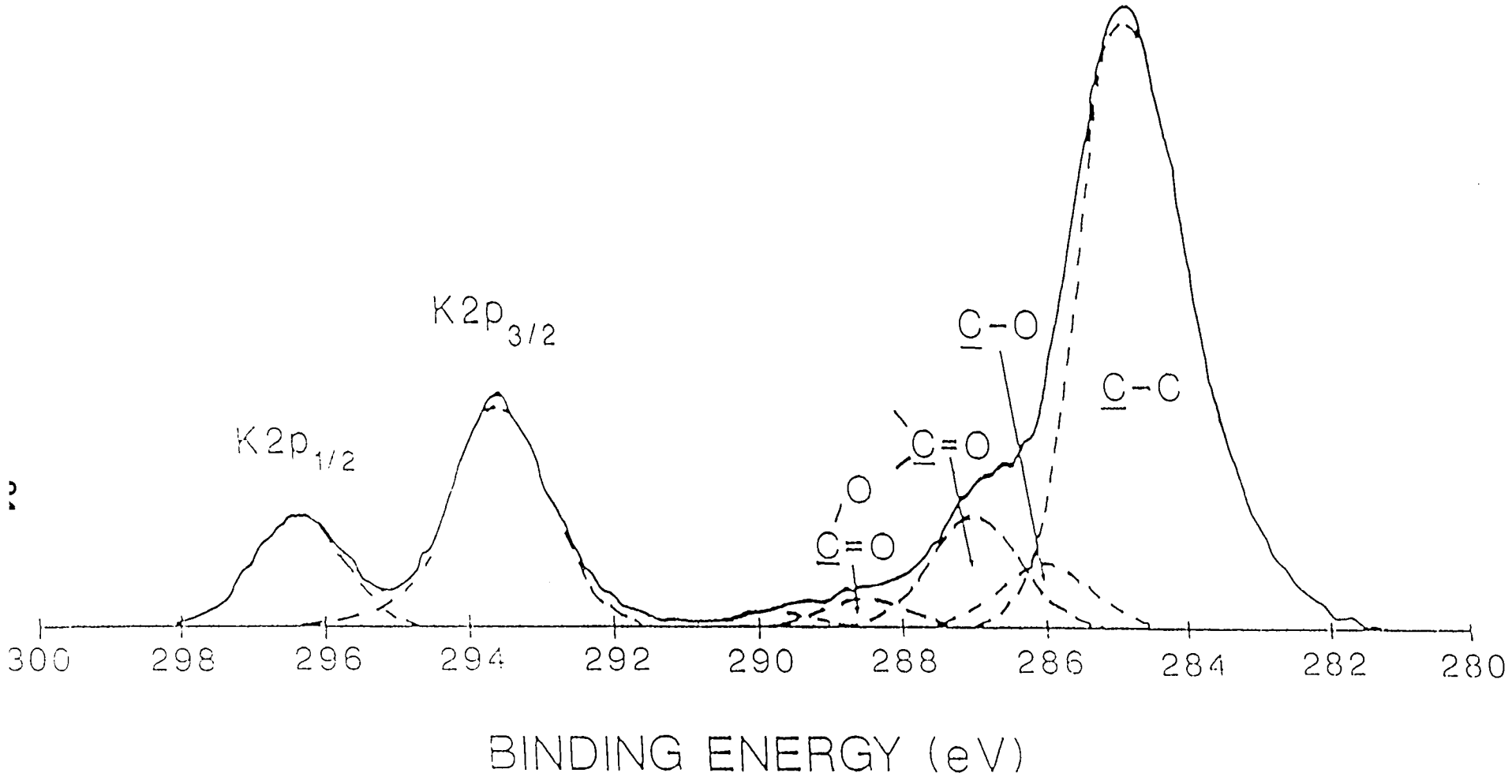

Figure 6.35: Deconvolution of Carbon XPS Peak for AS.

6.10.2 Role of SAS in the Sol to Gel Transformation

The sol to gel transformation of the A-91500 sub-fraction without SAS (AS-91500) was followed using ^2H NMR. These results were compared to those obtained for the A-91500 sub-fraction.

Figure 6.36 shows the ^2H NMR splittings plotted against concentration for various time periods. These results resemble those obtained for SAS-containing A-91500. At high concentrations, the deviation from linearity is noticeable after only 30 minutes. This is a reflection of aggregation resulting in reduced mobility and, therefore, a decrease in the splitting signal. The aggregation process progresses relatively quickly for this sub-fraction, and after 48 hours, changes in splitting for even the low concentrations ($\sim$1.0 wt%) can be seen.

Figures 6.37 and 6.38, showing the degree of aggregation over time, clearly demonstrate the effect of SAS on the sol to gel transformation for the A-91500 and AS-91500 sub-fractions. For both samples during the first 4 hours, no aggregation had occurred and, as a result, no change in the splitting signal was detected. As time progressed, the sol to gel transformation for the A-91500 samples proceeded very quickly. After 9 days the 2.0 wt% sample had reached 100%, corresponding to the state at which a stiff gel is formed. For the sample containing no SAS, AS-91500, the sol to gel transformation was much slower. After 9 days, the 2.0 wt% AS sample was only 35% aggregated.

In summary, these results show that the SAS particles significantly accelerate the sol to gel transformation. The organic matter on the surfaces of the SAS particles could be the source of additional attractive forces responsible for this observed accelerating effect. It is believed that this can be attributed to hydrophobic bonding (the tendency of nonpolar groups to adhere to one another in aqueous media).

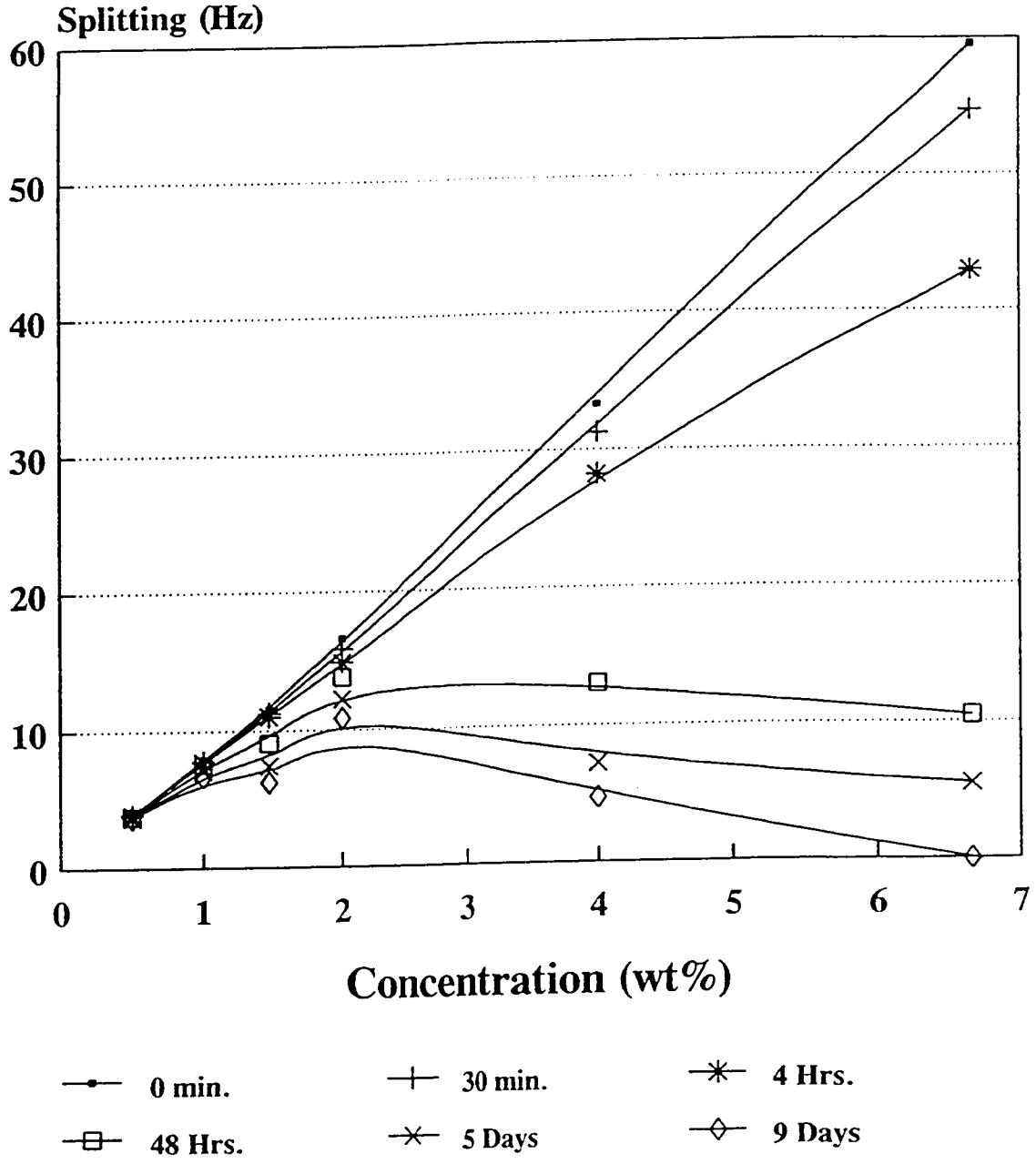

Figure 6.36: Splitting vs. Concentration for AS-91500.

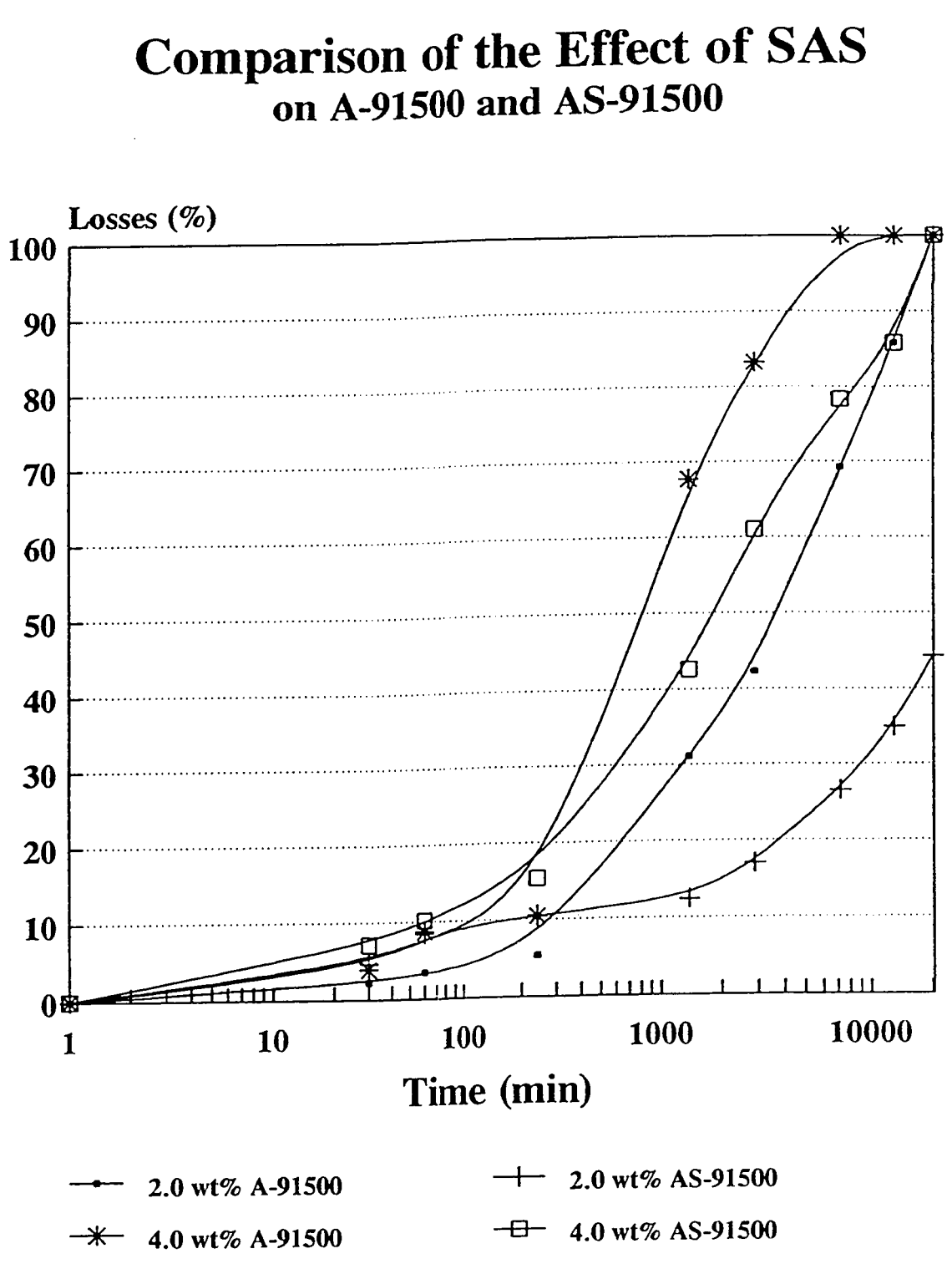

Figure 6.37: Losses vs. Time for A-91500 and AS-91500.

Comparison of the Effect of SAS
on the Sol to Gel Transformation of A-91500 and AS-91500

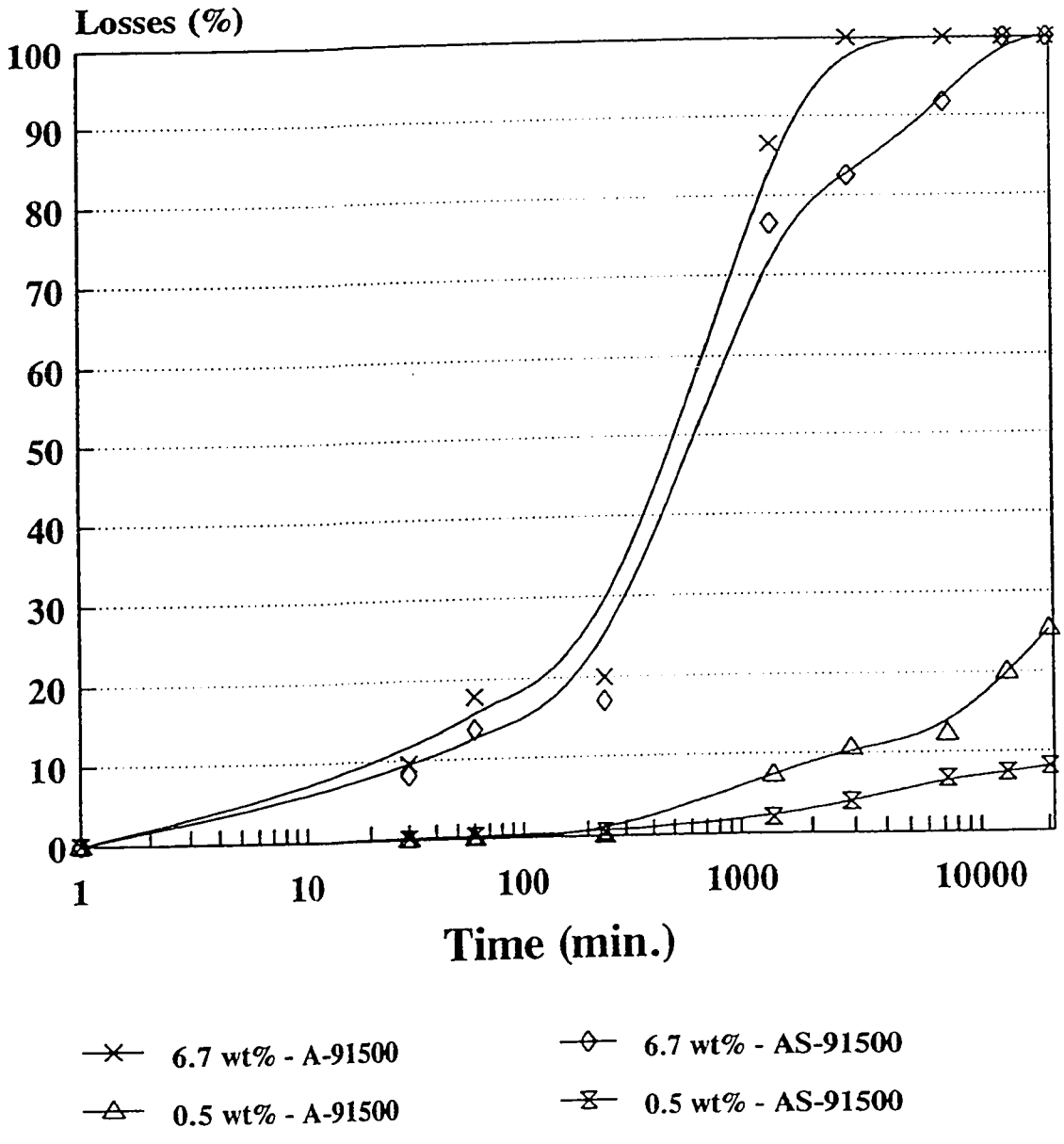

Figure 6.38: Losses vs. Time for A-91500 and AS-91500.

6.11 Effect of Water Chemistry

6.11.1 Sol to Gel Transformation in Distilled Water

The ultrafine clay particles are an integral part of oil sand sludge and cannot be avoided. It was hypothesized that sludge structure formation could be prevented by changing the water chemistry. To study the sol to gel transformation of the A-500 and A-91500 sub-fractions in distilled water, the natural electrolytes were washed out. A range of concentrations were prepared from each and the sol to gel transformation process was followed using ^{2}H NMR.

The percent change in splitting over time for A-500 and A-91500 is presented in Figures 6.39 and 6.40. These figures show that when distilled water was substituted for pond water, the sol to gel transformation was reduced significantly, if not completely halted. The results of this study prove that electrolyte concentration plays a significant role in sludge structure formation.

In distilled water the ionic atmosphere, or electrostatic double layer, around the particles is very thick and tends to screen the charges on the particles from each other. This thick double layer prevents the particles from coming close together, thereby preventing any interactions. Overall, the suspension is stable and the random movement of the particles is simply due to Brownian motion.

When pond water was substituted for distilled water, the electrolyte concentration of the aqueous media of the ultrafine particles increased, causing significant changes in the aggregation process. The increased electrolyte concentration caused the electrostatic double layer to be reduced. At this point, the particles were able to approach each other within distances where van der Waals attraction forces began to influence their interactions. When this happened, an equilibrium between attractive and repulsive forces was created. This equilibrium

Effect of Distilled Water
on the Sol to Gel Transformation of A-500

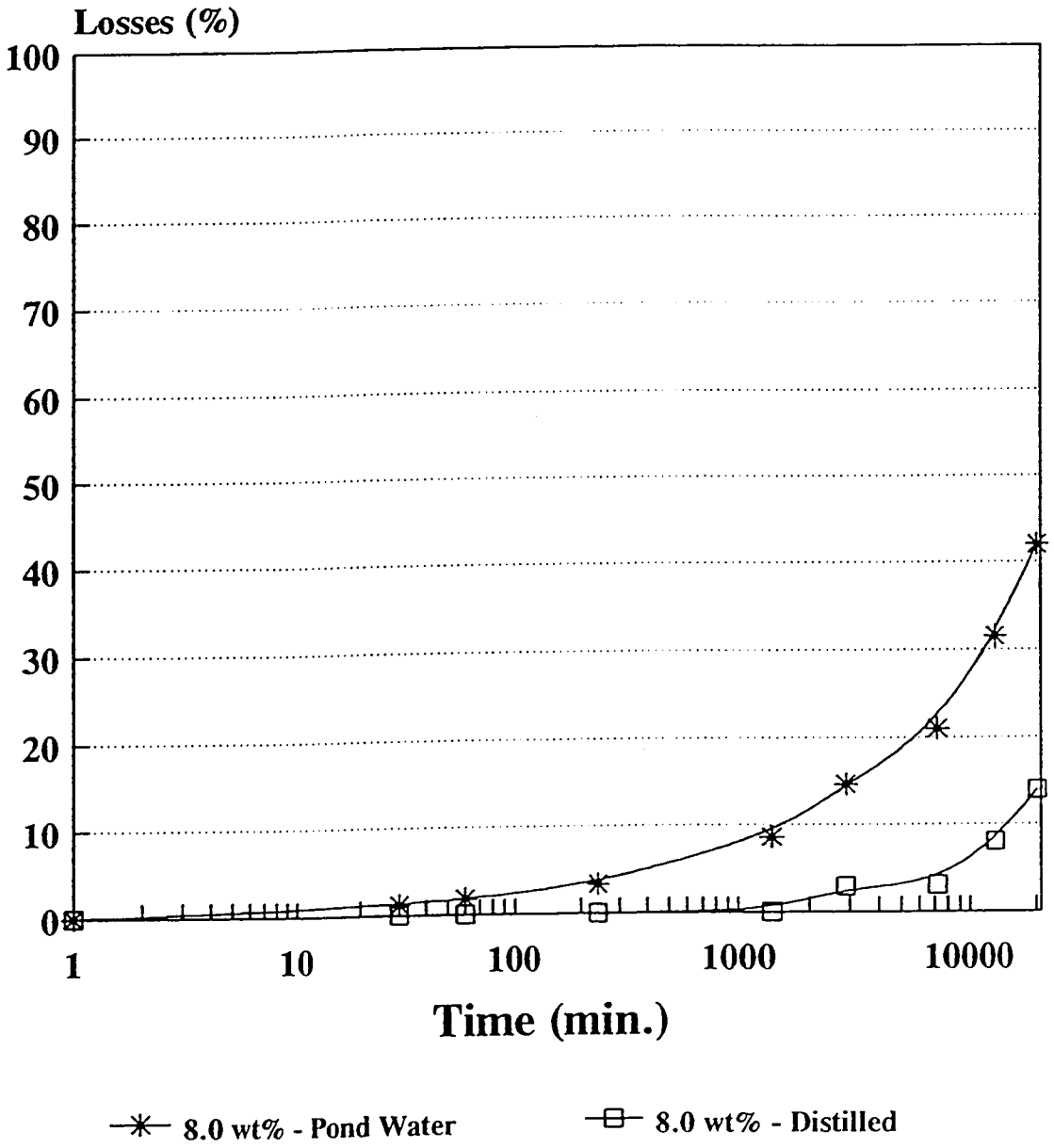

Figure 6.39: Losses vs. Time for A-500 in Distilled and Pond Water.

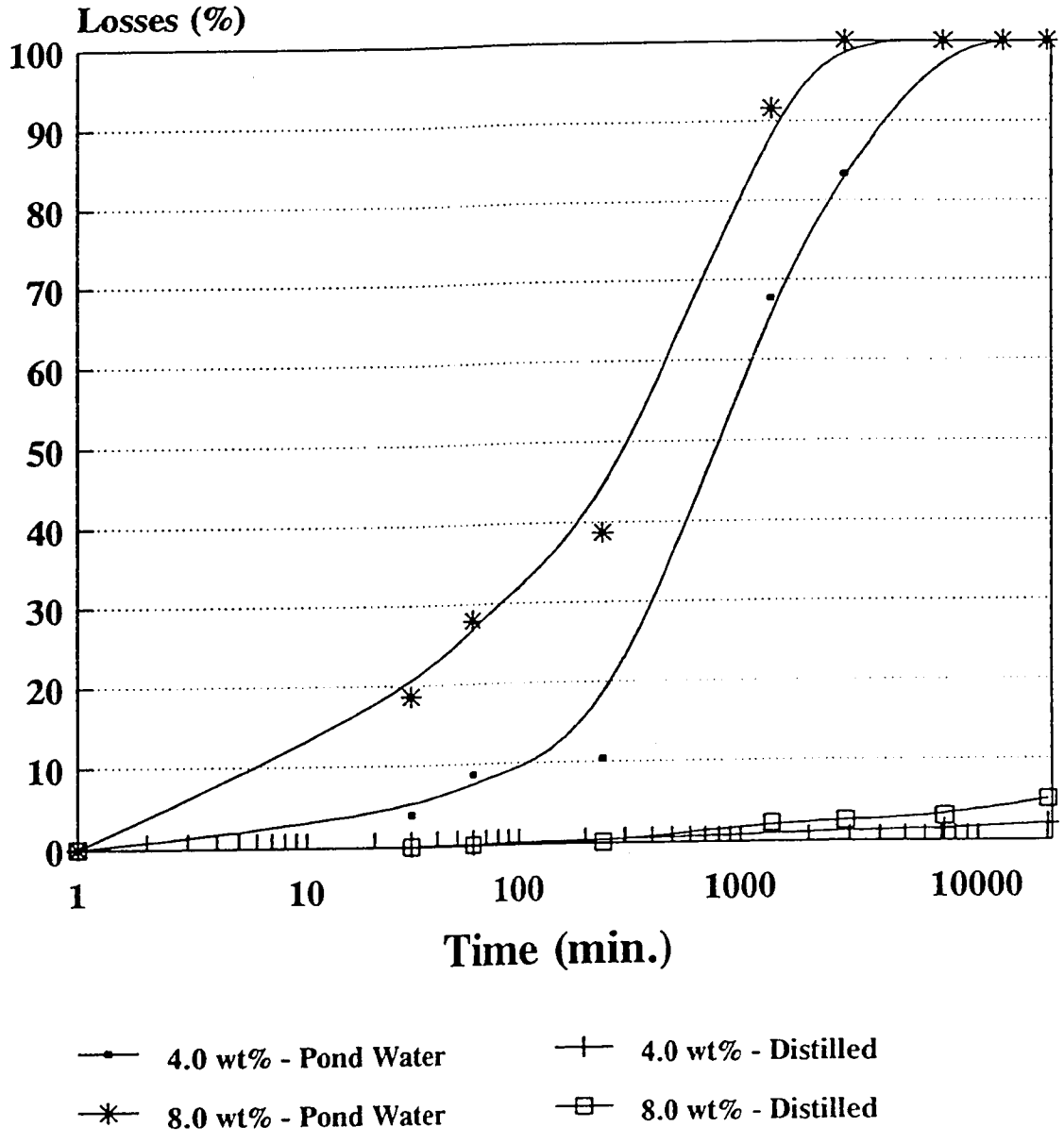

Figure 6.40: Losses vs. Time for A-91500
in Distilled and Pond Water.

appeared to be the main cause of the gel structure formation. In addition, the electrolyte concentration of the pond water caused the gel structure to exhibit thixotropic behaviour. As more particles were forced to come together, the structured network, that was being formed, caused large amounts of water to be trapped.

To summarize, in both distilled and electrolyte-containing pond water, interparticle attractive and repulsive forces operate simultaneously. The attractive forces are independent of the electrolyte concentration, but the repulsive forces decrease as the electrolyte concentration is increased. In distilled water the repulsive forces dominated, and the sol was stable (did not gel). However, in pond water the repulsive forces were reduced to the point at which the attractive forces began to be felt, and the sol to gel transformation occurred.

6.11.2 Gel To Coagulum Transformation of A-91500

During the sedimentation tests containing $AlCl_3$ and $CaCl_2$ coagulation occurred immediately. There was an immediate separation between a sediment and a clear supernatant. The supernatant liquid did not appear to contain any particulate solids and the transition between the two layers was very sharp. The position of the interface was read every two hours for the first twelve hours, and then once a day for two weeks.

After the two layers were formed, the interface moved downwards at a fairly constant rate for approximately two days. After two days, a progressive transition seemed to occur towards an aging period, where the sediment underwent a slow syneresis. The liquid-like sediment decreased extremely slowly after this point. These results are similar to those obtained by Zou and Pierre (1991) during their settling studies of montmorillonite clays.

During the sedimentation test containing NaCl, minimal settling of the solids could be observed. By the end of two weeks, only a very small amount of

supernatant was released from the suspension.

The effects of $AlCl_3$, $CaCl_2$, and NaCl on the sedimentation rate of 2.0 wt% of A-91500 suspensions are shown in Figure 6.41. The data indicate that the initial constant sedimentation rate increases and the final sediment volume decreases with cation valency. This is in qualitative agreement with the Schulze-Hardy rule. The rule states that the coagulative power of an electrolyte is determined by the valency of one of its ions, and the coagulating ion is always of opposite electrical sign to that of the particles. In these experiments, the cations are the predominant counter-ions, which is in agreement with the classical picture of plate-like clays having a net negative charge.

As the valency of the counter-ion was increased, the surface double layer around each clay particle became thinner, thereby allowing the van der Waals attraction forces to dominate. Collisions between the particles led to the formation of dense, compact aggregates which settled under gravity.

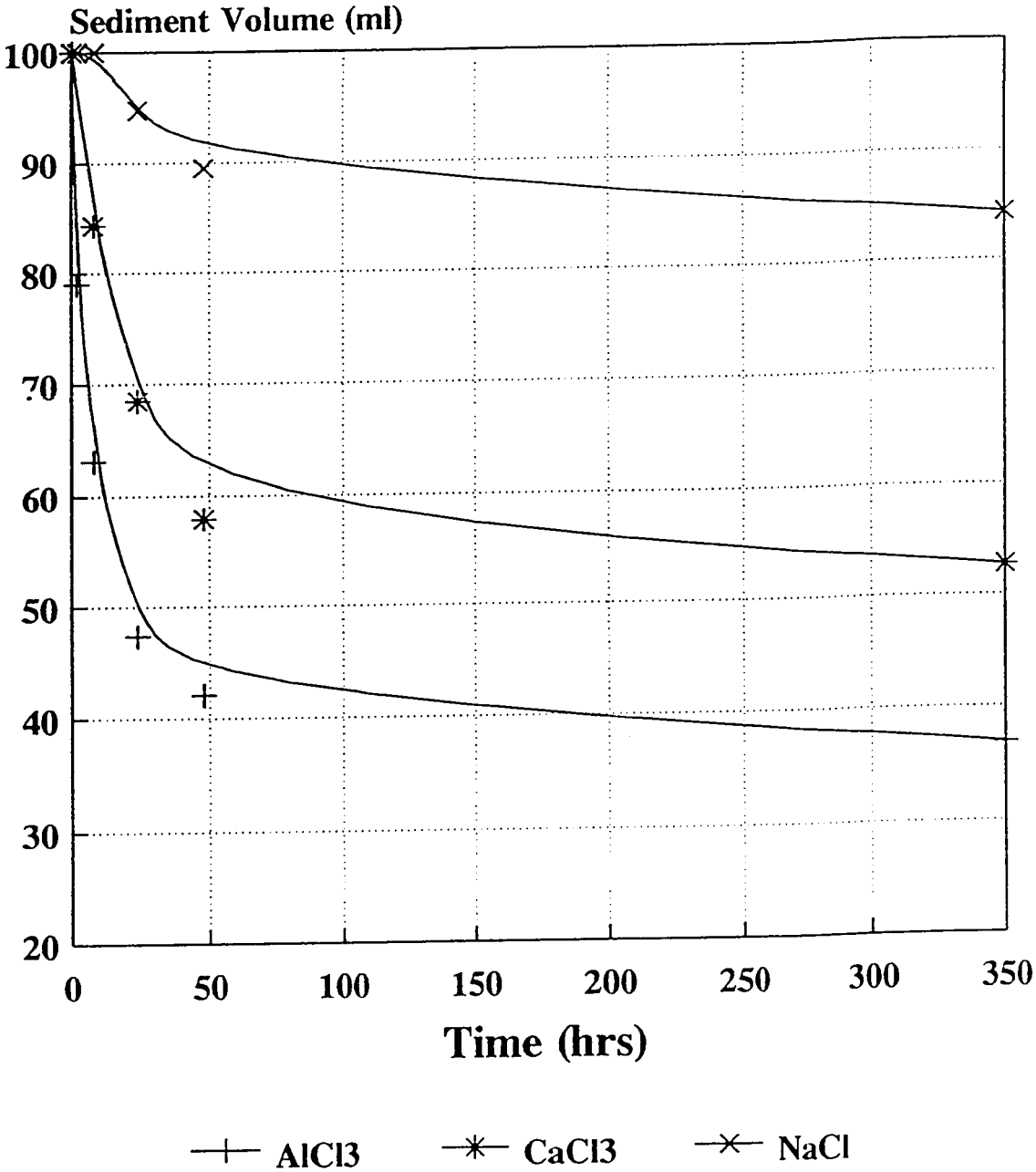

Figure 6.41: Sediment Volume vs. Time for A-91500

Chapter 7

Formation and Structure of Ultrafine Clay Particle Sol, Gel, and Coagulum

On the basis of the previous water chemistry studies, the following section is a summary of the particle interactions at different electrolyte concentrations.

Our studies of the ultrafine clay particles in distilled water showed that in this electrolyte-free environment, the face and edge double layers were sufficiently well developed to prevent any particle association by van der Waals attraction forces. As a result, the clay suspension remained in the state of a stable sol.

In the presence of pond water, having a pH of approximately 8.4[3], the double layers were compressed, reducing the electrostatic repulsion. The particles were able to approach each other within distances where the van der Waals attraction forces became active. As mentioned earlier, an equilibrium between attractive and repulsive forces appears to be set up and, thereby, causes the clay suspension to undergo a sol

[3] The clay particle surface is negatively charged and, at a pH of 8.4, the edges of the clay particle are also negatively charged (Swartzen-Allen and Matijevic, 1973).

to gel transformation. This process seems to occur at a shallow potential minimum (the secondary minimum on the DLVO potential diagram), thereby explaining why the gel network can be broken so easily by weak agitation.

At the electrolyte concentration of pond water, a three-dimensional structure was formed; therefore, it is proposed that two types of particle associations may be occurring: edge-to-face and edge-to-edge. The cubic card house structure formed by edge-to-face associations would consist of parallel plates held together by cross-linking particles perpendicular to the parallel plates.

It is, however, suspected that edge-to-edge associations are dominating. During similar studies of clay particle associations, Fukasawa and Tsujii (1988) stated that according to the DLVO theory, the potential curve of interaction between two particles has a maximum (V_{max}) to make a barrier against access of two particles. This V_{max} value, expressed in potential energy per unit area, is similar between the edge-to-edge and face-to-edge interactions. Therefore, the potential energy barrier between edge-to-edge interaction per particle would be lower than that between edge-to-face because of the smaller area of an edge than that of a face. These edge-to-edge associations would lead to the formation of ribbon-like aggregates. As these ribbons grow by the attachment of additional particles, they would begin to interact with each other by bridging. Eventually, a three-dimensional network structure of the ribbons would be created. Furthermore, Fukasawa and Tsujii stated that if aggregation of the ribbons had occurred at the primary minimum, a dispersion of strongly coagulated particles would be formed instead of a weak gel network.

Finally, additional electrolytes were added to the ultrafine clay suspension until coagulation was induced. The double layer of the negatively charged face was further compressed, bringing the particles into the primary minimum interaction range. Face-to-face association appears to have resulted and a dense sediment was formed, allowing significant amounts of water to be released.

Chapter 8

Conclusions

1. Ultrafine clay particles, capable of forming a highly porous, three-dimensional gel network, are the main components responsible for structure formation in Athabasca oil sand sludge.

2. The ultrafine particles are aluminosilicate clays, kaolinite and mica, with particle sizes in the range of 10 to 200 nm.

3. The ultrafine clay particles are able to form a gel in a very short time period (1 to 14 days), within which a large amount of water is trapped, and bitumen, fine and coarse solids become embedded.

4. The rigorous colloidal layer separation scheme, which was developed, does not alter the properties of the ultrafine clay particles.

5. The ^{2}H NMR technique was sensitive enough to accurately and effectively monitor the sol to gel transformation process within oil sand sludge. As well, the ^{2}H NMR data can be used to determine the gel onset concentration.

6. Particle size has a significant effect on the sol to gel transformation process. The gel forming propensity increases as particle size decreases. A decrease in particle size causes both the concentration of ultrafine particles and time required to form a stiff gel to decrease.

7. Gel formation for mixtures of different particle sizes was shown to be an additive property with no additional interactions occurring between the gel forming ultrafine clay particles.

8. The presence of coarse solids slows the rate of the sol to gel transformation process.

9. Removal of the poorly-crystalline inorganic components did not affect the gel forming propensity of the ultrafine clay particles.

10. The ultrafine clay particles can be separated into hydrophilic (AS) and biwetted (surface active solids, SAS) ultrafine particles. The SAS ultrafine particles significantly accelerate the rate of the sol to gel transformation. It appears that this is caused by hydrophobic bonding.

11. Water chemistry plays a significant role in sludge structure formation. The ultrafine clay particles could not gel in distilled water.

12. A gel to coagulum transformation was induced by significantly increasing the electrolyte concentration of the aqueous media. The sedimentation kinetics results from the gel to coagulum transformation study were in qualitative agreement with the Schulze-Hardy rule.

Chapter 10

Recommendations For Future Work

Carbon represented more than 40 atomic % of the particle surfaces of the SAS sub-fractions. As yet it is not known whether this organic matter completely covers the surfaces or occurs as patches of organics over the surfaces. It is recommended that these sub-fractions be investigated using secondary mass spectrometry.

Large quantities of electrolytes were added to the ultrafine clay suspension until coagulation was induced. Face-to-face association appears to have resulted and a dense sediment was formed, allowing significant amounts of water to be released. It is recommended that further coagulation studies be conducted. These studies could determine which electrolyte is most effective and the optimum coagulation concentration required.

References

AOSTRA, "AOSTRA: A 15 Year Portfolio of Achievement", AOSTRA Information Services, Calgary, Alberta, 26-27 (1990).

Babchin, A., V. Reitman, and K. Rispler, "Settling of Synthetic Sludges and Kaolinites", The Petroleum Society of CIM and AOSTRA 1991 Technical Conference, 21-24 April, 1991, Banff, Alberta, **91-127**, 1-7 (1991).

Biermans, V. and L. Baert, "Selective Extraction of the Amorphous Al, Fe, and Oxides Using an Alkaline Tiron Solution", Clay Minerals, **12**, 127-135 (1977).

Brinker, C.J. and G.W. Scherer, "Sol-Gel Science", Academic Press, Toronto (1990).

Camp, F.W., "Processing Athabasca Tar Sands - Tailings Disposal", The Canadian Journal of Chemical Engineering, **55**, 5, 581-591 (1977).

Clark, K.A., "Canadian Patent: Process of Extracting Oil From Tar Sands", File 27.A-54I, PRC 81/26, Item 184,PAA (1948).

Darcovich, K., L.S. Kotlyar, W.C. Tse, J.A. Ripmeester and B.D. Sparks "Wettability Study of Organic Rich Solids Separated From Athabasca Oil Sands", Energy and Fuels, **3**, 386-391 (1989).

Degens, E.T., "Geochemistry of Sediments", Prentice-Hall Inc., New Jersey (1965).

Derjaguin, B., and L.D. Landau, "Acta Physicochim. U.R.S.S.", Journal of Experimental and Theoretical Physics, **14**, 635-650 (1941) (reprinted **15**, 662, 1945).

Everett, D.H., "Basic Principles of Colloid Science", Royal Society of Chemistry Paperbacks, London (1988).

EVS Consultants, "The Microbial Characteristics of Oil Sands Tailings Sludge", EVS Consultants' Report No. 3/532-01, Prepared For AOSTRA, Calgary, Alberta, 1-8 (1992).

Fitzgerald, J.J., "Black Gold With Grit", Gray's Publishing Ltd., Sidney, British Columbia (1978).

Fukasawa, J. and K. Tsujii, "Higher-Order Structure Formation of Ultrafine Boehmite Particles in Sols, Gels, and Dried Materials", Journal of Colloid and Interface Science, **125**, 1, 155-161 (1988).

Grandjean, J., and P. Laszlo, "Deuterium Nuclear Magnetic Resonance Studies of Water Molecules Restrained by Their Proximity to a Clay Surface", Clay and Clay Minerals, **37**,5, 403-408 (1989).

Grandjean, J., and P. Laszlo, "Multinuclear Magnetic Resonance Studies of Structure and Dynamics at the Interface of Clay Materials", Spectroscopic Characteristics of Minerals and Their Surfaces, American Chemical Society, Washington, D.C. (1990).

Hakala, M.R. and T.C. Wong, "Phase Structure and Orientational Order of Water in the Lyotropic Mesophase of the Hexadecyltriethyl-Ammonium Bromide-Water-Pentanol System by Deuterium and Oxygen-17 NMR", Langmuir, **2**, 83-89 (1986).

Hall, E.S. and E.L. Tollefson, "Stability of Oil Sand Sludge", Energy Processing, **72**, 38 (1980).

Hartman, R.J., "Colloid Chemistry", Houghton Mifflin Company, New York (1934).

Iler, R.K., "The Chemistry of Silica", John Wiley and Sons, New York, (1979).

Israelachvili, J.N., "Adhesion Forces Between Surfaces in Liquids and Condensable Vapours", Surface Science Reports, **14**, 3, 109-159 (1992).

Kessick, M.A., "Structure and Properties of Oil Sands Clay Tailings", The Journal of Canadian Petroleum Technology, **1**, 49-52 (1979).

Kodama, H. and G.J. Ross, "Application of the Tiron Dissolution Method to Remove and Characterize Poorly Crystalline and Noncrystalline Inorganic Components in Soils", Soil Science Society American Journal, 1-25 (1991).

Kotlyar, L.S., A. Majid, and B.D. Sparks, "A Study of Factors Affecting the Stability of Tailings Sludge Produced by the Hot Water Bitumen Extraction

Process", The Petroleum Society of CIM and AOSTRA 1991 Technical Conference,21-24 April, 1991, Banff, Alberta, **91-117**, 1-16 (1991).

Kotlyar, L.S., B.D. Sparks, and H. Kodama, "Isolation and Characterization of Organic Rich Solids Present in Athabasca Tailings Pond Sludge", AOSTRA Journal of Research, **9**, 1-17 (1990).

Kotlyar, L.S., "Gel Forming Attributes of Colloidal Solids From Fine Tails Formed During Extraction of Bitumen From Athabasca Oil Sands by the Hot Water Extraction Process", Report to Fine Tails Fundamentals Consortium c/o AOSTRA (in press) (1992).

Kotlyar, L.S., "Gel Forming Propensity of Ultrafines From Fine Tails in Distilled and Pond Water", Report to Fine Tails Fundamentals Consortium c/o AOSTRA (in press) (1992).

Metcalf and Eddy, Inc., "Wastewater Engineering: Treatment, Disposal, and Reuse", 3rd Ed., McGraw-Hill Publishing Co., Toronto (1991).Mikula, R.J., C. Payette,

V. Munoz, and W.W. Lam, "Microscopic Observation of Structure in Oil sand Sludge", The Petroleum Society of CIM and AOSTRA 1991 Technical Conference, 21-24 April, 1991, Banff, Alberta, **91-120**, 1-9 (1991).

NEDAPAC, "Some Methods For Treating Tar Sands Tailings - Part 1", National Engineering Design and Planning and Computation Co. Ltd, Edmonton, Alberta, 1-5 (1973).

Parfitt, G.D., "Dispersion of Powders in Liquids", 3rd Ed., Applied Science, London (1981).

Pashley, R.M., "Hydration Forces Between Mica Surfaces in Aqueous Electrolyte Solutions:, Journal of Colloid and Interface Science, **80**, 1, 153-162 (1981).

Ripmeester, J.A., L.S. Kotlyar, and B.D. Sparks, "^{2}H NMR and the Sol to Gel Transition in Suspensions of Colloidal Clays", Colloids and Surfaces, (in press), (1992).

Schutte, R., J.A. Czarnecki, and J.K. Liu, "Structure of Sludge", The Petroleum Society of CIM and AOSTRA 1991 Technical Conference, 21-24 April, 1991, Banff, Alberta, **91-119**, 1-9 (1991).

Scott, J.D., and M.B. Dusseault, "Behaviour of Oil Sand Tailings Sludge", The Petroleum Society of CIM, 33rd Annual Technical Meeting, Calgary, Alberta, 1-20 (1982).Searle, A.B. and R.W. Grimshaw, "The Chemistry and Physics of

Syncrude Canada Ltd, "Syncrude Analytical Methods For Oil Sand and Bitumen Processing", Syncrude Research Co., Edmonton, Alberta, **58** (1979).

Tadros, T.F., "The Effect of Polymers on Dispersion Properties", Academic Press, New York, (1982).

Van de Ven, T.G.M., "Colloidal Hydrodynamics", Academic Press, New York (1989).

Van Olphen, H., "An Introduction to Clay Colloid Chemistry", Interscience Publishers, New York, 1st Ed. (1963).

Van Olphen, H., "An Introduction to Clay Colloid Chemistry", Interscience Publishers, New York, 2nd Ed. (1976).

Van Olphen, H., "An Introduction to Clay Colloid Chemistry", Interscience Publishers, New York, 3rd Ed. (1990).

Verwey, E.J. and J.T.G. Overbeek, "Theory of the Stability of Lyophobic Colloids", Elsevier, New York (1948).

Viani, B.E., P.F. Low, and C.B. Roth, "Relation Between Interlayer Force and Interlayer Distance in the Swelling of Montmorillonite", Journal of Colloid and Interface Science, **96**, 1, 229-244 (1984).

Woessner, D.E. and B.S. Snowden, Journal of Colloid and Interface Science, **30**, 54-60 (1969).

Wong, T.C. and M.R. Hakala, "On the Determination of the Orientational Probability Distribution of Water in Heterogeneous Systems From ^{2}H and ^{17}O Quadrupolar Splittings", Chemical Physics Letters, **119**, 85-88 (1985).

Yong, R.N. and A.J. Sethi, "Mineral Particle Interaction Control of Tar Sand Sludge Stability", The Journal of Canadian Petroleum Technology, **17**, 4, 76-83 (1978).

Zou, J. and A.C. Pierre, "Mixture of Colloidal and Non-Colloidal Particles: Packing Patterns of Montmorillonite Particles in Aqueous Media", Journal of the Canadian Ceramic Society, **60**, 3, 51-56 (1991).

Appendix A

Mass Balances

SLUDGE FRACTIONATION USING DISTILLED WATER

Mass Balance on Suncor Sludge

Table A.1: Solids Distribution of A-200 Sub-Fraction

Fraction	% of Initial A-200 Sub-Fraction (Dry Basis)	% of Total Sludge (Dry Basis)	Solids Content, %
A-200	72.6	3.68	38.03
A-500	16.5	0.84	18.47
A-1500	6.5	0.33	9.06
A-91500	4.4	0.23	0.104
Total =	**100 %**	**5.08 %**	

Table A.2: Solids Distribution of A-500 Sub-Fraction

Sub-Fraction	% of Initial A-500 Sub-Fraction (Dry Basis)	% of Total Sludge (Dry Basis)	Solids Content, %
A-200	29.62	1.80	22.62
A-500	40.63	2.46	24.78
A-1500	12.14	0.74	11.24
A-91500	17.61	1.07	0.44
Total =	**100 %**	**6.07 %**	

Table A.3: Solids Distribution of A-1500 Sub-Fraction

Sub-Fraction	% of Initial A-1500 Sub-Fraction (Dry Basis)	% of Total Sludge (Dry Basis)	Solids Content, %
A-200	0.0	0.0	N/A
A-500	35.91	0.70	12.96
A-1500	24.63	0.48	9.22
A-91500	39.46	0.76	0.373
Total =	**100 %**	**1.94 %**	

Table A.4: Total Solids Distribution of Suncor Oil Sand Sludge.

Fraction	% of Total Sludge (Dry Basis)
Free B + BS	8.72
Sediment	77.74
A-200	5.48
A-500	4.00
A-1500	1.55[a]
A-91500	2.51[b]

[a] Further study showed that A-1500 was a flocculated mixture of A-500 and A-91500 (57 wt% and 43 wt%, respectively).

[b] 2.51 wt% = 0.76 (from initial A-200) + 1.07 (from initial A-500) + 0.23 (from initial A-1500) + **0.45** (from initial A-91500 - could not be separated further into other sub-fractions).

SLUDGE FRACTIONATION USING DISTILLED WATER

Mass Balance on Suncor Sludge With SAS Removed

Table A.5: Solids Distribution of AS-200 Sub-Fraction.

Sub-Fraction	% of AS-200 Sub-Fraction	% of Total Sludge (Dry Basis)	Solids Content, %
AS-200	86.0	2.44	29.05
AS-500	14.0	0.40	12.52
AS-1500	0	0	-
AS-91500	0	0	-
Total =	**100 %**	**2.84 %**	

Table A.6: Solids Distribution of AS-500 Sub-Fraction.

Sub-Fraction	% of AS-500 Sub-Fraction (Dry Basis)	% of Total Sludge (Dry Basis)	Solids Content, %
AS-200	35.41	0.56	15.03
AS-500	52.33	0.82	16.82
AS-1500	5.25	0.08	4.79
AS-91500	7.01	0.11	0.06
Total =	**100 %**	**1.57 %**	

Table A.7: Solids Distribution of AS-1500 Sub-Fraction.

Sub-Fraction	% of AS-1500 Sub-Fraction (Dry Basis)	% of Total Sludge (Dry Basis)	Solids Content, %
AS-200	4.04	0.08	3.49
AS-500	10.78	0.22	7.86
AS-1500	17.22	0.35	10.68
AS-91500	67.96	1.39	0.29
Total =	**100 %**	**2.04 %**	

Table A.8: Total Solids Distribution of Suncor Oil Sand Sludge.

Fraction	% of Total Sludge (Dry Basis)
Free B + BS	8.72
Sediment	77.74
SAS	6.12
AS-200	3.08
AS-500	1.44
AS-1500	0.43[c]
AS-91500	2.47[d]

[2c] Further study showed that AS-1500 was a flocculated mixture of AS-500 and AS-91500 (57 wt% and 43 wt%, respectively).

[d] 2.47 wt% = 0.11 (from initial AS-500) + 1.39 (from initial AS-1500) + **0.97** (from initial AS-91500 - could not be separated further into other sub-fractions).

Appendix B

^{2}H NMR Residual Splitting Data

SUNCOR COLLOIDAL SUB-FRACTIONS

^{2}H NMR RESIDUAL SPLITTING DATA

B.1) A-200 Sub-Fraction in Pond Water:

Conc. wt%	0 min.	30 min.	1 Hr.	4 Hrs.	23 Hrs.	48 Hrs.	5 Days	9 Days	14 Days
1.93	0	0	0	0	0	0	0	0	0
6.15	0	0	0	0	0	0	0	0	0
9.77	0	0	0	0	0	0	0	0	0
13.65	0	0	0	0	0	0	0	0	0

B.2) A-200 Sub-Fraction in Distilled Water

Conc. wt%	0 min.	30 min.	1 Hr.	4 Hrs.	23 Hrs.	48 Hrs.	5 Days	9 Days	14 Days
2.0	0	0	0	0	0	0	0	0	0

6.0	0	0	0	0	0	0	0	0	0
9.8	0	0	0	0	0	0	0	0	0

B.3) A-500 Sub-Fraction in Pond Water

Conc. wt%	0 min.	30 min.	1 Hr.	4 Hrs.	23 Hrs.	48 Hrs.	5 Days	9 Days	14 Days
0.52	3.08	3.05 0.990	3.05 0.990	3.05 0.990	3.034 0.985	3.015 0.979	2.981 0.968	2.957 0.960	2.47 0.80
1.0	5.73	5.73 1.00	5.73 1.00	5.72 0.998	5.70 0.994	5.63 0.983	5.37 0.937	5.174 0.903	5.02 0.88
1.53	9.31	9.276 0.996	9.276 0.996	9.254 0.994	9.13 0.981	8.97 0.963	8.79 0.944	8.072 0.867	7.64 0.82
2.02	12.51	12.50 0.999	12.46 0.995	12.39 0.990	12.18 0.974	11.90 0.951	11.72 0.937	10.65 0.851	10.1 0.81
3.41	21.46	21.16 0.986	21.16 0.986	21.06 0.981	20.63 0.961	20.49 0.954	20.02 0.933	17.23 0.803	16.3 0.76
6.00	38.73	38.30 0.989	38.06 0.983	37.76 0.975	36.79 0.950	35.21 0.909	32.72 0.845	28.58 0.738	25.3 0.65
7.98	52.56	51.92 0.988	51.60 0.982	50.83 0.967	48.06 0.914	44.82 0.853	41.51 0.790	36.00 0.685	30.5 0.58
20.22	155.1	149.8 0.966	144.5 0.931	142.7 0.920	112.6 0.726	90.11 0.581	82.51 0.532	42.04 0.271	0 gel

4.) A-500 Sub-Fraction in Distilled Water:

Conc. wt%	0 min.	30 min.	1 Hr.	4 Hrs.	23 Hrs.	48 Hrs.	5 Days	9 Days	14 Days
0.5	3.29	3.29 1.00	3.29 1.00	3.29 1.00	3.29 1.00	3.29 1.00	3.29 1.00	3.29 1.00	3.29 1.00
1.0	5.85	5.85 1.00	5.85 1.00	5.85 1.00	5.85 1.00	5.85 1.00	5.85 1.00	5.85 1.00	5.85 1.00

1.5	9.87	9.87 1.00	9.87 1.00	9.87 1.00	9.87 1.00	9.87 1.00	9.87 1.00	9.68 0.981	9.38 0.95
2.12	12.01	12.01 1.00	12.01 1.00	12.01 1.00	12.01 1.00	12.01 1.00	12.01 1.00	11.51 0.958	10.4 0.88
4.27	24.95	24.95 1.00	24.95 1.00	24.95 1.00	24.95 1.00	24.95 1.00	25.58 1.025	24.40 0.978	22.4 0.90
6.01	35.67	35.67 1.00	35.67 1.00	35.67 1.00	35.67 1.00	35.67 1.00	35.67 1.00	34.17 0.958	31.8 0.89
7.92	48.65	48.65 1.00	48.65 1.00	48.65 1.00	48.65 1.00	48.65 1.00	47.24 0.971	45.30 0.931	42.0 0.86
19.33	157.5	156.4 0.993	156.4 0.993	156.1 0.991	145.1 0.921	140.0 0.889	128.7 0.817	125.7 0.798	115. 0.73

B.5) A-1500 Sub-Fraction in Pond Water:

Conc . wt%	0 min.	30 min.	1 Hr.	4 Hrs.	23 Hrs.	48 Hrs.	5 Days	9 Days	14 Days
1.0	6.966	6.959 0.999	6.958 0.999	6.903 0.991	6.834 0.981	6.820 0.979	6.778 0.973	6.757 0.970	6.74 0.97
1.5	10.68	10.67 0.999	10.65 0.997	10.56 0.989	10.39 0.973	10.36 0.970	10.34 0.968	10.26 0.961	10.0 0.94
2.02	14.69	14.66 0.998	14.55 0.990	14.44 0.983	14.25 0.970	13.99 0.953	13.78 0.938	13.46 0.917	12.8 0.87
4.01	29.83	29.30 0.982	29.10 0.975	28.52 0.956	27.30 0.915	26.22 0.879	24.85 0.833	22.52 0.755	19.8 0.66
5.95	46.10	44.11 0.957	43.21 0.937	40.39 0.876	37.11 0.805	33.34 0.723	25.55 0.554	19.34 0.419	14.1 0.31
7.96	63.94	60.12 0.940	58.81 0.920	50.19 0.785	43.91 0.687	33.75 0.528	26.85 0.420	18.96 0.297	15.4 0.24

B.6) A-91500 Sub-Fraction in Pond Water:

Conc. wt%	0 min.	30 min.	1 Hr.	4 Hrs.	23 Hrs.	48 Hrs.	5 Days	9 Days	14 Days
0.5	3.958	3.958 1.00	3.958 1.00	3.958 1.00	3.669 0.927	3.538 0.894	3.470 0.877	3.166 0.800	2.96 0.75
1.0	7.675	7.644 0.996	7.611 0.992	7.59 0.989	6.491 0.846	4.89 0.637	4.39 0.572	4.221 0.550	4.06 0.53
1.47	11.55	11.38 0.985	11.24 0.973	11.10 0.961	8.839 0.765	6.076 0.526	5.37 0.465	4.620 0.400	4.00 0.35
2.00	15.86	15.51 0.978	15.32 0.966	15.01 0.947	10.93 0.689	9.15 0.577	4.88 0.308	2.247 0.142	0 gel
4.06	33.27	31.97 0.961	30.39 0.913	29.81 0.896	10.74 0.323	5.547 0.167	0 gel	0 gel	0 gel
6.72	57.16	51.73 0.905	46.99 0.822	45.78 0.801	7.688 0.135	0 gel	0 gel	0 gel	0 gel
7.80	69.72	56.75 0.814	50.24 0.721	42.74 0.613	5.827 0.084	0 gel	0 gel	0 gel	0 gel

B.7) A-91500 Sub-Fraction in Distilled Water:

Conc. wt%	0 min.	30 min.	1 Hr.	4 Hrs.	23 Hrs.	48 Hrs.	5 Days	9 Days	14 Days
0.5	2.92	2.92 1.00	2.92 1.00	2.92 1.00	2.92 1.00	2.92 1.00	2.92 1.00	2.92 1.00	2.92 1.00
1.0	5.85	5.85 1.00	5.85 1.00	5.85 1.00	5.85 1.00	5.85 1.00	5.85 1.00	5.85 1.00	5.85 1.00

1.5	9.13	9.13 1.00	9.13 1.00	9.13 1.00	9.13 1.00	9.13 1.00	9.13 1.00	9.13 1.00	9.13 1.00
2.0	12.05	12.05 1.00	12.05 1.00	12.05 1.00	12.05 1.00	12.05 1.00	12.05 1.00	12.05 1.00	12.0 5 1.00
3.98	25.36	25.36 1.00	25.36 1.00	25.36 1.00	25.36 1.00	25.18 0.993	25.01 0.986	24.90 0.982	24.9 0.98
6.5	46.08	46.08 1.00	46.08 1.00	46.08 1.00	46.08 1.00	45.94 0.997	45.77 0.993	45.69 0.992	45.7 0.99
8.39	87.78	87.69 0.999	87.64 0.998	87.21 0.994	85.89 0.978	85.58 0.975	85.84 0.970	84.88 0.967	84.1 0.96

RECOMBINED vs. ORIGINAL COLLOIDAL FRACTIONS
NMR SPLITTING DATA

B.8) Original Colloidal Fraction (in Pond Water)

Conc.	0 min	30 mn	1 Hr.	4 Hrs	23 Hrs	48 Hrs	5 Day	9 Day	14 Dy
0.5	2.835	2.775 0.979	2.775 0.979	2.771 0.977	2.768 0.976	2.741 0.967	2.59 0.914	2.43 0.857	2.26 0.797
1.0	5.852	5.823 0.995	5.764 0.985	5.706 0.975	5.530 0.945	5.448 0.931	4.895 0.836	4.617 0.789	4.442 0.759
1.5	8.797	8.735 0.993	8.621 0.980	8.551 0.972	8.520 0.968	8.257 0.939	7.616 0.866	6.785 0.771	6.512 0.740
2.0	12.12	11.84 0.977	11.80 0.974	11.74 0.969	11.60 0.958	10.74 0.886	9.869 0.814	8.963 0.739	7.708 0.636
4.0	25.58	24.21 0.946	23.99 0.938	23.11 0.904	22.06 0.862	19.91 0.778	17.30 0.676	13.25 0.518	11.12 0.435
5.96	39.75	36.68 0.923	35.97 0.905	32.19 0.810	29.03 0.730	25.65 0.645	17.77 0.447	13.56 0.341	8.394 0.211
8.02	53.44	48.47 0.907	47.35 0.886	39.41 0.737	30.55 0.572	23.79 0.445	16.06 0.301	10.74 0.201	0 gel

B.9) Recombined Colloidal Fraction

Conc.	0 min.	30 mn	1 Hr.	4 Hrs.	23 Hrs	48 Hrs	5 Day	9 Day	14 Dy
0.5	2.941	2.940 0.999	2.935 0.998	2.923 0.994	2.903 0.987	2.864 0.974	2.651 0.901	2.649 0.901	2.643 0.899
1.0	5.742	5.731 0.998	5.713 0.995	5.695 0.992	5.644 0.983	5.593 0.974	5.478 0.954	5.070 0.883	4.885 0.851
1.5	8.882	8.846 0.996	8.802 0.991	8.758 0.986	8.660 0.975	8.541 0.962	8.285 0.933	7.727 0.870	7.422 0.836
2.0	12.47	12.37 0.992	12.28 0.985	12.12 0.972	12.07 0.968	11.64 0.933	10.96 0.878	10.16 0.814	9.578 0.768
4.03	26.04	25.28 0.971	25.08 0.963	24.01 0.922	23.59 0.906	22.20 0.853	19.44 0.746	17.00 0.653	15.21 0.584
6.0	39.79	38.04 0.956	37.61 0.945	34.81 0.875	32.76 0.823	29.80 0.749	21.46 0.539	16.32 0.410	14.40 0.362
7.97	52.89	49.98 0.945	49.03 0.927	43.01 0.813	38.73 0.732	30.60 0.578	20.72 0.392	13.34 0.252	8.145 0.154

^{2}H NMR DATA
GEL FORMER MIXTURES
(A-500 / A-91500 Mixtures)

B.10) 25 wt% - A-500 / 75 wt% - A-91500 (in Pond Water)

Conc.	0	30 min	1 Hour	4 Hours	23 Hours	48 Hours	5 Days	9 Days	14 Days
0.48	3.576	3.576 1.00	3.576 1.00	3.417 0.956	3.317 0.928	3.254 0.910	3.201 0.895	2.936 0.821	2.876 0.804
1.0	7.186	7.186 1.00	7.14 0.994	7.042 0.980	7.165 0.997	6.799 0.946	6.618 0.921	6.375 0.887	6.330 0.881
1.5	11.11	11.05 0.995	11.00 0.990	10.80 0.972	10.63 0.957	10.31 0.928	9.942 0.895	9.751 0.878	9.393 0.845
2.01	15.15	15.04 0.993	14.98 0.989	14.66 0.968	14.13 0.933	13.70 0.904	12.69 0.838	11.90 0.786	10.84 0.716
2.5	19.33	19.20 0.993	19.08 0.987	18.20 0.941	17.96 0.929	17.07 0.883	15.99 0.827	14.10 0.729	11.72 0.606
3.5	27.38	27.16 0.992	26.97 0.985	24.60 0.898	23.80 0.869	21.96 0.802	19.52 0.713	14.65 0.535	10.62 0.388
4.0	30.92	30.69 0.992	30.37 0.982	26.71 0.864	25.72 0.832	23.09 0.747	16.40 0.530	11.68 0.378	10.32 0.334
5.96	47.38	46.31 0.977	45.71 0.965	38.34 0.809	33.28 0.702	23.39 0.494	13.64 0.288	9.855 0.208	6.776 0.143
7.95	64.82	62.42 0.963	61.27 0.945	38.58 0.595	27.62 0.426	19.05 0.294	11.44 0.177	0 gel	0 gel

B.11) 50 wt% - A-500 / 50 wt% - A-91500 (in Pond Water)

Conc.	0	30 min	1 Hour	4 Hours	23 Hours	48 Hours	5 Days	9 Days	14 Days
0.5	3.576	3.576 0.986	3.494 0.977	3.426 0.958	3.333 0.932	3.297 0.922	3.254 0.910	3.201 0.895	2.978 0.833
1.0	7.043	7.043 1.00	7.015 0.996	6.896 0.979	6.767 0.961	6.698 0.951	6.245 0.887	6.184 0.878	6.001 0.852
1.48	10.36	10.34 0.998	10.29 0.994	9.983 0.964	9.850 0.951	9.422 0.910	8.929 0.862	8.911 0.860	8.576 0.828
2.0	14.27	14.18 0.994	14.14 0.991	13.71 0.961	13.43 0.941	12.90 0.904	12.04 0.844	11.36 0.796	10.47 0.733
2.5	17.63	17.49 0.992	17.44 0.989	16.90 0.958	16.87 0.956	16.37 0.928	15.43 0.875	14.64 0.830	12.95 0.733
3.5	25.56	25.30 0.990	25.22 0.987	24.09 0.943	23.61 0.924	22.48 0.880	21.15 0.828	18.70 0.732	15.24 0.596
3.98	29.19	28.86 0.989	28.78 0.986	26.34 0.902	25.92 0.888	24.20 0.829	20.77 0.711	17.43 0.597	14.41 0.494
6.0	44.89	43.71 0.974	43.23 0.963	37.15 0.827	35.01 0.780	28.50 0.635	18.35 0.409	14.50 0.323	10.83 0.241
7.98	60.80	58.96 0.970	58.28 0.958	46.98 0.773	37.88 0.623	27.81 0.457	18.43 0.303	15.07 0.248	12.94 0.213

B.12) 75 wt% - A-500 / 25 wt% - A-91500 (in Pond Water)

Conc.	0	30 min	1 Hour	4 Hours	23 Hours	48 Hours	5 Days	9 Days	14 Days
0.5	3.244	3.244 1.00	3.224 0.994	3.157 0.973	3.006 0.927	2.978 0.918	2.667 0.822	2.602 0.802	2.540 0.783
1.0	6.651	6.628 0.997	6.618 0.995	6.603 0.993	6.591 0.991	6.558 0.986	6.205 0.933	6.032 0.907	5.972 0.898
1.48	9.722	9.683 0.996	9.644 0.992	9.602 0.988	9.498 0.977	9.382 0.965	9.018 0.928	8.781 0.903	8.562 0.881
2.0	13.21	13.17 0.996	13.03 0.986	12.92 0.978	12.74 0.964	12.58 0.952	12.19 0.922	11.66 0.882	11.26 0.852
2.5	17.32	17.22 0.994	17.03 0.983	16.86 0.974	16.85 0.973	16.46 0.951	16.36 0.944	15.48 0.894	14.18 0.819
3.5	24.17	23.93 0.990	23.66 0.979	23.42 0.969	23.19 0.959	22.72 0.940	22.20 0.919	20.95 0.867	18.68 0.773
4.0	27.00	26.68 0.988	26.21 0.971	25.46 0.943	25.05 0.928	23.74 0.879	21.71 0.804	20.10 0.744	17.80 0.659
5.95	41.43	40.85 0.986	39.98 0.965	37.74 0.911	35.74 0.863	33.03 0.797	26.75 0.646	22.50 0.543	19.62 0.474
7.98	57.19	56.03 0.980	53.82 0.941	49.65 0.868	45.45 0.795	38.89 0.680	28.36 0.496	23.55 0.412	20.98 0.367

A-200/500/91500 MIXTURES

NMR SPLITTING DATA

B.13) 25 wt% - A-200 / 75 wt% - A-500 (in Pond Water):

Conc.	0 min.	30 min.	1 Hr.	4 Hr.	23 Hrs.	48 Hrs.	5 Days	9 Days	14 Day
1.0	5.613	5.613 1.00	5.613 1.00	5.747	5.930	5.943	5.72 0	5.408	4.334
1.5	8.779	8.779 1.00	8.779 1.00	8.845	8.799	8.722	8.63	8.112 0.922	6.722 0.764
2.0	12.18	12.17 0.999	12.153 0.997	12.075 0.991	11.86 0.974	11.63 0.954	11.5 0.95	11.530 0.946	8.607 0.706
4.0	25.46	25.44 0.999	25.38 0.997	24.85 0.976	24.62 0.967	24.12 0.947	23.9 0.94	22.48 0.883	20.55 0.807
6.0	38.61	38.57 0.999	38.50 0.997	38.01 0.984	36.24 0.939	35.23 0.912	34.1 0.88	31.93 0.827	29.23 0.757
8.0	53.75	52.40 0.975	51.25 0.953	50.32 0.936	47.41 0.882	44.79 0.833	43.8 0.82	40.78 0.759	33.66 0.626
10.0	69.88	67.36 0.964	65.28 0.934	63.17 0.904	57.37 0.821	53.17 0.761	51.8 0.74	43.31 0.620	35.14 0.503

B.14) 50 wt% - A-200 / 50 wt% - A-500

Conc.	0 min.	30 min.	1 Hr.	4 Hr.	23 Hrs.	48 Hrs.	5 Days	9 Days	14 Days
1.0	0	0	0	0	4.949	4.804 0.971	4.433 0.896	3.868 0.782	3.074
1.5	0	0	0	6.346	7.230	7.033	6.578	5.811	4.771
2.0	7.176			9.468	9.428 0.996	9.363 0.989	9.014 0.952	8.04 0.843	6.536 0.686
4.0	17.57			20.23	19.41 0.959	19.41 0.959	19.06 0.942	17.39 0.860	14.30 0.707
6.0	31.18			30.30 0.972	29.39 0.942	28.39 0.910	27.94 0.896	27.37 0.878	24.10 0.773
8.0	44.73			41.96 0.938	38.69 0.865	37.96 0.849	35.22 0.787	32.11 0.718	26.21 0.586
10.0	51.06			46.36 0.908	42.48 0.832	41.15 0.806	40.48 0.793	35.21 0.690	30.93 0.606

B.15) 75 wt% - A-200 / 25 wt% - A-500

Conc.	0 min.	30 min.	1 Hr.	4 Hr.	23 Hrs.	48 Hrs.	5 Days	9 Days	14 Days
1.0	0	0	0	0	4.77	4.504	4.008 0.840	3.299 0.692	3.628 0.551
1.5	0	0	0	0	7.018	6.733	5.934 0.846	5.15 0.734	3.989 0.568
2.0	0	0	8.60	8.757	8.97	8.865	8.195	6.624	5.132
4.0	17.51		19.62	19.91	19.30	18.71	17.51	14.10	11.02
6.0	26.47			28.97	29.18	29.33	28.76	26.95	24.01
8.0	38.67		40.30	37.96	42.49	40.22	40.14	37.46	31.14

10.0				52.23	49.31	46.12	46.85	41.40	29.05 0.556

B.16) 25 wt% - A-200 / 75 wt% - A-91500

Conc.	0 min.	30 min.	1 Hr.	4 Hr.	23 Hrs.	48 Hrs.	5 Days	9 Days	14 Days
1.0									
1.5	10.35		10.23 0.988	10.22 0.986	10.14 0.979	9.896 0.956	9.54 0.921	8.702 0.840	7.644 0.738
2.0	14.15		13.78 0.974	13.57 0.959	13.55 0.958	13.06 0.923	12.39 0.876	11.02 0.779	9.35 0.661
4.0	29.53		27.75 0.939	26.81 0.908	25.58 0.866	23.85 0.808	20.19 0.684	12.78 0.433	7.164 0.243
6.0	45.29		39.36 0.869	38.71 0.855	34.62 0.764	24.81 0.548	16.13 0.356	9.005 0.199	0 gelled
8.0	66.08		54.25 0.821	52.93 0.801	45.40 0.687	33.77 0.511			

B.17) 50 wt% - A-200 / 50 wt% - A-91500

Conc.	0 min.	30 min.	1 Hr.	4 Hr.	23 Hrs.	48 Hrs.	5 Days	9 Days	14 Days
1.0	0		5.281	5.536	5.850	5.664	5.338	4.85	4.15
1.5	8.00		8.538	8.762	8.887	8.538	8.525	7.705	6.571
2.0	11.52		11.36 0.986	11.35 0.986	11.35 0.986	11.08 0.962	10.74	9.356	7.836
4.0	25.75		23.66 0.919	23.46 0.911	22.25 0.864	21.30 0.827	20.04 0.778	16.73 0.650	11.84 0.460
6.0	39.74		35.94 0.904	35.61 0.896	32.49 0.817	27.06 0.681	21.53 0.542	10.62 0.267	0 gel

8.0	55.79		48.07 0.862	45.30 0.812	34.87 0.625	6.41 0.115	0 gel	0 gel	0 gel

B.18) 75 wt% - A-200 / 25 wt% - A-91500

Conc.	**0 min.**	**30 min.**	**1 Hr.**	**4 Hr.**	**23 Hrs.**	**48 Hrs.**	**5 Days**	**9 Days**	**14 Days**
1.0	0	0	0	0	4.961	4.582 0.924	4.168 0.840	3.498 0.705	2.932 0.591
1.5	0	0	0	0	6.899	6.603 0.957	5.995 0.869	5.149 0.746	4.421 0.641
2.0	7.968		8.140	8.198	9.257	9.063	8.672	7.238 0.782	5.832 0.630
4.0	17.97		20.13	20.34	18.25	18.27	16.85	14.72	12.83 0.630
6.0	27.41		27.49	28.41	26.23	24.93	23.61	18.14 0.639	0 gel
8.0	41.36		39.85 0.963	37.42 0.905	34.17 0.826	28.02 0.677	22.02 0.532	0 gel	0 gel

B.19) 25 wt% - A-200 / 75 wt% - (A-500/91500)

Conc.	**0 min.**	**30 min.**	**1 Hr.**	**4 Hr.**	**23 Hrs.**	**48 Hrs.**	**5 Days**	**9 Days**	**14 Days**
1.0	0	0	5.232	5.281	5.471	5.375	5.361	5.353	4.371
1.5	8.288	8.288 1.00	8.288 1.00	8.557	8.493	8.290	8.126	8.033	6.753
2.0	11.63	11.55 0.993	11.41 0.981	11.30 0.971	11.29 0.970	11.29 0.970	11.25 0.967	10.54 0.906	8.848 0.761
4.0	23.56	23.23 0.986	22.91 0.972	21.78 0.924	21.56 0.915	21.42 0.909	20.75 0.881	18.68 0.793	15.97 0.678
6.0	37.86	36.46 0.963	34.68 0.916	33.22 0.877	31.66 0.836	29.07 0.768	27.03 0.714	20.92 0.552	16.74 0.442

8.0	49.51	47.39 0.957	45.34 0.916	42.43 0.857	38.73 0.782	31.87 0.644	25.53 0.516	21.71 0.438	0 gel

B.20) 50 wt% - A-200 / 50 wt% - (A-500/91500)

Conc.	0 min.	30 min.	1 Hr.	4 Hr.	23 Hrs.	48 Hrs.	5 Days	9 Days	14 Days
1.0	0		4.603	4.658	5.291	5.149	4.834	4.173	3.411
1.5	0		6.886	6.488	7.53	7.259	7.204	6.101	5.231
2.0	8.332		9.852	9.786	9.979	9.896	9.53	8.258	6.832
4.0	20.75		20.59 0.992	20.31 0.979	19.79 0.954	19.35 0.933	19.31 0.931	17.91 0.863	15.45
6.0	30.75		29.40 0.956	28.84 0.938	28.07 0.913	26.54 0.863	24.90 0.810	22.44 0.730	0 gel
8.0	42.90		40.14 0.936	39.08 0.911	37.73 0.879	34.32 0.800	28.35 0.661	23.57 0.549	0 gel

B.21) 75 wt% - A-200 / 25 wt% - (A-500/91500)

Conc.	0 min.	30 min.	1 Hr.	4 Hr.	23 Hrs.	48 Hrs.	5 Days	9 Days	14 Days
1.0	0	0	0	0	4.339	4.069 0.938	3.756 0.866	3.100 0.714	2.448 0.564
1.5	0	0	0	0	6.580	6.210 0.944	5.84 0.888	4.80 0.729	3.718 0.565
2.0	0	0	0	0	8.926	8.26 0.925	7.712 0.864	6.392 0.716	5.118 0.573
4.0	15.82		18.53	18.01 0.972	17.75 0.958	16.95 0.915	16.34 0.882	14.47 0.781	12.99 0.701

6.0	28.38		27.83 0.981	27.78 0.979	25.29 0.891	24.65 0.869	23.58 0.831	22.67 0.799	16.53 0.583
8.0	44.45		37.08 0.834	35.60 0.801	34.40 0.774	33.25 0.748	30.71 0.691	27.63 0.622	0 gel

Tiron Treated A-91500 Sample

NMR Splitting Data

B.22) Tiron Treated and Untreated A-91500 Sub-Fractions in Pond Water:

Conc wt%	0 min.	30 min.	1 Hr	4 Hrs.	23 Hrs.	48 Hrs.	5 Days	9 Days	14 Days
2.0 Tiron Treated	15.21	14.46 0.951	14.21 0.934	13.45 0.884	11.48 0.755	10.56 0.694	8.097 0.532	6.073 0.40	1.83 0.12
2.0 Not Treated	15.86	15.51 0.978	15.32 0.966	15.01 0.947	10.93 0.689	9.15 0.577	4.88 0.308	2.247 0.142	0 gel

SUNCOR COLLOIDAL SUB-FRACTIONS WITHOUT SAS NMR DATA

B.24) AS-500 Sub-Fraction Without SAS in Pond Water:

Conc.	0 min.	30 min	1 Hr.	4 Hrs	23 Hrs	48 Hrs	5 Days	9 Days	14 Days
0.5	3.669	3.637 0.991	3.628 0.989	3.621 0.987	3.594 0.980	3.197 0.871	3.007 0.820	2.917 0.795	2.818 0.768
1.0	7.724	7.714 0.999	7.689 0.995	7.670 0.993	7.606 0.985	7.379 0.955	7.334 0.950	6.984 0.904	6.721 0.870
1.5	11.45	11.42 0.997	11.38 0.994	11.36 0.992	11.17 0.975	11.14 0.972	11.05 0.965	10.90 0.952	10.67 0.932
1.97	15.43	15.38 0.996	15.32 0.993	15.30 0.991	14.95 0.969	14.94 0.968	14.73 0.954	14.55 0.943	14.03 0.909

4.27	34.13	33.94 0.994	33.85 0.992	33.74 0.989	32.72 0.959	32.05 0.939	31.28 0.916	30.41 0.891	29.02 0.850
5.96	49.11	48.36 0.985	47.98 0.977	46.82 0.953	45.26 0.922	43.51 0.886	41.03 0.835	38.46 0.783	35.77 0.728
8.13	66.80	65.69 0.983	65.13 0.975	63.55 0.951	59.86 0.896	56.97 0.853	51.92 0.777	46.61 0.698	34.20 0.512

B. 25) AS-91500 Sub-Fraction Without SAS in Pond Water:

Conc.	0 min.	30 min	1 Hr.	4 Hrs.	23 Hrs	48 Hrs	5 Days	9 Days	14 Days
0.5	3.95	3.945 0.999	3.938 0.997	3.930 0.995	3.868 0.979	3.794 0.961	3.686 0.933	3.659 0.926	3.629 0.919
1.04	7.892	7.805 0.989	7.793 0.987	7.758 0.983	7.694 0.975	7.542 0.956	7.114 0.901	6.711 0.850	6.53 0.827
1.46	11.50	11.22 0.976	11.07 0.963	10.97 0.954	10.25 0.891	9.785 0.851	8.715 0.768	7.853 0.683	6.991 0.608
2.0	16.59	15.83 0.954	15.20 0.916	14.85 0.895	14.54 0.876	13.78 0.830	12.19 0.735	10.81 0.651	9.238 0.557
4.02	33.29	31.26 0.939	29.95 0.899	28.19 0.847	19.12 0.574	12.97 0.390	7.225 0.217	4.735 0.142	0 gel
6.65	59.56	54.73 0.919	51.37 0.863	42.88 0.720	14.00 0.235	10.41 0.175	5.522 0.093	0 gel	0 gel

Appendix C

Gel Onset Concentration Determination Graphs

Gel Onset Concentration Determination
A-500, A-1500, and A-91500

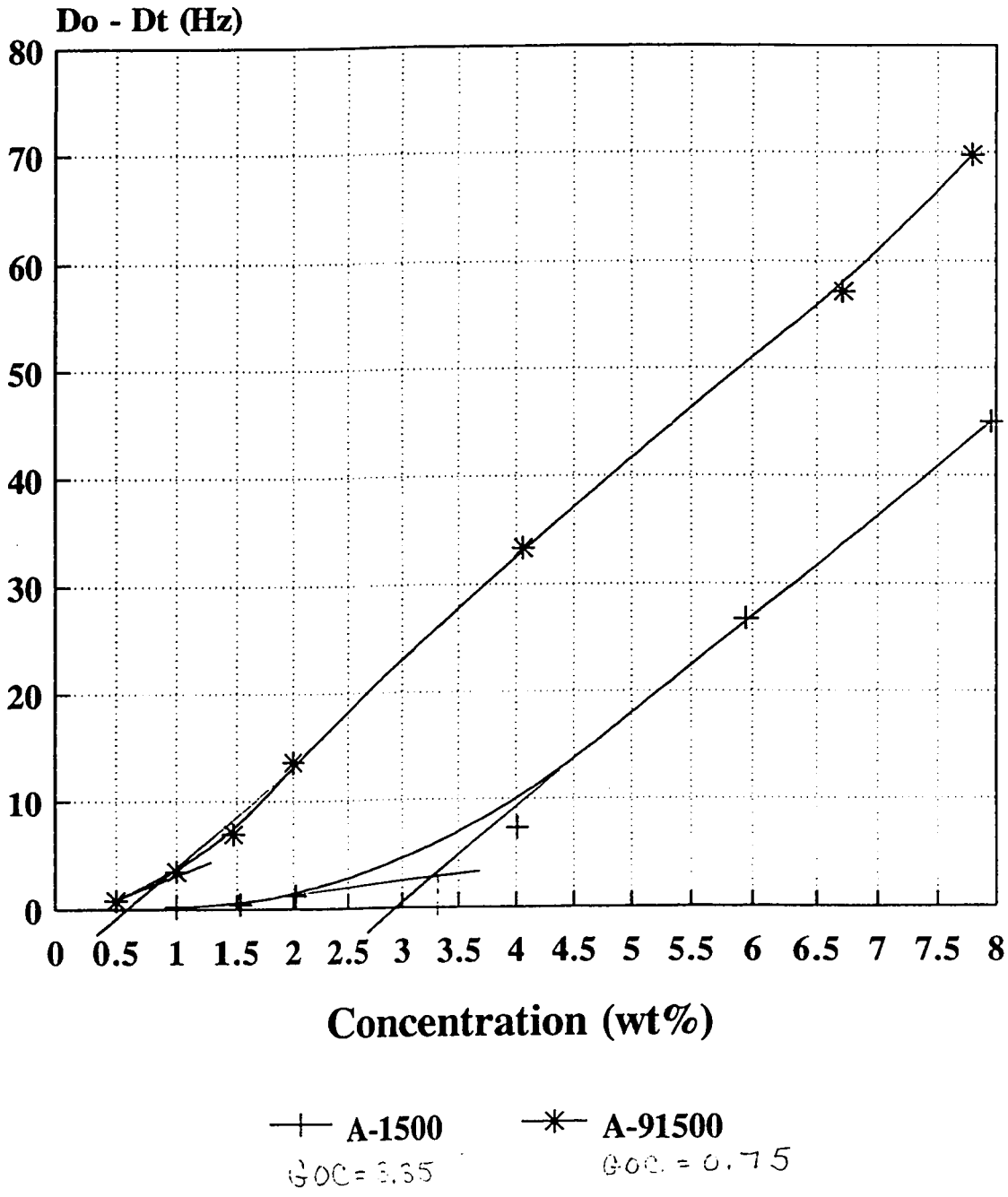

Results taken after 9 days.

Gel Onset Concentration Determination
A-500, A-1500, and A-91500

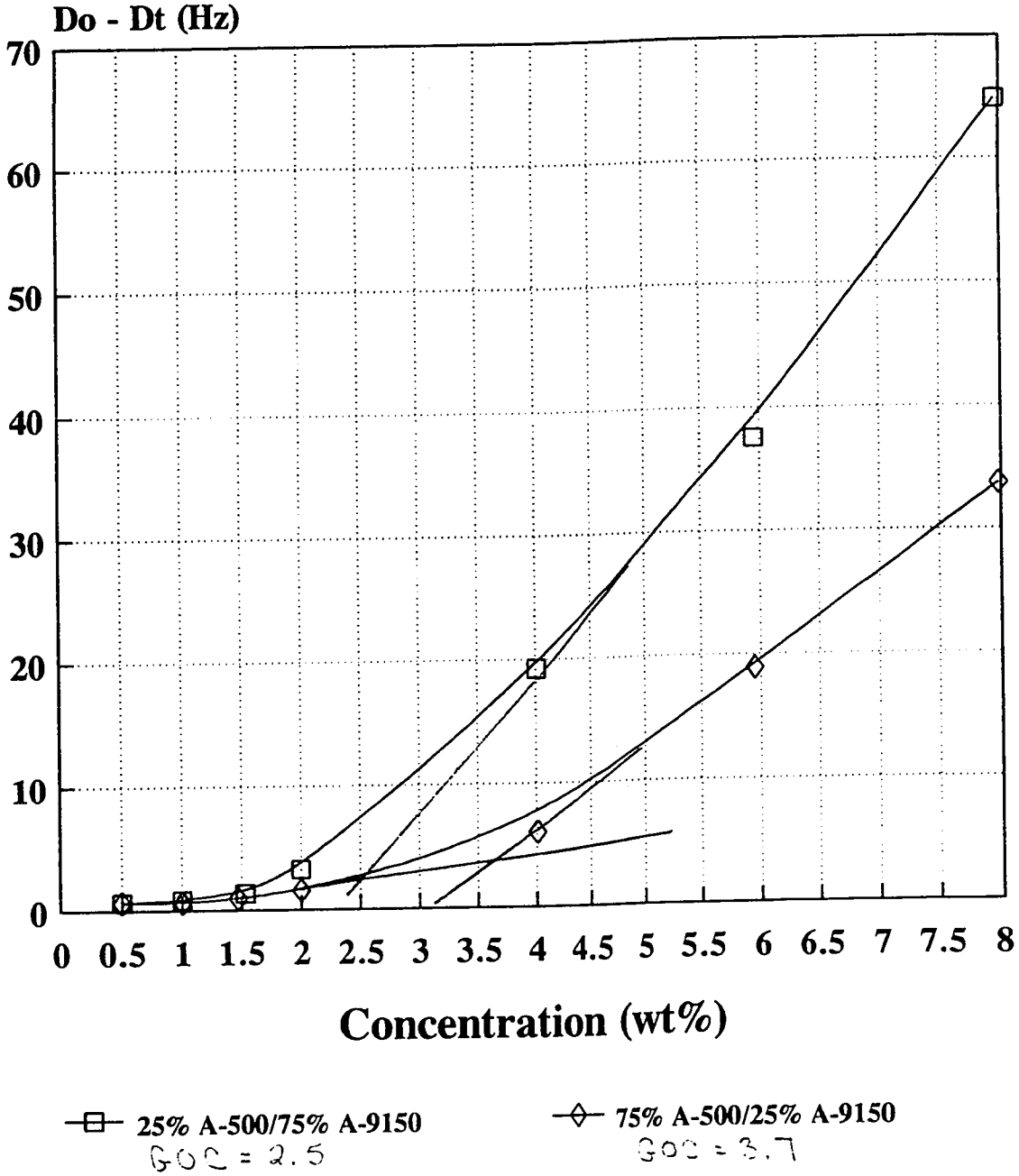

Results taken after 9 days.

Gel Onset Concentration Determination
A-500, A-1500, and A-91500

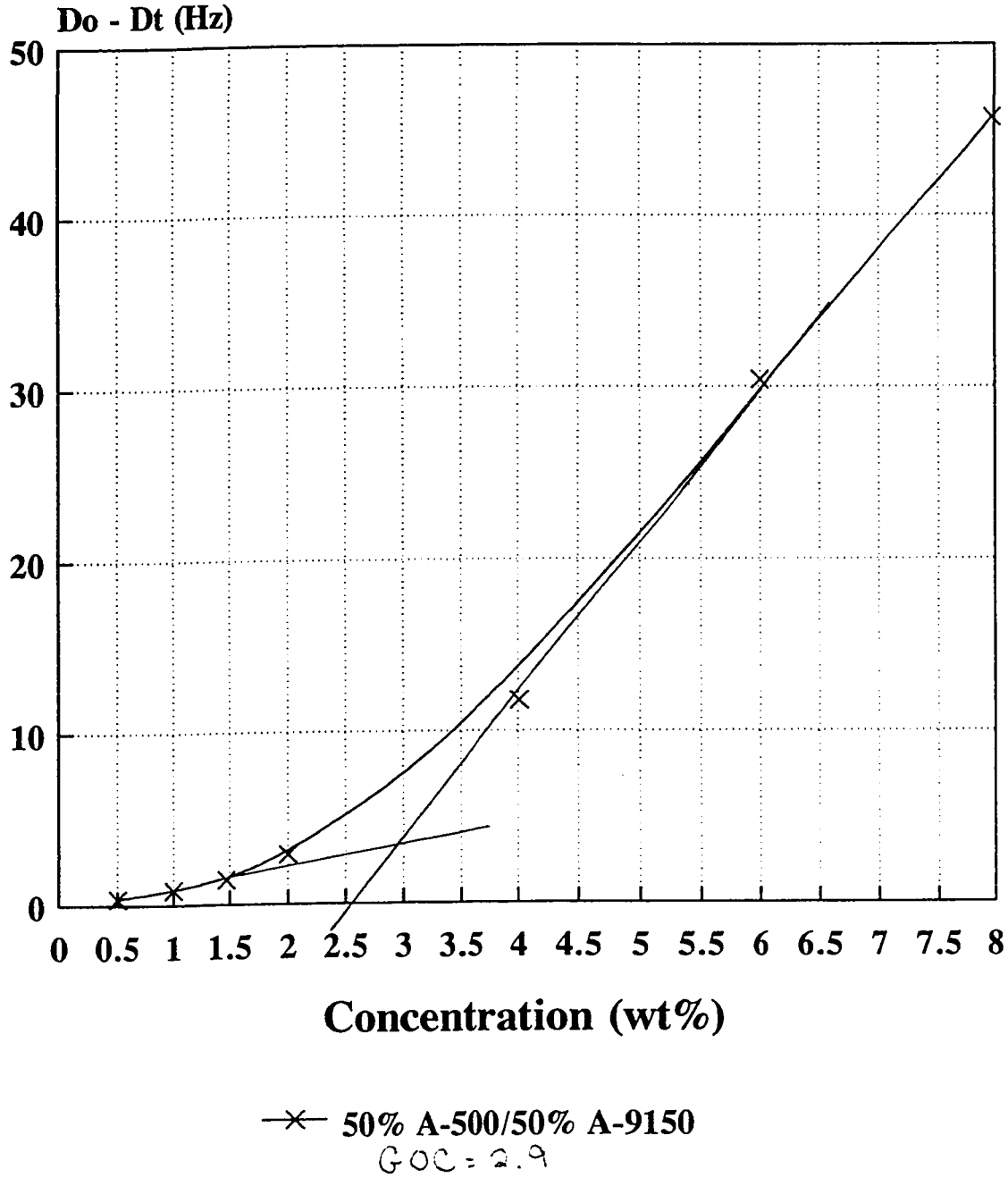

Results taken after 9 days.

Gel Onset Concentration Determination
A-500, A-1500, and A-91500

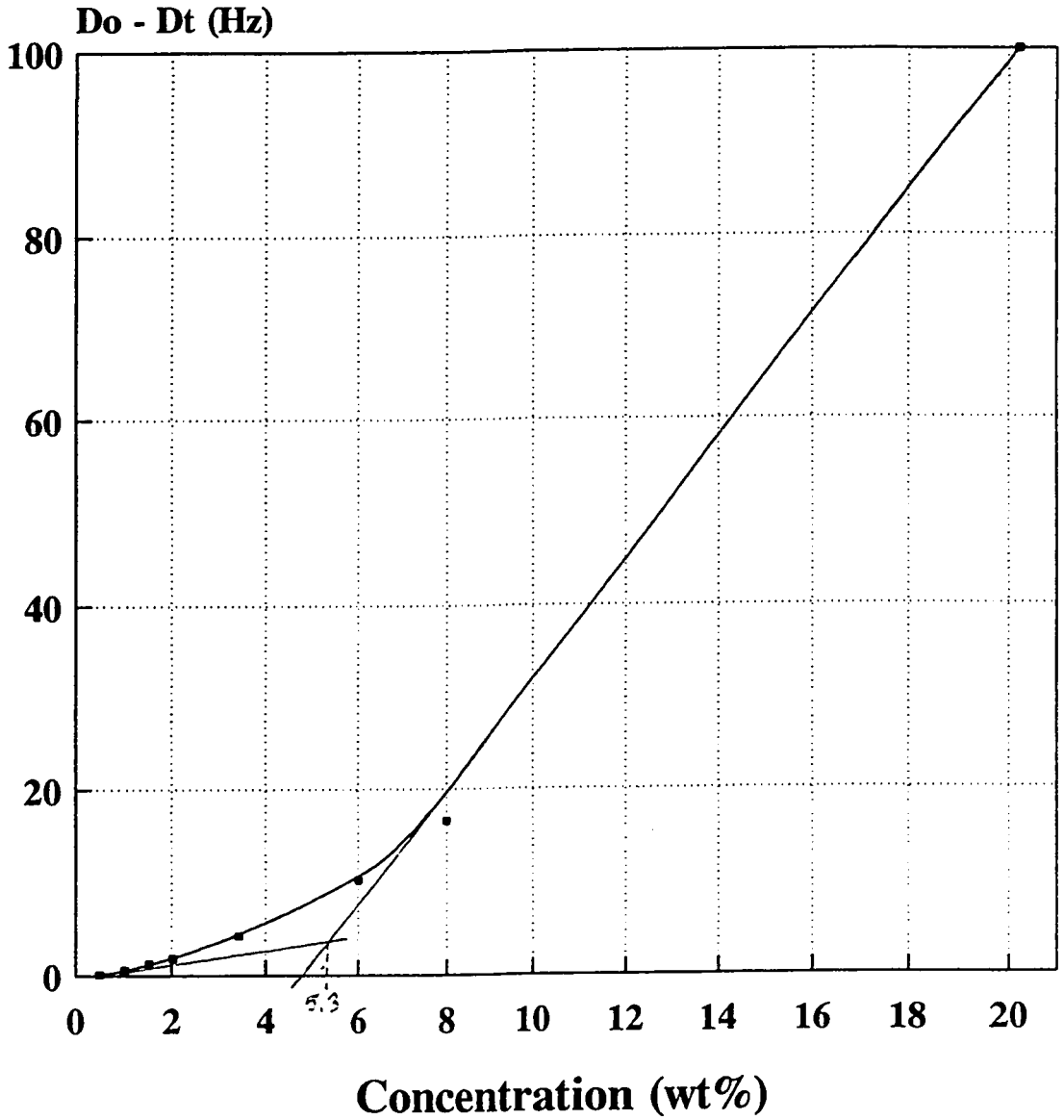

Results taken after 9 days.